CRANFIELD UNIVERSITY

Francesco Lonardoni

DISCOVERY AND QUANTIFICATION OF PROTEINS OF BIOLOGICAL RELEVANCE THROUGH DIFFERENTIAL PROTEOMICS AND BIOSENSING

Cranfield Health

PhD thesis
Academic Year: 2009 - 2012

Supervisors: Dr. Alessandra Maria Bossi
Dr. Iva Chianella

April 2012

UNIVERSITA' DEGLI STUDI DI VERONA
&
CRANFIELD UNIVERSITY

CRANFIELD HEALTH

PhD thesis

Academic Year 2009 - 2012

Francesco Lonardoni

DISCOVERY AND QUANTIFICATION OF PROTEINS OF BIOLOGICAL RELEVANCE THROUGH DIFFERENTIAL PROTEOMICS AND BIOSENSING

Supervisors: Dr. Alessandra Maria Bossi
Dr. Iva Chianella

April 2012

This thesis is submitted in partial fulfilment of the requirements for the degree of Doctor of Philosophy co-tutela between the University of Verona and Cranfield University.

ABSTRACT

Medical diagnosis is the process of attempting to determine and/or identify a possible disease or disorder. This process is revealed by biomarkers, defined by The Food and Drug Administration (FDA) as “characteristics that are objectively measured and evaluated as indicators of normal biologic processes, pathogenic processes, or pharmacologic responses to a therapeutic intervention”. The process of biomarker discovery has been boosted in the last years by proteomics, a research discipline that takes a snapshot of the entire wealth of proteins in an organism/ tissue/ cell/ body fluid. An implementation of the analysis methods can help in isolate proteins present in the low range of concentrations, such as biomarkers very often are. An established biomarker can further be measured with the help of biosensors, devices that can be employed in the point-of care diagnostics.

This PhD thesis shows and discusses the results of three projects in the field of protein biomarkers discovery and quantification. The first project exploited proteomics techniques to **find relevant protein markers for Intrauterine Growth Restriction** (IUGR) in cordonal blood serum (UCS) and amniotic fluid (AF). A 14 proteins in UCS and 11 in AF were successfully identified and found to be differentially expressed.

Molecularly Imprinted Polymers (MIPs) directed towards proteins and peptides containing phosphotyrosine were then produced, with the final goal of **selectively extracting phosphopeptides** from a peptide mixture. An alteration of the phosphorylation pattern is in fact often associated to important diseases such as cancer. The polymers were produced as nanoparticles, that were characterised with Dynamic Light Scattering (DLS) and Atomic Force Microscopy (AFM). A recipe was also tested for binding capacity towards phosphotyrosine.

A Surface Plasmon Resonance (SPR) biosensor to **quantify hepcidin hormone** was finally produced. This is the major subject in iron homeostasis in vertebrates and marker of iron unbalance diseases. A calibration curve

was made and affinity/kinetic parameters for the ligand employed were measured.

Keywords:

IUGR, 2D-PAGE, phosphoproteomics, MIPs, nanoparticles, hepcidin, biosensors.

AIM AND OBJECTIVES OF THE THESIS

The general outline of my 3 year PhD period work focuses on the discovery and quantification of protein biomarkers. This **general aim** is branched in different research subjects.

Medical diagnosis is the process of attempting to determine and/or identify a possible disease or disorder. Diagnostics has made many steps forward in the last decades with the advent and progress of powerful techniques, such as imaging techniques (NMR, PET), mass spectrometry, bioinformatics and genomic tools. Big leaps have been made also specifically in the biochemical field, particularly in the identification and quantitative evaluation of molecules whose presence in the human body increases or decreases following a pathological condition.

The Food and Drug Administration (FDA) defines a biomarker as “a characteristic that is objectively measured and evaluated as an indicator of normal biologic processes, pathogenic processes, or pharmacologic responses to a therapeutic intervention”. Biomarker discovery is a long process which starts from the study of the characteristics of the organism of interest. The genomic approach reveals the potential characteristics of the organism, subsequently expressed in a protein pattern through the transcriptional and translational steps, eventually followed by the post-translational modifications.

The “proteome” is defined as the entire wealth of PROTEins expressed by the genOME. This is a very kaleidoscopic entity, different from subject to subject and different in different stages of life, or in different situations to which an organism can be exposed. Proteins are subjected to Post Translational Modifications (PTMs, e.g. glycosylation, phosphorylation, deamidation, splicing) and these runaway modifications often correlate with alterations from the normal setup. A proteomic approach takes a picture of a particular stage of life of an organism, and permits a comparison to be made

between the different general protein patterns in different situations, e.g. from a normal to a disease state.

Due to the large number of different proteins (thousands in a single cell) and their high differential expression (which can span 10 orders of magnitude in human blood) a single stage of separation is not sufficient to analyze them singularly. First of all prefractionation techniques to separate different parts of a cell (membrane, cytosol, nuclei, etc.) or different fractions of a liquid (blood, urine, cerebrospinal fluid, synovial fluid) are needed to reduce the complexity. Then orthogonal techniques have to be applied. These techniques exploit the different physical-chemical characteristics of proteins, e.g. molecular mass, isoelectric point, hydrophilicity. Nowadays the most established technique to take a snapshot of this changing entity is 2D gel electrophoresis (2-DE). Other orthogonal techniques are being used as well. MudPIT (Multidimensional Protein Identification Technology), for example, combines Strong Cation Exchange chromatography (SCX) and Reversed Phase chromatography (RP) to separate proteins and peptides in liquid phase on-line, and has the advantage to be directly interfaced to a mass spectrometer (MS) improving sensitivity and resolution.

Particular fractions of the proteome can be separately analysed. One important case is phosphorylation, the most widespread and studied PTM. Also in this case there are most established techniques to selectively catch and analyse phosphorylated proteins and peptides, with the aim of characterising phosphorylation pathways and finding abnormalities in their regulation, frequently in many diseases such as cancer or neurodegeneration. In order to improve our understanding of these networks, and with the aim of finding new drug targets or biomarkers, improvements at all levels of the analysis are needed. One critical step is the enrichment of phosphopeptides, which is currently not efficient enough to allow for a comprehensive coverage of this chemically heterogeneous class of molecules.

Once a protein or peptide of biological value is found, its relevance as a biomarker has to be validated against a wide group of subjects. Then its

routine measurement can be included in health screenings, possibly carried out with fast and cheap methods. Regarding this goal, biosensors can be particularly suitable. These are devices made of: a bioreceptor molecule, able to bind to or react with the analyte of interest; a transducing system that converts the biological event into an electric signal, and a data analysis system, that processes this signal in order to display the measured parameter(s) to the operator. These devices generally have the advantage that they can be employed directly where needed, i.e. at or near the patient, in what is called “point-of-care diagnostics”. This could reduce the time to make clinical management decisions.

My 3 years PhD period has evolved in this panorama, spanning from the biomarkers/drug targets discovery to assays/biosensors development.

The first project that I followed exploited proteomic techniques with the **objective** of finding relevant protein markers for Intrauterine Growth Restriction (IUGR) in cordonal blood and amniotic fluid, to shed some light on the pathology mechanisms and to furnish a tool for an early diagnosis of the disease. The pathology has great relevance, being present in 4% of all pregnancies and strongly related to stillbirth. The biochemical markers already used in clinics are not precise enough in the diagnosis, therefore a proteomic screen seemed to be the right approach in order to take a snapshot of the alteration of the protein pattern and find new potential clinical markers.

I then moved onto the production of Molecularly Imprinted Polymers, with the final **goal** of selectively extracting phosphopeptides from a peptide mixture and thus find alternatives for the grasp of the phosphoproteome. Improvements at all levels of phosphoproteomics are in fact needed. In particular, new materials could help in the step of sample enrichment. Phosphoproteins and phosphopeptides are in fact highly underrepresented with respect to their non-phosphorylated counterparts and the currently used materials catch only a fraction of their chemically heterogeneous population.

Finally I stepped into the biosensors field, **focusing** my work on the detection and quantification of hepcidin peptide hormone. This is the major subject in

iron homeostasis in vertebrates and of marker of iron imbalance diseases. The problem has an outstanding clinical relevance, given that anemias affect over one-half billion people all over the world. The recently discovered hepcidin hormone showed problems in its measurement, given its chemical/physical characteristics. The approach that I followed was the development of an SPR biosensor through the use of part of its natural receptor on macrophages and duodenal enterocells: the hepcidin binding domain on ferroportin. This seemed to be a promising way to tackle the problem and introduce a potential point-of-care testing device into the clinic.

All this work has been done keeping fixed one idea in my mind: everybody that works in this field faces the challenge and has the inspiring aim of improving, maybe just a bit and in a not immediately clear way, the health of all of us.

The proteomics work discussed in this thesis was carried out in the Mass Spectrometry and Proteomics lab at the Biotechnology Department of the University of Verona (Italy), in collaboration with the Department of Environmental Medicine and Public Health and the Department of Gynecological Sciences and Reproductive Medicine of Padova (Italy), that provided the biological samples. This study was approved by the Ethical Committee of Padova University Hospital, after obtaining written informed consent from the mothers of the foetuses.

The work on Molecularly Imprinted Polymers and the development of the SPR biosensor was performed in the Biochemical Methodologies and Molecular Imprinting Laboratory at the Biotechnology Department of University of Verona (Italy) and in the School of Cranfield Health of Cranfield University (Bedfordshire, UK). The results obtained are here discussed and evaluated.

ACKNOWLEDGEMENTS

In the end of this 3 year period I would like to thank firstly my italian supervisors Dr. Alessandra Bossi, Dr. Daniela Cecconi and Dr. Iva Chianella.

Dr. Rita Polati also deserves a first place in the “thank you” page for her support in the most challenging moments.

A special thought has to be addressed to people in Smart Polymers group in Cranfield Health: Prof. Sergey Piletsky for his leadership, Dr. Michael Whitcombe for his competence and to Dr. Dhana Lakshmi for her friendship.

A long list of friends should be here mentioned: I just would like to shake my ideal hand to Dr. Antonio Lapenna, that has been a nice companion for the thoughtless moments in Cranfield and to Dr. Piyush Sindhu Sharma for his still lasting deep friendship.

Finally, my family deserves the biggest acknowledgement: without them I would not be here now. And to my guardian angel: you know you are always on my mind.

TABLE OF CONTENTS

LIST OF FIGURES

LIST OF TABLES

LIST OF EQUATIONS

LIST OF ABBREVIATIONS

2D-PAGE	Two Dimensional Polyacrylamide Gel Electrophoresis
AA	Acrylamide
AC	Abdominal Circumference
AF	Amniotic Fluid
AFM	Atomic Force Microscopy
AQUA	Absolute Quantification of proteins
BPD	Bipariethal Diameter
CHAPS	3[(3-cholamidopropyl) dimethylammonium]-1-propanesulfonate
CID	Collision Induced Dissociation
CPP	Calcium Phosphate Precipitation
CRL	Crown-Rump Length
DC	Detergent Compatible
DHB	Dihydroxybenzoic Acid
DLS	Dynamic Light Scattering
DPIC	Diphenyliodonium chloride
DTT	Dithiothreitol
ECD	Electron Capture Dissociation
ECL	Enhanced Chemiluminescence
EDC	1-ethyl-3-(3-dimethylaminopropyl) carbodiimide
ELISA	Enzyme-Linked Immuno Sorbent Assay
ERLIC	Electrostatic Repulsion - Hydrophilic Interaction Chromatography
ESI	Electrospray Ionisation
ETD	Electron Transfer Dissociation
Eth	Ethanolamine
FL	Femur Length
Fmoc-	Fluorenylmethyloxycarbonyl-
GO	Gene Ontology
HAMMOC	Hydroxy Acid Modified Metal Oxide Chromatography
HAP	Hydroxyapathite
HBD	Hepcidin Binding Domain

HC	Head Circumference
HH	Hereditary Haemocromatosis
HILIC	Hydrophilic Interaction Chromatography
HSA	Human Serum Albumin
ICPL	Isotope-Coded Protein Label
IDA	Iminodiacetic Acid
IEF	Isoelectric Focusing
IFC	Integrated Microfluidic Cartridge
IMAC	Immobilised Metal Affinity Chromatography
IP	Immunoaffinity Purification
IPG	Immobilised pH Gradient
IT	Ion Trap
iTRAQ	isotope Tags for Relative and Absolute Quantification
IUGR	Intra Uterine Growth Restriction
k_D	Equilibrium Dissociation constant
LCQ	Liquid Chromatography Quadrupole
LTQ	Linear Trap Quadrupole
MALDI	Matrix Assisted Laser Desorption Ionisation
MB	Methylene blue
MIP	Molecularly Imprinted Polymer
MOAC	Metal Oxide Chromatography
MP	Multiplex Proteomics
MS	Mass Spectroscopy
MSA	Multi-Stage Activation
MW	Molecular Weight
M/Z	Mass/charge ratio
NHS	N-hydroxysuccinimide
NTA	Nitrilotriacetic Acid
OD	Optical Density
PAC	Phosphoramidate Chemistry
PAIs	Protein Abundance Indexes
pdMS3	phosphorylated directed fragmentation
pI	Isoelectric point

PVDF	Polyvinylidene Difluoride
QQQ	Triple Quadrupole
RAS	Renin-Angiotensin System
RP	Reversed Phase
RU	Responsive Units
SALDI	Surface Assisted Laser Desorption/Ionisation
SAX	Strong Anion exchange chromatography
SCX	Strong Cation exchange chromatography
SDS	Sodium Dodecyl Sulphate
SEM	Scanning Electron Microscopy
SGA	Small for Gestational Age
SILAC	Stable Isotope Labeling with Amino acids in Cell culture
SIMAC	Sequential elution from IMAC
SPM	Scanning Probe Microscopy
SPR	Surface Plasmon Resonance
SSP	Standard Spot numbering
TBP	Tributylphosphine
TED	Tris(carboxymethyl)ethylenediamine
TEM	Transmission Electron Microscopy
TOF	Time-Of-Flight
TSIA	Toluensulphinic Acid
UC	Umbilical Cord
WCX	Weak Cation Exchange
XIC	Extracted Ion Chromatogram
XPS	X-ray Photoelectron Spectroscopy

1 CHAPTER

DISCOVERY OF NEW PROTEIN MARKERS FOR INTRAUTERINE GROWTH RESTRICTION

1.1 Introduction

Foetus growth is a complex process driven basically by four factors: maternal, placental, genetic and external (Gardosi J, 2006). All these factors are intimately correlated in determining a harmonic growth of the foetus. An unbalance of one or more of them can determine lesser or greater alterations in the foetus' wellbeing. In modern hospitals foetus growth is monitored throughout the pregnancy with several exams at well determined periods of the expected 40 weeks of gestation. Ecography is the most renowned method, by which different metric parameters are measured: head circumference (HC), biparietal diameter (BPD), femur length (FL), abdominal circumference (AC), crown-rump length (CRL) and humerus length (HL) (Fig. 1-1) (Mandruzzato G, 2008). Other routine exams are cardiotocography (foetus heart beat), eco-Doppler (evaluation of blood flux from mother to foetus and *vice-versa*) and mother's urine and blood analysis (biochemical analysis).

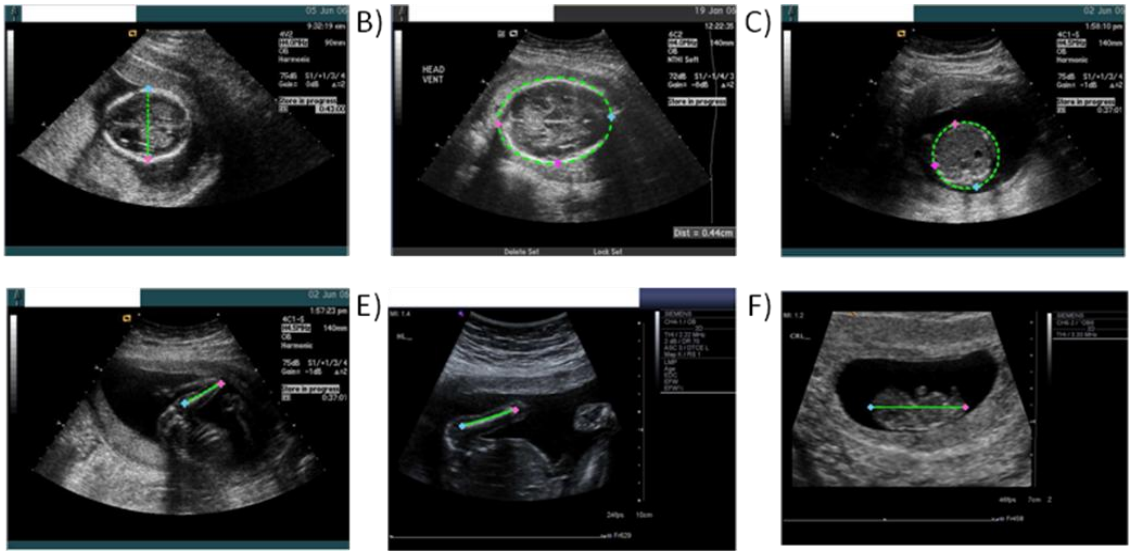

Fig. 1-1. Foetal segmentation measured through ecography: A) BPD, B) HC, C) AC, D) FL, E) HL, F) CRL (Pictures taken from: Carneiro G, Georgescu B, Good S, Comaniciu D, IEEE Transactions on Medical Imaging 2008, 27, 1342-1355).

The foetus weight is normally estimated through ecographic measurements, e.g. AC as single parameter has a good correlation with the weight (Mandruzzato G, 2008) and normally follows a sigmoidal trend, therefore it is more pronounced in the middle of the gestational period (Fig. 1-2). Customised growth charts made on homogeneous populations are available and are used in order to assess the normal increase of the foetus weight (Breeze ACG, 2007).

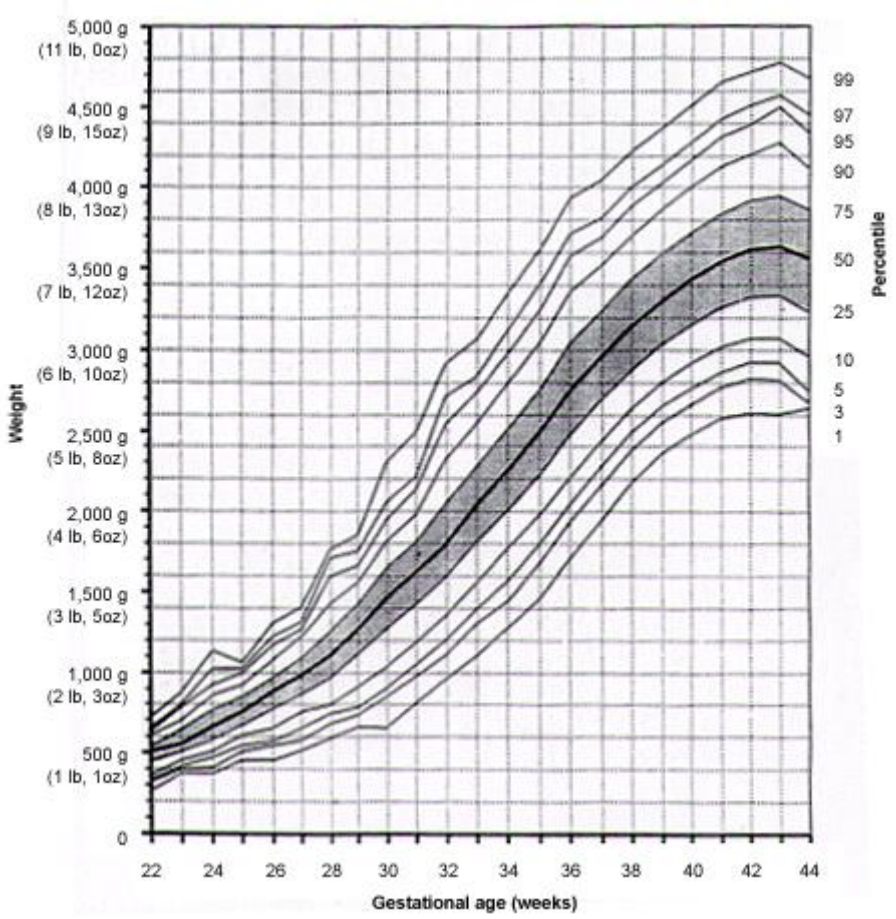

Fig. 1-2. Sigmoidal trend of foetus' weight increase during the gestational period (Picture taken from: Peleg D, Kennedy CM, Hunter SK. Am Fam Physician. 1998 Aug 1;58(2):453-460).

When the weight is less than the 10th customised centile we speak about a small for gestational age foetus (SGA). This small size can be physiological, i.e. due to factors like parity or altitude that normally reduce the weight, otherwise a pathological condition can be present and it has to be carefully considered by obstetricians. In this case we speak about intrauterine growth restriction (IUGR). The discrimination between SGA and IUGR is normally determined through a series of ecographic measurements with 2 weeks of delay between measurements: if the growth shows an accentuated slowdown, a pathological condition is present, and actions have to be taken in order to secure the best health condition for the foetus and the mother. This condition is in fact related to serious problems for the foetus, both perinatally, carrying increased morbidity

and mortality, and in adult life, bringing metabolic and cognitive deficits (Bernstein G, 2000). Apart from cases where hormonal therapy is effective (Hui L, 2008) no proven therapy in uterus is nowadays available, and a decision has to be taken whether to let the foetus grow in adverse conditions or program the delivery. This decision is normally taken considering the gestational age, which has to be evaluated as more precisely as possible (Mandruzzato G, 2008). Obstetrical management is therefore critical, and subjected to regulation by law and juridical disputes. In this context legal medicine plays a role in ascertaining when an improper obstetrical management was present, having consequences as health problems of the foetus and/or the mother (Loue S). The growing number of juridical disputes raises the need of a precise determination of the period when the pathological condition emerged (damage timing) and if it was not seen. This determination can be made *a posteriori*, evaluating the presence of biomarkers in cordonal blood serum or amniotic fluid.

Amniotic fluid (AF), routinely used for prenatal diagnosis, contains large amounts of proteins produced by the amnion epithelial cells, foetal tissues, foetal excretions, and placental tissues. Additionally, molecules originating from maternal circulation are released in the amniotic cavity. The biochemical composition of AF is modified throughout pregnancy and its protein profile reflects both physiological and pathological changes affecting the foetus and the mother (Jauniaux E, 1994, Kolialexi A, 2007). Identification of changes in the balance of proteins, therefore, may be used to detect a particular type of pathology, or to identify a specific genetic disorder. Potential biomarkers in AF have already been identified in cases of inflammation and premature rupture of foetal membranes (Brenner, 2004, Vuadens F, 2003).

Umbilical cord (UC) blood drawn from the doubly clamped umbilical cord at delivery reflects the foetal blood compartment. Along these lines, the cord blood levels of various growth factors and hormones have been related to size at birth by several groups (Amarilyo G, 2010, Neta GI, 2010). Protein S100B is a recently identified UC blood protein able to assess newborn brain damage (Gazzolo D, 2004). Other established markers of anoxia are umbilical cord

blood pH, uric acid, cytokines and lactate levels in umbilical vein (Hellstrom-Westas L, 1995, Huang CC, 1999).

The purpose of this project is to investigate the differential protein expression levels in UC serum (UCS) and amniotic fluid (AF) in IUGR, to produce information on the causes and mechanisms of prenatal disorders and reveal possible markers for postnatal complications and disease progression. Moreover, as said before, new markers for precision and accuracy improvement of damage timing are needed, in order to assess possible responsibilities of an improper obstetrical treatment.

The chosen experimental technique is two-dimensional polyacrylamide gel electrophoresis (2D-PAGE), a well-established tool for proteomic analysis that can be used to compare patterns of protein expression in various biological materials under physiological and pathological conditions. MS, in association with bioinformatics, provides the tool for the identification of protein spots on 2D-PAGE maps. In the next paragraph this technique will be explained in detail.

1.2 Two-dimensional gel electrophoresis (2D-PAGE)

In 2D-PAGE proteins in a sample are separated in two dimensions according respectively to their isoelectric point (pI) and molecular mass (MW). The technique includes sample preparation, protein separation through gel electrophoresis, protein detection, digestion of the differentially expressed proteins and their identification with MS and bioinformatic tools (Fig. 1-3).

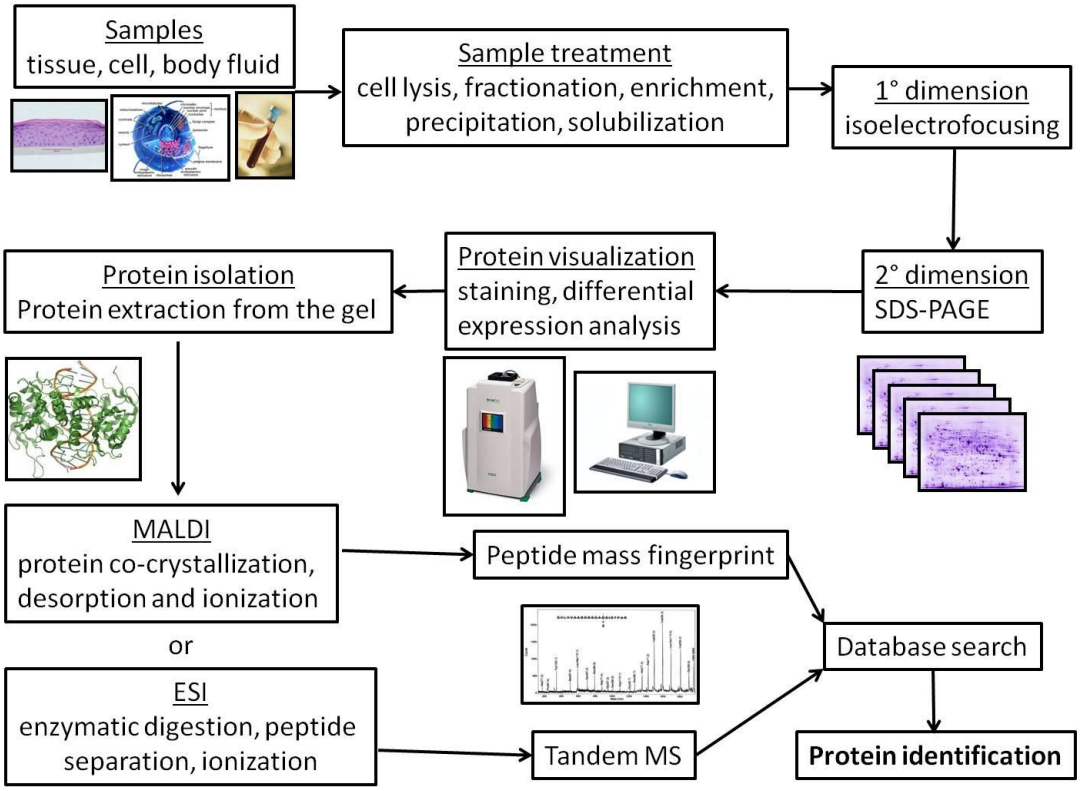

Fig. 1-3. Workflow of a clinical proteomics analysis, i.e. regarding clinical samples and molecular medicine studies. MALDI: Matrix Assisted Laser Desorption Ionisation; ESI: Electrospray Ionisation.

1.2.1 Sample preparation

Normally as a first step proteins are extracted from a complex medium, such as a cell culture or a body fluid, and treated to remove impurities such as nucleic acids, lipids, salts and sugars. This step can be done for example on serum samples through acetone precipitation and centrifugation: impurities will be mostly present in the supernatant and proteins can be isolated as a pellet. These are subsequently solubilised in a highly dispersive media, such as 7M urea, 2M thiourea plus 3% surfactant (e.g. 3[(3-cholamidopropyl) dimethylammonium]-1-propanesulfonate, “CHAPS”, a sulfobetainic zwitterionic detergent) Tris buffer. In order to remove nucleic acids a prolonged centrifugation at high speed (e.g.14000 x g x 40’) is usually effective, otherwise the use of ampholytes can suit the purpose of precipitating them, subsequently removed by centrifugation. In order to improve solubilisation, sulphur bridges are broken by the use of a reducing agent, such as tributhylphosphine (TBP)

and –SH groups are prevented from reforming links through iodoacetamide or acrylamide (AA) blocking. This operation also avoids the creation of fake omo and etero-oligomers due to –SH recombination (Harry JL, 2000).

1.2.2 Protein separation

The samples are then loaded onto polyacrylamide strips with an immobilised pH gradient (IPG strips) and the applied voltage induces proteins to migrate depending on their charge, along the strip. When they are in a region where the pH corresponds to their pI they stop, due to a null net charge. This first separation is further amplified with a second dimension. The IPG strips are equilibrated in a solution containing sodium dodecyl sulphate (SDS), which binds to proteins proportionally to the number of amino acid residues (about 1 SDS molecule for every 2 residues), conferring to every protein a negative charge proportional to its molecular weight. The strip is then interfaced on a side of a polyacrylamide gel slab through agarose gel bridging. A second electrophoretic migration along the gel matrix separates proteins with the same pI but different MW. More maps are produced with different samples to evaluate the statistical variation, both analytical and biological.

1.2.3 Detection of proteins

Protein spots in the gel are then stained to be visualised and therefore to evaluate protein amounts. A common stain is colloidal Coomassie blue (Neuhoff V, 1988), while other stains are SyproRuby. RuBPS (both fluorescent) (Yan JX, 2000) and Silver staining (the most sensitive but at the same time difficult to control for not reaching an equilibrium in the staining process) (Shevchenko A, 1996). Each of these methods is compatible with the downstream MS analysis.

The gel images are then acquired and digitised, to be further analysed with dedicated software such as PDQuest, Melanie, Phoretic and Progenesis Gel images are superimposed to match protein spots, in order to compare quantities of the same protein between the gels and find modulations of expression between groups of samples. The level of appreciable differential expression depends on the number of replicates, e.g. with 10 replicates a 1.5 times modulation is appreciable (Hunt SMN, 2005).

1.2.4 Protein digestion

Once protein spots with a significant differential expression have been found their identity needs to be inferred. MS methods are the most powerful and versatile available with this purpose. First of all the protein spots need to be cut out from the gel, then they are submitted to proteolytic digestion with an enzyme such as trypsin, that cleaves peptide bonds in proximity of a C-terminal lysine or arginine and generates peptides of suitable length for MS analysis (Fig. 1-4).

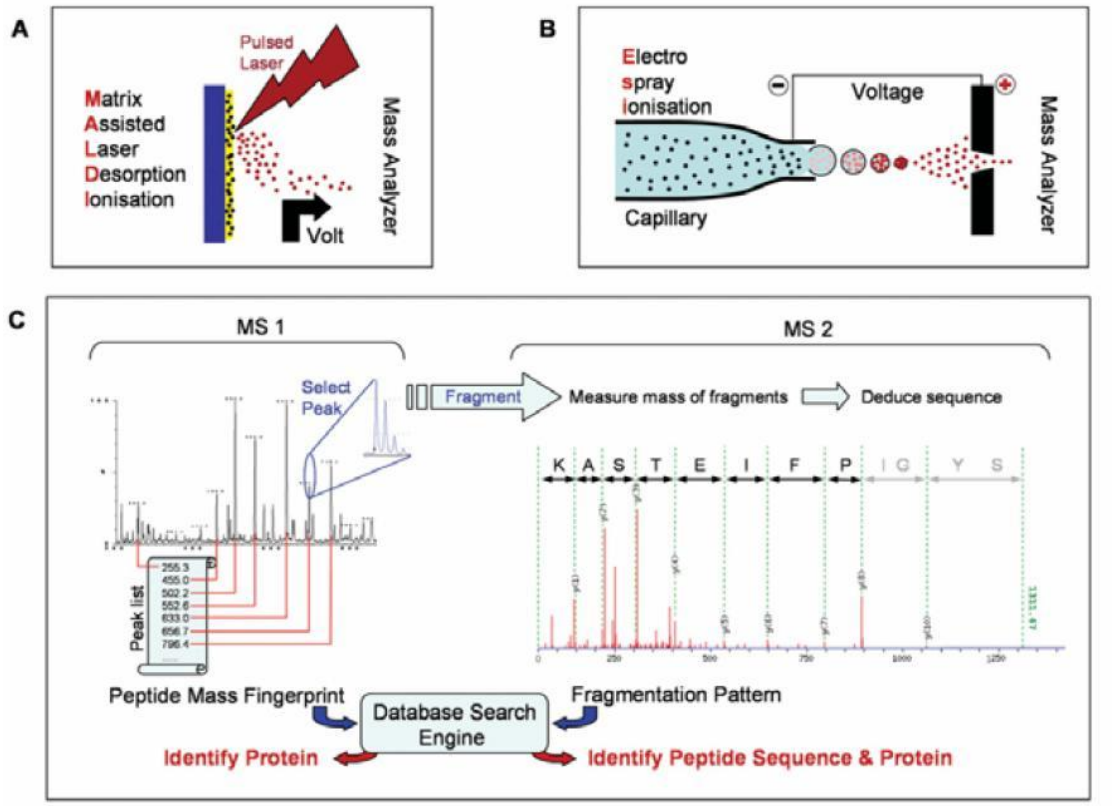

Fig. 1-4. Mass Spectroscopy methods. In proteomics mostly MALDI and ESI methods are used to ionise proteins and/or peptides, subsequently fragmented to give a MS^1 spectrum. A further fragmentation of the most abundant peptides gives the MS^2 spectrum.

1.2.5 Protein identification

The identification of proteins through mass spectroscopy relies on the accurate measurement of protein and peptide masses.

A mass spectrometer is a device made essentially of three components:

1) an ionizing source, that in this case ionises proteins and peptides;

2) a mass analyser, that resolves the ions in dependence of their mass/charge ratio (m/z);

3) a detector, that reveals the ions resolved by the mass analyser.

In proteomic studies two ionisation methods are generally employed: Matrix Assisted Laser Desorption Ionisation (MALDI) and Electrospray Ionisation (ESI) (Chen, 2008). In MALDI peptides are co-crystallised in a matrix with molecules such as sinapinic acid or alpha-cyano-4-hydroxycinnamic acid. A laser impulse then softly desorbs and ionises the peptides, whose m/z is measured, usually with Time-Of-Flight detectors (TOF). The combination of more peptide masses is associated with a specific protein (peptide fingerprint). In order to deepen the analysis a further fragmentation of peptides can be performed, via a second collision chamber and another TOF analyser (MALDI-TOF/TOF). The collision with helium atoms, electrons or other collision agents such as electron transferring molecules induces the backbone fragmentation in correspondence of peptide bonds, permitting to infer the peptide sequence through calculation of mass difference of adjacent peaks (tandem MS/MS).

In ESI-MS, instead, peptides firstly separated with an HPLC column are ionised with an electrospray system. The preferred detectors for this system are Ion Trap (IT) and triple quadrupole (QQQ).

The peptide sequence is the first step in protein identification, and its reliability is expressed through a score, calculated as $S= -10Log_{10}(p)$. The parameter p is the probability that a sequence match between MS and database data is a random event, and is given by the ratio between the significance threshold of random match chosen E and the number of proteins in the database N.

For example, if during a search 500,000 peptides fell within the window of mass tolerance chosen and the significance threshold chosen is 0.05 (1 in a 20 chance to be a false positive) the corresponding score threshold would be S= -

$10Log_{10}(E/N) - 10Log_{10}(0.05/500000) = 70$. The protein score is given by the sum of the scores of individual peptides.

Other parameters to be included in mass spectrum analysis are mass tolerance, the presence of modifications (e.g. –SH blocking with AA) and the N- or C-terminal amino acid depending on the lysing enzyme used. The mass spectrum is a forest of peaks, and the highest are submitted to further fragmentation. The results of fragmentation are analysed with software packages such as MASCOT (at the Matrix Science server) or SEQUEST to correlate the peptide sequences with those usually derived from genomic data. These data can be found in dedicated protein databases such as SWISSPROT maintained by the Swiss Institute for Bioinformatics and the European Bioinformatics Institute, or the USA government-funded National Center for Biotechnology Information (NCBI).

A successful protein identification depends on many parameters, such as the number of successfully identified peptides, their uniqueness for a protein and the sequence coverage. Nevertheless there can be ambiguities, and a 100% assignment is not always possible (that is why mass spectroscopists speak about “correlation” and not “identification”) (Chen, 2008). A MASCOT score for a peptide above 30 is usually considered enough to have a good correlation.

1.2.6 Bioinformatics

Once a reasonable correlation between MS data and a protein has been obtained, it becomes a potential candidate as a marker of disease or of drug treatment. In order to have a complete understanding of its role, its molecular functions (e.g. enzyme), cellular or extracellular districts where it is present (e.g. cytoplasma) and biological processes in which it is involved (e.g. glucose oxidation) need to be known. This study, called Gene Ontology (GO) can be performed with one of the many software packages available, such as SWISSPROT or GeneCards, curated by the Crown Human Genomic Centre at the Weizmann Institute of Science in Israel (Bairoch A, 2000).

The next step is inserting the protein in the nets of processes in which it is involved, this time with the help of dedicated software packages such as Kioto Encyclopedia of Genes and Genomes (KEGG, hosting more than 150,000 pathway maps) or Reactome.

1.3 Materials and methods

1.3.1 Umbilical cord blood and amniotic fluid withdraw

The study, approved by the Ethical Committee of Padova University Hospital (Padova, Italy), was performed after obtaining written informed consent from the mothers of the foetuses. Ten IUGR and ten AGA full-term singleton neonates, all of Italian origin, were included in the study. Offspring of mothers with a birth weight below the 10th customised centile were characterised as IUGR. The Gestation Related Optimal Weight computer-generated program was used to calculate the customised centile for each pregnancy, taking into consideration significant determinants of birth weight, such as maternal height and booking weight, ethnic group, parity, gestational age and gender. The choice of the neonates excluded the cases where a chromosomal pathology, child-dependent disease or maternal consumption of xenobiotics were present.

Umbilical cord blood samples (UCS) were withdrawn from double clamped umbilical cord of singletons, from full-term deliveries performed with caesarean section. UCS was obtained after clotting for 30-45 min at room temperature followed by centrifugation at 3000g for 20 min in BD Vacutainer® glass serum tube, then samples were added to protease inhibitors (Roche) and frozen straightaway at -80°C until the analysis.

Amniotic fluid (AF) samples were obtained through withdrawal by syringe after amniotic sac resection, and treated with the same procedure as serum, omitting the clotting step.

1.3.2 Protein sample preparation

The samples of UCS were albumin and IgG depleted (with ProteoPrep Blue Depletion kit, Sigma). Proteins, from UCS and AF, were precipitated with 4 volumes of acetone at -20°C for 2 h and then resuspended in a solubilising solution: 7 M urea (Sigma, Sigma-Aldrich Corporation, St. Louis, MO, USA), 2 M thiourea (Sigma), 3% CHAPS (Sigma), and 20 mM Tris (Sigma). Centrifugation at 14000 x g at 4°C for 40 min was performed to get rid of incidentally present nucleic acids.

The samples were then incubated with 5 mM tributylphosphine (Sigma) and 20 mM acrylamide (Sigma) for 60 minutes at room temperature to reduce protein

disulphide bonds and alkylate the cysteine thiolic groups. The reaction was blocked by the addition of 10 mM ditiothreitol (DTT, Sigma). Protein concentration was evaluated by Detergent Compatible (DC) Protein assay (Bio-Rad Labs., Hercules, CA, USA) based on the Lowry method.

1.3.3 Two-dimensional gel electrophoresis and image analysis

UCS and AF protein fractionation by 2-DE were performed as reported by Cecconi el al. (Cecconi D, 2008). Briefly, 450 µl of each sample (containing 3 mg/ml of protein) was separated by 17 cm pH 3-10 NL IPG strip, and the total product time x voltage applied was 70000 Vh for each strip. The second dimensional separation was done using 8-18%T gradient SDS-PAGE, applying 40 mA for each gel for 3 min, then 2 mA/gel for 1 h, and 20 mA/gel until the track dye, bromophenol-blue, reached the anodic end of the gels. After 2-DE, the proteins were detected by Sypro Ruby. The image analysis of the 2D gels replicates was performed by PDQuest software (Bio-Rad), version 7.3. Each gel was analysed for spot detection, background subtraction and protein spot optical density (OD) intensity quantification. The gel image showing the highest number of spots and the best protein pattern was chosen as a reference template, and spots in this standard gel were then matched across all gels. Spot quantity values were normalised in each gel by dividing the raw quantity of each spot by the total quantity of all the spots included in the standard gel. Gels were divided in two groups (control and IUGR samples) and, for each protein spot, the average spot quantity value and its variance coefficient in each group were determined. Data were log transformed and analysed with Student's t-test, then spots giving significant results ($p < 0.01$) were verified visually to exclude artefacts.

1.3.4 Mass spectrometry and protein identification

Spots showing a statistically significant differential expression were carefully cut out from 2-D Sypro Ruby stained gels and subjected to in-gel trypsin digestion (Neuhoff V, 1988). Briefly, spots were destained with three washing steps: 50mM NH_4HCO_3, 50% 50mM NH_4HCO_3 (v/v), 50% acetonitrile, 100%

acetonitrile, and dried at 37°C for 30 min. The gel pieces were then swollen in digestion buffer containing 50mM NH_4CO_3 and 12.5ng/ml of trypsin (modified porcine trypsin, Promega, Madison, WI) and the digestion proceeded at 37°C overnight. The supernatants were collected and peptides were extracted in an ultrasonic bath (twice with 50% acetonitrile, 50% H_2O v/v with 1% formic acid, once with acetonitrile). Finally tryptic peptides were dried by vacuum centrifugation. Peptides from 8 µl of each sample were then separated by reversed phase (RP) nano-HPLC-Chip technology (Agilent Technologies, Palo Alto, CA, USA) online-coupled with a 3D ion trap mass spectrometer (model Esquire 6000, Bruker Daltonics, Bremen, Germany). The chip was composed of a Zorbax 300SB-C18 (150mm × 75µm, with a 5µm particle size) analytical column and a Zorbax 300SB-C18 (40 nL, 5µm) enrichment column. The complete system was fully controlled by ChemStation (Agilent Technologies) and EsquireControl (Bruker Daltonics) software. The scan range used was from 300 to 1800 m/z. For tandem MS experiments, the system was operated with automatic switching between MS and MS/MS modes. The three most abundant peptides of each m/z were selected to be further isolated and fragmented. The MS/MS scanning was performed in the normal resolution mode at a scan rate of 13,000 m/z per second. A total of five scans were averaged to obtain an MS/MS spectrum. Database searches were conducted using the MS/MS ion search of Mascot against all entries of the non-redundant NCBI database with the following parameters: specific trypsin digestion, up to one missed cleavage; fixed and variable modifications: propionamide (Cys) and oxidation (Met), respectively; peptide and fragment tolerances: ± 0.9 Da and ± 0.9 Da, respectively, and peptide charges: +1, +2 and +3. For positive identification, the score of the result of [- 10 x $Log_{10}(p)$] had to be over the significance threshold level ($p < 0.01$) and at least 2 different peptides ($p < 0.05$) had to be assigned.

1.3.5 Protein validation by Western Blot analysis

Protein samples were precipitated with cold acetone at -20°C for 2 hours and centrifuged at 14,000 x g for 10 min. The pellets obtained were dried and resuspended with Laemmli's sample buffer (62.5 mM Tris-HCl, pH 6.8, 25% glycerol, 2% SDS, 0.01% Bromophenol Blue, 5% ß-mercaptoethanol) through 5

min heating in boiling water. A 1-D SDS-PAGE separation on 10%T acrylamide gel in Tris/glycine/SDS buffer was then performed. The separated proteins were transferred to a PVDF membrane through electroblotting and equal protein loading in each lane (60 μg) was verified by Ponceau red staining. The membranes were treated with primary and secondary antibodies at the appropriate dilutions (see Tab. 1-2) and bound antibody was detected by Enhanced Chemiluminescence (ECL) Western blotting detection system (Millipore, USA). Western blots were scanned by a ChemiDoc instrument (Bio-Rad) and images were analysed using Quantity One image processing software (Bio-Rad).

1.3.6 Classification of Proteins

Functional annotation was obtained by assignment of Gene Ontology (GO) terms for the identified proteins. GO analysis was performed with the help of GeneCards database (http://www.genecards.org), classifying each protein with respect to its molecular function and biological process in which it is involved.

1.4 Results

The typical high resolution 2-DE protein pattern of IUGR and control neonates, obtained from UCS and AF protein extracts, are reported in Fig. 1-5 and Fig. 1-6. By PDQuest analysis we measured differential protein expression by analysing the 10 biological replicates of 2-DE maps obtained for each group.

A total of 18 and 13 spots (matched across all the replica 2D maps) were found to be differentially expressed ($p < 0.01$) in UCS and AF respectively. Spots selected from the differential analysis were subjected to RP-HPLC-ESI-MS/MS analysis for protein identification.

The unique differentially expressed proteins identified were 14 in UCS, and 11 in AF samples. In Tab. 1-1, the successfully identified proteins corresponding to up- or down-regulated spots in UCS and AF are shown, together with the gene names, the standard spot number (SSP), the identification parameters and the indication of their gene ontology (GO) annotation (biological process and molecular function). Protein GO classification indicate that 21% of proteins are involved in inflammatory response, 20% in immune response, while a smaller

proportion are related to transport, blood pressure, and coagulation. Figure 8 shows the distribution of the identified proteins as a pie chart, categorised according to the biological process in which they are involved.

Western Blot analysis, performed to determine the level of expression of five candidate proteins (complement C3-alpha chain (C3), serotransferrin (TF), kininogen light chain (KNG1), apolipoprotein J (CLU), and angiotensinogen (AGT) identified by 2-DE analysis are shown in Fig. 1-7. The relative protein expression in both samples was normalised through staining with Ponceau Red which permits an appreciation of the total protein amount. Trends of changes in the same direction as those detected in the 2D gel analyses were detected for all the proteins. The quantitative difference between the results obtained by 2D electrophoresis and by Western Blot suggested that most changes detected by the former technique specifically involve post-translationally modified forms, which can be only separated in 2D maps (Fig. 1-5, Fig. 1-6).

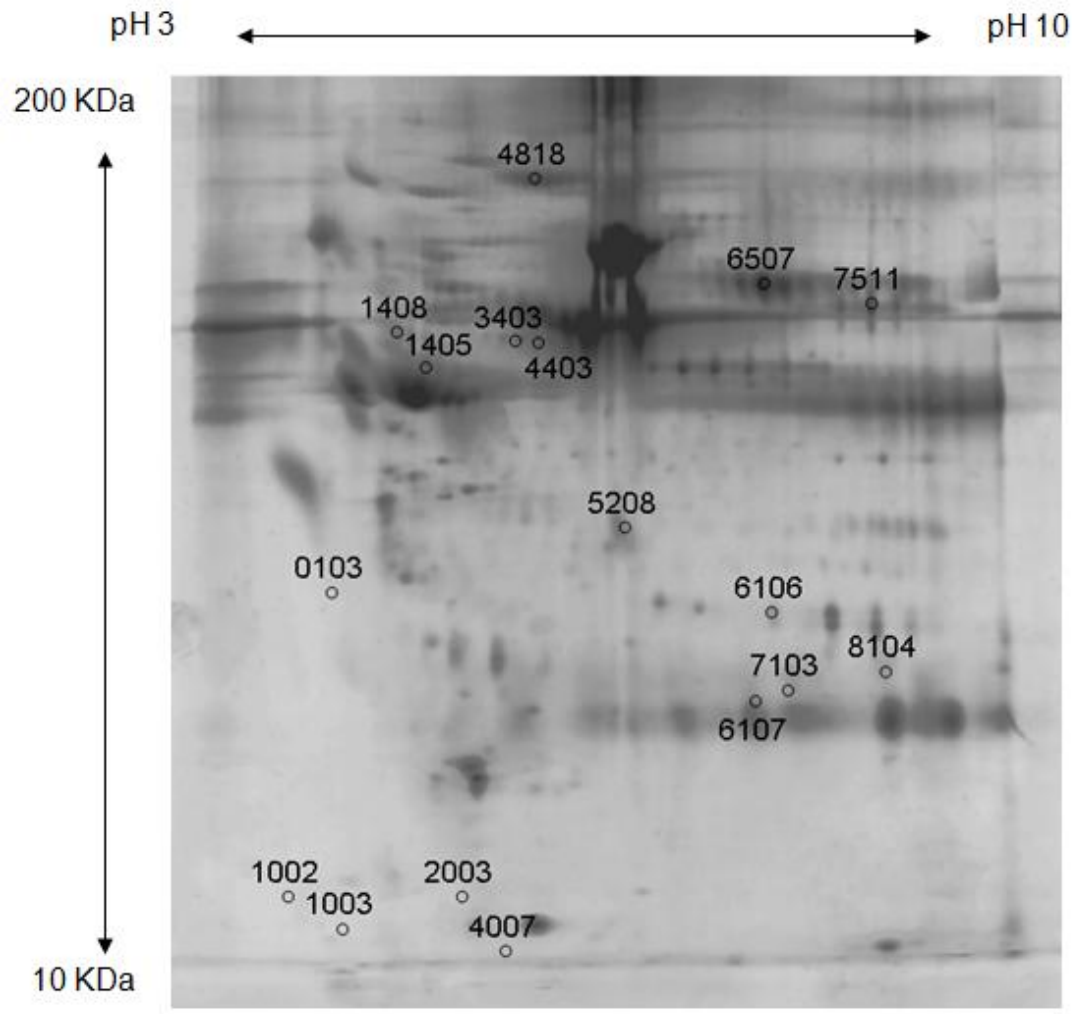

Fig. 1-5. 2D-PAGE map of UCS with spots of differentially expressed proteins pinpointed with an SSP (Standard Spot numbering), assigned by PDQuest software).

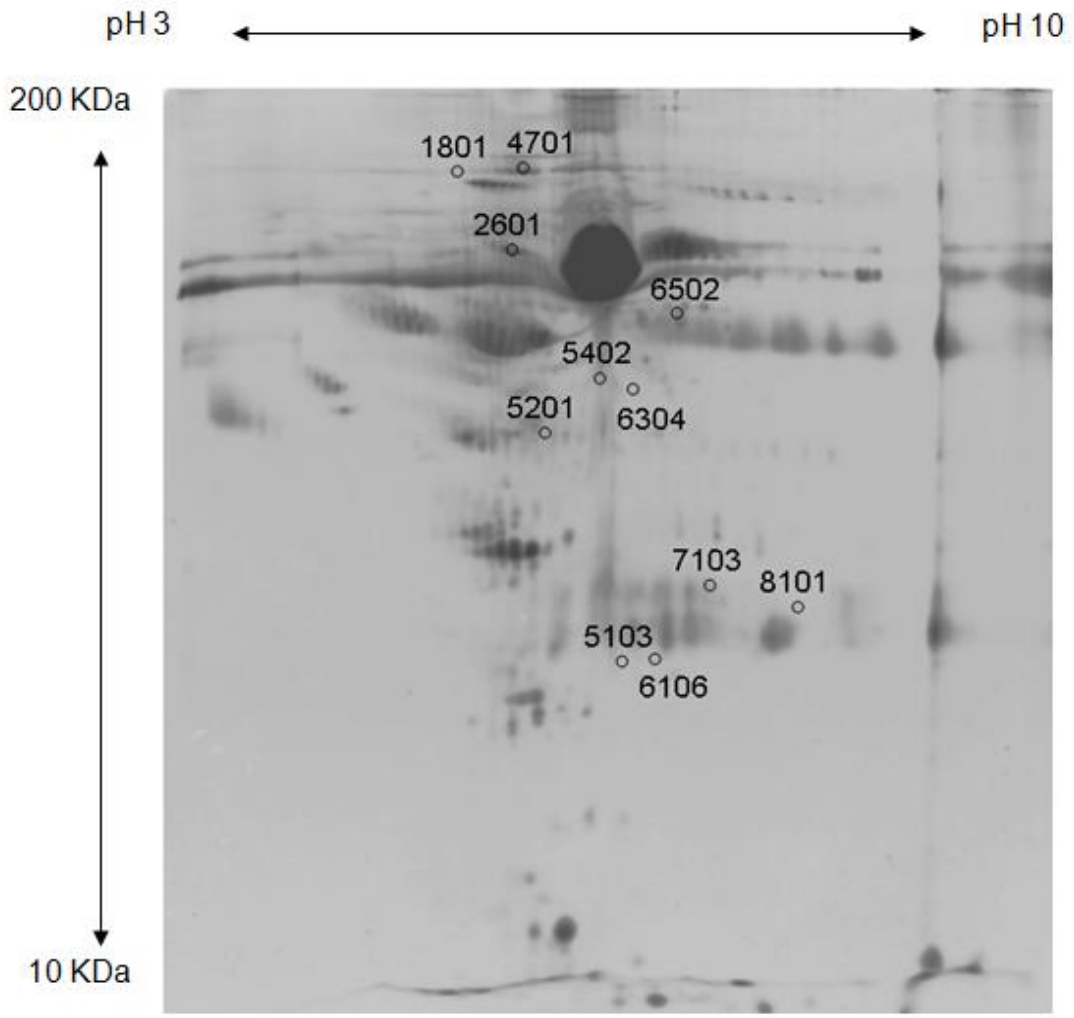

Fig. 1-6. 2D-PAGE map of AF with spots of differentially expressed proteins pinpointed with an SSP (Standard Spot numbering), assigned by PDQuest software).

Tab. 1-1. Identified proteins that are differentially expressed in UCS and AF of IUGR newborns through 2-DE.

Protein name	Gene name	IUGR sample	Spot no. [a]	NCBI acc. #	Mr (kDa) exp/ theor	pI exp/ theor	No. of peptides identified	Mascot score [b]	Sequence Coverage (%) [c]	Molecular function GO term	Biological process GO term	Fold of variation IUGR/C [d]
Alpha-1-B-glycoprotein	A1BG	AF	2601	gi|69990	85/51.9	5.4/5.6	15	445	30	protein binding	crisp-3 binding	–2.0
Alpha-2-macroglobulin	A2M	UCS	4818	gi|177870	125/163.2	5.3/6.0	5	106	2	endopeptidase inhibitor	complement pathway	– 1.6
Angiotensinogen	AGT	UCS	1405	gi|532198	55/53.1	4.8/5.8	13	448	23	vasoconstrictor	Regulation of vasoconstriction	– 1.6
Apolipoprotein J	APOA1	UCS	0103	gi|178855	30/48.8	4.3/6.3	2	69	6	phospholipid binding	lipid transport	> 20
Carbonic anhydrase 1	CA1	AF	7103	gi|4502517	30/28.8	6.9/6.6	12	356	34	carbonate dehydratase activity	one-carbon metabolic process	+ 12.8
Ceruloplasmin	CP	AF	4701	gi|1620909	150/115.4	5.5/5.4	9	274	11	ferroxidase activity	ion transport	–1.8
Complement Component C3, Chain A	C3	UCS	7511	gi|78101267	60/71.1	7.2/6.8	14	730	30	endopeptidase inhibitor	inflammatory response	– 2.0
Complement Component C3b, Chain B	C3	UCS	3403	gi|118137965	55/103.9	5.2/5.2	3	122	4	endopeptidase inhibitor	inflammatory response	– 1.6
Complement Component C3b, Chain B	C3	UCS	4403	gi|118137965	55/103.9	5.2/5.2	18	509	19	endopeptidase inhibitor	inflammatory response	– 1.6
Complement Component C3c, Chain B	C3	UCS	8104	gi|78101270	25/21.5	7.3/5.8	7	172	31	endopeptidase inhibitor	inflammatory response	– 2.2
Complement component C4	C4A	UCS	1002	gi|179674	15/192.7	4.2/6.6	3	54	1	endopeptidase inhibitor	inflammatory response	– 2.6
Complement factor B	CFI	AF	6502	gi|291922	65/85.4	6.5/6.5	13	307	12	peptidase	inflammatory response	– 1.2
Fibrinogen beta chain	FGB	AF	5201	gi|2781208	45/37.6	5.8/5.8	7	206	15	protein binding	blood coagulation	>20
Fibrinogen beta chain	FGB	UCS	5208	gi|119625341	34/50.4	5.6/8.6	5	202	13	protein binding	blood coagulation	+ 8.5
Hemoglobin gamma-G	HBG2	UCS	1003	gi|31725	13/17.0	4.7/5.9	2	132	20	oxygen transporter activity	oxygen transport	> 20
Hemoglobin gamma-G	HBG2	UCS	2003	gi|183885	13/16.6	5.2/6.4	3	141	28	oxygen transporter activity	oxygen transport	> 20
Ig kappa 4 light chain	IGKV4-1	UCS	6107	gi|170684576	20/24.1	6.7/6.2	6	124	22	antigen binding	immune response	– 1.8

Ig lambda chain V-IV region	BCRL4	UCS	7103	gi|87901	20/15.5	6.8/7.7	3	123	25	antigen binding	immune response	− 1.7
Ig lambda chain V-IV region	BCRL4	UCS	8104	gi|87901	20/15.5	7.3/7.7	5	97	25	antigen binding	immune response	− 2.2
Ig light chain	IGKJ	AF	5103	gi|149673887	25/23.4	6.0/7.0	7	186	34	antigen binding	immune response	>20
Keratin, type II cytoskeletal 1	KRT1	UCS	4007	gi|11935049	12/66.0	5.5/8.2	5	141	6	protein binding	cytoskeleton organisation	+ 2.1
Keratin, type II cytoskeletal 1	KRT1	UCS	6106	gi|119395750	27/66.0	6.8/8.2	13	398	17	protein binding	cytoskeleton organisation	− 1.9
Kininogen-1 isoform 2	KNG1	UCS	1408	gi|4504893	55/47.9	4.6/6.3	11	333	21	endopeptidase inhibitor	regulation of vasoconstriction	− 1.8
Serotransferrin	TF	UCS	6507	gi|4557871	70/77.0	6.6/6.8	12	429	19	ferric iron binding	iron ion transport	− 1.5
Serum albumin	ALB	AF	1801	gi|28592	150/69.3	5.2/6.0	1	51	2	transport	carrier protein	>20
Serum albumin	ALB	AF	5402	gi|6013427	60/69.2	6.0/5.9	9	364	15	transport	carrier protein	>20
Serum albumin	ALB	AF	6106	gi|157830361	30/47.3	6.3/6.0	11	152	9	transport	carrier protein	>20
Serum albumin	ALB	AF	6304	gi|27692693	55/47.3	6.2/6.0	19	506	30	transport	carrier protein	–1.5
Serum albumin	ALB	AF	8101	gi|27692693	30/47.3	7.4/6.0	17	427	22	transport	carrier protein	>20

[a] Spot numbers refer to 2D gels of Figure 1-5 and 1-6.

[b] Score is $-10\log_{10}(p)$, where *p* is the probability that the observed match is a random event,
based on the NCBI database using the MASCOT searching program as MS/MS data.

[c] Amino acid sequence coverage for the identified protein.

[d] Fold of variation in expression in IUGR/C ratio: increased protein (+), decreased protein(-).

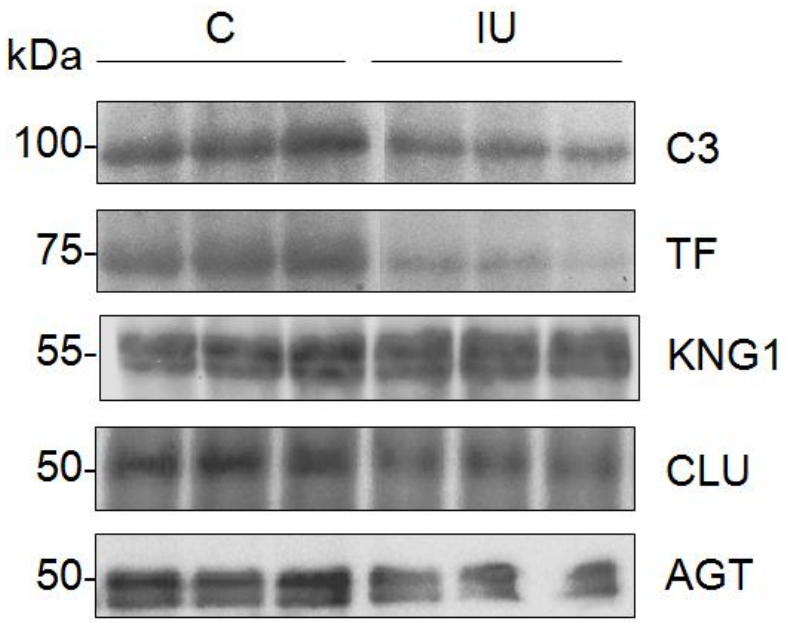

Fig. 1-7. Protein expression validation with Western blot analysis for five proteins. Film images with the relative protein expression were normalised by Ponceau red staining. Film images were captured with GS710 densitometer (Bio-Rad) and analysed with Quantity One software to calculate the band intensities (OD).

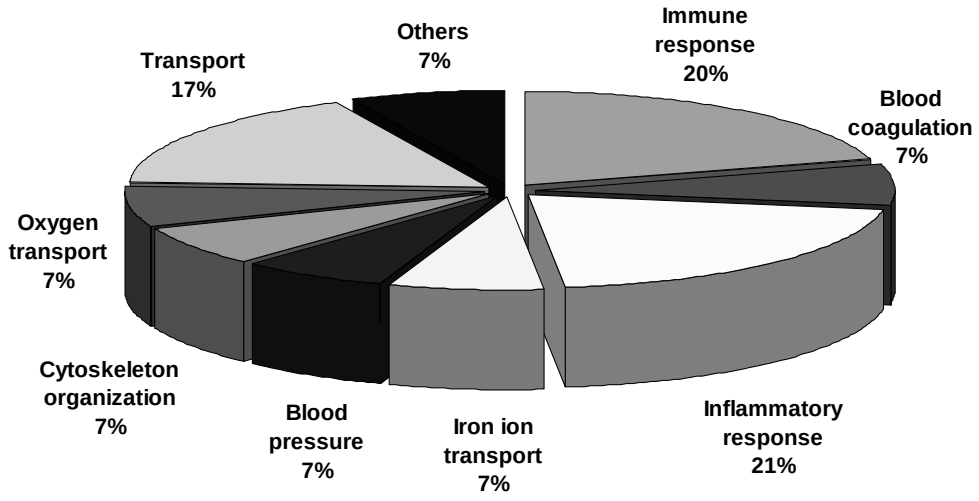

Fig. 1-8. Protein GO categorisation. Distribution of the identified proteins according to the biological process(es) in which they are involved. GO analysis was performed by using GeneCards database.

Tab. 1-2. The different primary and secondary antibodies used for Western Blot analysis, with the corresponding dilutions.

Primary antibody	**Dilution**
Mouse anti-complement C3B-alpha (Chemicon)	1:1000
Mouse anti- angiotensinogen (Abnova)	1:2000
Mouse anti-transferrin HTF-14 (GeneTex)	1:1000
Mouse anti-clusterin CLI-9 (GeneTex)	1:2000
Rabbit anti-kininogen1 (GeneTex)	1:2000
Secondary antibody	**Dilution**
Goat anti-mouse IgG, HRP conjugated (Millipore)	1:5000
Donkey anti-rabbit IgG, HRP conjugated (Amersham)	1:10000

1.5 Discussion

The differentially expressed proteins identified in both umbilical cord serum and amniotic fluid samples of IUGR and AGA neonates are described and discussed in the following paragraphs.

1.5.1 Coagulation and IUGR

The association between coagulation disorders and IUGR has already been demonstrated by several publications (Bellart J, 1998, Benedetto C, 2010, Ducloy-Bouthors AS, 2010). A low grade activation of the coagulation system is in fact suggested as one possible factor in the pathogenesis of IUGR. Accordingly, it has been reported that heparin treatment significantly improved the growth of the growth-restricted foetus (Persson B L, 1982, Yu YH, 2010, Yu YH, 2004). Among the proteins that play a pivotal role in coagulation there is fibrinogen, which is converted by thrombin into fibrin to form a clot. Interestingly, it has been demonstrated that the G/A polymorphism at position - 455 of the

beta-fibrinogen gene may enhance the physiological increase in fibrinogen levels during pregnancy and thereby predispose to obstetric complications (Camilleri R S, 2004, von Tempelhoff G F, 2009). In line with these findings, we found that fibrinogen was up-regulated in UCS as well as in AF of IUGR samples.

Another protein also related to coagulation is alpha 2-macroglobulin (A2M) which is a protease inhibitor with both anticoagulant and procoagulant properties (it neutralises alpha-thrombin, plasmin, and activates protein C) (Cvirn G, 2002). In some studies A2M has been negatively correlated with birth weight: infants with lower birth weight had higher cord serum A2M concentrations as compared to those with higher birth weight (Goldenberg RL, 1991, Cliver SP, 1993). Our data stands in contrast with these findings, indeed we reported a down-regulation of A2M in UCS of mothers of IUGR infants. An explanation of this discrepancy may depend on the modulation of different PTM-modified isoforms.

1.5.2 Immune mechanisms and IUGR

Another mechanism that seems to be involved in IUGR development is the inflammatory response, which interestingly has been linked to the coagulation process state (Lipinski S, 2010, Girardi G, 2008). Normal pregnancy is associated with increased concentrations of maternal plasma complement components. Complement activation may in fact compensate for the decreased adaptive immunity observed in normal pregnancy, and is aimed to protect the host (mother and/or foetus) from microorganisms and other potential antigens (Richani K, 2005, Tincani A, 2010).

The available data on the relationship between complement activation and growth retardation appear to be conflicting: some studies have reported that complement levels were significantly lower in mothers of SGA infants than in controls (Labarrere C, 1985) suggesting that the immunological derangement leads to placental lesions and growth restriction. On the contrary, others indicate that complement activation is associated with IUGR and other pathological outcomes of pregnancy (such as preeclampsia and recurrent spontaneous abortions) (Labarrere CA, 1986). In particular, it has been reported

that C5 (Girardi G, 2008), as well as C3a activation (Lynch AM, 2010), are crucial intermediary events (in the first trimester of pregnancy) in the pathogenesis of IUGR. In this study we found that IUGR newborns are related to down-regulation of C3, C3b, C3c, C4 complement components in UCS, as well as down-regulation of complement factor B in AF samples respectively. Our findings emphasise the central role of complement proteins modulation as a key process implicated in poor pregnancy outcomes.

1.5.3 Blood pressure alteration and IUGR

Pregnancy is a physiological condition characterised by a progressive increase of the different components of the renal renin-angiotensin system (RAS). RAS is involved not only in the regulation of blood pressure and fluid-electrolyte homeostasis, but has also a role in the human placenta development throughout gestation: angiotensin II for example inhibits human trophoblast invasion (Xia Y, 2002). Alterations in RAS have been already observed in IUGR offspring and may play a key role in the aetiology of IUGR hypertension (Zohdi V, 2007, Grigore D, 2007). Interestingly, it has been reported that maternal and foetal angiotensinogen Thr235 genotypes are associated with an increased risk of IUGR (Zhang XQ, 2003, Zhang X, 2007), as well as of preeclampsia, which is a medical condition in which hypertension arises in pregnancy (Bouba I, 2003). Here we reported that angiotensinogen is down-regulated in UCS of IUGR newborns. Further studies are needed to understand whether the decreased angiotensinogen we identified is the Thr235 variant or not, and to prove whether the data obtained are consistent with previous reports from other workers.

Another protein related to blood pressure control is kininogen, which belong to plasma kallikrein-kinin system (KKS) that plays a role not only in blood pressure (via modulation of RAS system), but also in inflammation, coagulation and pain. Kininogen is a thiol protease that circulate as two different isoforms produced by alternative splicing, high molecular weight (HK) and low molecular weight kininogen (LK). Cleavage of HK by plasma kallikrein results in kininogen heavy chain (63 kDa), light chain (58 kDa) and modified light chain (45 kDa). It has been reported that downregulation of plasma HK precedes the onset of preeclampsia (20-week gestation) (Blumenstein M, 2009).

In agreement with these observations, we found that the kininogen modified light chain (45 kDa) was down-regulated in UCS of IUGR newborns. Moreover, it has been reported that reduced levels of vasodilator substances, such as prostacyclin and kallikrein, may have a causal role in IUGR (Salas SP, 1993, Salas SP, 2007).

1.5.4 Iron and copper homeostasis, oxidative stress and IUGR

Copper and iron metabolism are known to be linked and to play a pivotal role during pregnancy: transferrin (Tf) is the main protein regulating Fe homeostasis, whereas ceruloplasmin (CP) is the major copper-carrying protein which acts as a circulating ferroxidase enzyme, able to oxidise ferrous ions to less toxic ferric forms. Together ceruloplasmin and transferrin act as an antioxidative system. Iron deficiency during pregnancy is common and has serious consequences both in the short and the long term such as foetal growth retardation and cardiovascular problems in the adult offspring. Similarly, Cu deficiency, although not so common, also has deleterious effects (Gambling L, 2003, Andersen HS, 2007). Here we shown that serotransferrin was down-regulated in UCS, while ceruloplasmin was decreased in AF of IUGR newborns.

Several studies have shown a link between altered iron homeostasis and growth retardation: a decrease in transferrin receptor 1 has been reported in IUGR placentas (Mando C, 2010); elevated maternal ferritin was related to an increased risk of IUGR (Soubasi V, 2010), while a decrease of serum concentrations of total and highly sialylated serotransferrins was detected in severe preeclampsia (Wu Y, 2003). In addition, concerning copper homeostasis, it has been demonstrated that in IUGR placentas the level of Cu was significantly reduced (Zadrozna M, 2009), and that ceruloplasmin levels were decreased in small for dates babies (Salimonu LS, 1992, Airede AI, 1998).

1.6 Conclusion

Our results support the conclusion that the IUGR condition alters the expression of proteins, some of which are involved in the coagulation process, immune mechanisms, blood pressure and iron and copper homeostasis control. The

identification of proteins, whose expression is altered by IUGR, may contribute to improve the understanding of this important clinical condition, leading to the individuation of candidate proteins that could be further investigated as biomarkers. The real importance of all of these candidates require further validation *in vitro* and *in vivo*; nevertheless, they could represent promising diagnostic targets, and shed a ray of hope for a target-oriented therapy of IUGR.

2 Chapter

MOLECULARLY IMPRINTED POLYMERS FOR PHOSPHOPROTEOMICS

2.1 Introduction

The present project is aimed at developing a pre-fractionation approach for proteomics based on selective polymeric materials, to be used prior to proteome analysis for selecting classes of proteins on the basis on homogeneous functional criteria.

2.2 A particular fraction of the proteome

Post-translational modifications (PTMs) are processing events that change the properties of a protein by proteolytic cleavage or by addition of a modifying group to one or more amino acids. Far from being mere “decorations”, PTMs of a protein determine its activity state, localisation, turnover, and interactions with other proteins. In signalling, for example, kinase cascades are turned on and off by the reversibile addition and removal of phosphate groups, and in the cell cycle ubiquitination marks cyclins for destruction at defined time points (Mann M, 2003).

Other examples of the biological effects of protein modifications are attachment of fatty acids for membrane anchoring and association, glycosylation for protein half-life, targeting, “cell-cell” and “cell-matrix” interactions. Consequently, the analysis of proteins and their PTMs is particularly important for the study of the physio-pathology (Baumann M, 2004).

2.3 Phosphoproteomics

2.3.1 Introduction

Phosphorylation is the most widespread and studied Post Translational Modification (PTM) in proteins (Collins MO, 2007).

It is involved in almost all cell functions: metabolism, osmoregulation, transcription, translation, cell cycle progression, cytoskeletal rearrangement, cell

movement, apoptosis, differentiation, regulation of the signal transduction pathways, intercellular communication during the development and functioning of the nervous system (Graves J, 1999, Hunter T, 2000, Sickmann A, 2001).

The phosphorylation/dephosphorylation process is regulated by the switch kinases/phosphatases. Kinases add a phosphate group to a receptive side chain of an amino acid; phosphatases instead catalyse the hydrolysis of a phosphoester bond (Raggiaschi R, 2005, Thingholm TE, 2009). The effect of the addition or subtraction of a phosphate group is the modification of enzymatic activity, protein-protein interaction and cellular localisation.

Phosphorylation is not a unique process: often a single protein can display more than a single site suitable for the process, often catalysed by different kinases. For example, glycogen synthase contains at least 9 phosphorylation sites, and its modulation is performed by at least 5 protein kinases acting on different sites of the protein (Nelson L, 2004). A misregulation of the phosphorylation processes can cause severe damage to the cells, leading to diseases such as cancer, diabetes or neurodegeneration (Clevenger CV, 2004, Zhu X, 2002).

The most common kind of phosphorylation in eukaryotes is O-phosphorylation, on serine, threonine and tyrosine with a ratio of 1800/200/1 (Grønborg M, 2002, Kersten B, 2006). Other sites of phosphorylation can be histidine, lysine, arginine, glutamic acid, aspartic acid and cysteine (Sickmann A, 2001), even though these are less studied due to the lability of the chemical bonds involved and the subsequent necessity to use very special techniques to analyse them.

It is estimated that 2-4% of eukaryotic genes are associated with kinases and phosphatases (there are about 500 kinase and 100 phosphatase genes in the human genome) (Manning G, 2002, Twyman RM, 2004, Venter JC, 2001). Around 100,000 phosphorylation sites may exist in the human proteome, the majority of which are presently unknown (Zhang H, 2002). The importance of studying phosphorylation was marked by the success of the cancer drug *Gleevec*, the first to inhibit a specific kinase, which gave definitely an impulse to the research on kinases and their substrates as potential drug targets (Manning G, 2002).

The comprehensive analysis of protein phosphorylation should include: identification of phosphorylated proteins and of their sites of phosphorylation, how these phosphorylations modify the biological activity of the protein and the identity of the kinases and phosphatases involved in the process.

2.3.2 A delicate analysis

Working in phosphoproteomics presents a series of hurdles in the analytical strategy.

The first issue concerns the reversible nature of phosphorylation. The study of phosphoproteins necessitates their isolation from a cell extract or a sub-cellular compartment. Subsequently to cell lysis, however, many enzymes such as phosphatases become active, determining the degradation of the proteins and detachment of phosphate groups from their sites. Also kinases can express their action, confusing the picture of which phosphate groups are biologically relevant (Raggiaschi R, 2005). Working at low temperature helps significantly in slowing down these processes, but it's not enough. In order to stop the action of these enzymes it is essential to add a specific mix of inhibitors of proteases and phosphatases to the cell extracts (Thingholm TE, 2008) while in order to inhibit kinases, EDTA, EGTA or kinase inhibitors are added. It is also important to choose an inhibition mix that does not interfere with downstream analytical methods, such as phospho-specific enrichment methods.

Another issue relates to the characterisation of phosphoproteins which is mostly performed through Mass Spectrometric (MS) methods after enzymatic digestion. The detection of phosphopeptides (FPs from now on) with MS is hampered by the presence of their non-phosphorylated partners; moreover, the efficiency of ionisation is higher for the latter species, also generally more abundant in the sample (this fact is referred to as "low stoichiometry" of phosphorylation).

It follows that enrichment methods are necessary to extract the phosphoproteins or the FPs from the sample. There are various methods to choose from, depending to the kind of sample and the aims of the study.

2.3.3 Detection of phosphoproteins

The detection of phosphoproteins in a sample still relies on optimised “classical” methods.

2.3.3.1 Isotopic labelling of phosphoproteins

One of the oldest methods used to study phosphoproteins is metabolic labelling with ^{32}P and ^{33}P. This consists of nourishing living cells or organisms with substances labelled with these radioactive isotopes which are incorporated into the synthesised proteins. Following lysis of the cells, the protein population is isolated through 1-DE or 2-DE, visualised on the gels with autoradiography or acquired digitally with Phosphorimager systems. This method is still largely employed, because of its simplicity and reliability when working with “live” systems *in vitro* or *in vivo* (Eymann C, 2007).

A comparison between the performances of ^{32}P and ^{33}P in labelling the proteins indicates that ^{33}P gives neater images and higher resolution, even though a longer exposure time is required with, respect to ^{32}P (Guy GR, 1994).

Apart from the safety and environmental implications in using radioactive isotopes, this method has other drawbacks. First of all it is not compatible with some downstream methods, such as MS. Furthermore it can only be applied on viable cells, since the radioactive isotopes have to be taken from the media and metabolised: it cannot therefore be applied to post-mortem tissues or biopsies.

In *in vivo* studies, cells are incubated with ^{32}P, however the presence of ATP reservoirs within the cells can interfere with the labelling, reducing the efficiency of the method (Steen H, 2001). Furthermore, ^{32}P is toxic to the cells, and over time can cause damage (Hu VW, 2001).

In *in vitro* studies, proteins are incubated with specific kinases in the presence of [γ-^{32}P]-ATP and, under specific conditions, the radioactive atom is incorporated into amino acid residues. Due to the unnatural presence of kinase with respect to the target protein, the phosphorylation of a different target frequently occurs instead of the natural one (promiscuity) (Graham ME, 2007).

2.3.3.2 Western Blotting employing phosphospecific antibodies

Western blotting is a quite an old technique. It is based on the selective binding of an antibody to a protein, transferred from a 1D or 2D gel to a nitrocellulose or polyvinylidene difluoride (PVDF) membrane support and subsequently revealing the antibody-marked spot with some visual method (Magi B). The key role is played by the antibody, which should be specific for the protein epitope of interest: in this case epitopes are phosphoserine, phosphothreonine and phosphotyrosine. The selectivity and affinity characteristics of the antibody are of major importance, in order to perform specific recognition and limit false positives. While excellent anti-phosphotyrosine antibodies have been developed (e.g. (PY)20, (PY)100 and 4G10 hybridoma clones), better antibodies are still needed for phosphoserine and phosphothreonine. Antibodies generated against pSer and pThr, in fact, very often necessitate use of a consensus sequence flanking the phosphoamino acid; this might be due to the lower immunogenicity of pSer/pThr compared to pTyr (Schmidt SR, 2007).

Grønborg et al. performed a test for specificity and reliability of anti-phosphoserine and anti-phosphothreonine antibodies (Grønborg M, 2002). They made a large scale differential analysis of phosphorylated proteins, succeeding in identifying phosphorylation sites and FPs not identified with dedicated prediction software. The combination of high resolution 2-DE techniques and the Enhanced ChemiLuminescence (ECL) system give improved sensitivity to the method, i.e. intensification of around 1000 times of the light emitted from a spot (Kaufmann H, 2001).

Although Western blotting is an efficient technique to reveal even small amounts of protein (10^{-10} mol), its use in quantitative analysis is limited by the variability of the amount of proteins that can be transferred to the membrane.

2.3.3.3 Direct staining of phosphoproteins

The easiest way to detect phosphoproteins in a sample is the direct staining with a phosphospecific dye after a SDS-PAGE gel. Many attempts have been made during the 1970's (Steinberg TH, 2003), but all these methods faced problems in terms of sensitivity and of non-specificity, e.g. the inability to discriminate between phosphorylated and non-phosphorylated proteins or to detect phosphotyrosine. Quite recently a novel fluorescent dye has been introduced: Pro-Q Diamond. This dye selectively binds to phosphoproteins requiring a very simple experimental protocol. The sensitivity of the stain depends on the number of phosphorylated residues of the proteins: the detection limit was 16 ng for pepsin (1 phosphorylated residue) and 2 ng for casein (8 phosphorylated residues) (Schulenberg B, 2003). Thus, the method is very useful for a preliminary screening, but still not sufficient for a comprehensive analysis of the phosphoproteome.

The dye is also compatible with MS and with Multiplex Proteomics (MP), i.e. simultaneously detecting phosphoproteins and total proteins (e.g. these latter stained with SYPRO Ruby dye) on the same 2D gel. The combination of the two staining methods permits distinguishing poorly represented but highly phosphorylated proteins from highly represented but poorly phosphorylated ones, comparing the results from the two different colorations.

2.3.3.4 Detection of phosphoproteins employing protein phosphatases

The presence or absence of a phosphate group on a protein is enough to change its pI and subsequently its position in the first dimension of a 2D gel. That's why, by employing a phosphatase enzyme, it is possible to modify the position of a protein spot on a map and thus determine its nature comparing the maps before and after the treatment. Software has been also developed that can predict the pI shift due to the addition/removal of a phosphate group, which can be of the order of 1-2 pH units (Kumar Y, 2004). As an example, Yamagata et al. exploited the specific enzymatic activity of k-phosphatase (kPPase) on phosphoserine, phosphothreonine, phosphotyrosine and phosphohistidine residues to identify novel phosphoproteins in cultured rat fibroblasts (Yamagata A, 2002).

The methods employing phosphatases, however, are not suitable for quantitative analysis, mainly because of the complexity of the analysis and the variable efficacy of the enzymatic action.

2.3.4 Selective enrichment of phosphoproteins and FPs

The identification of the PTM sites on a protein is generally performed by using MS approaches. On most occasions, the only enrichment of the sample in phosphoproteins followed by protease-specific digestion and MS analysis is not sufficient to identify the sites of phosphorylation present (due to the general low stoichiometry of the phosphorylation), thus a second enrichment step at the FP level is often also required.

Some commercial kits for phosphoprotein and FP enrichment are available, offering ease of use and reproducibility; nevertheless it has been clearly demonstrated that the methods available differ in the specificity of isolation and in the set of phosphoproteins and FPs isolated (Bodenmiller B, 2007), strongly suggesting that no single method is sufficient for a comprehensive phosphoproteome analysis. Strategies for phospho-specific enrichment are shown in Fig. 2-1.

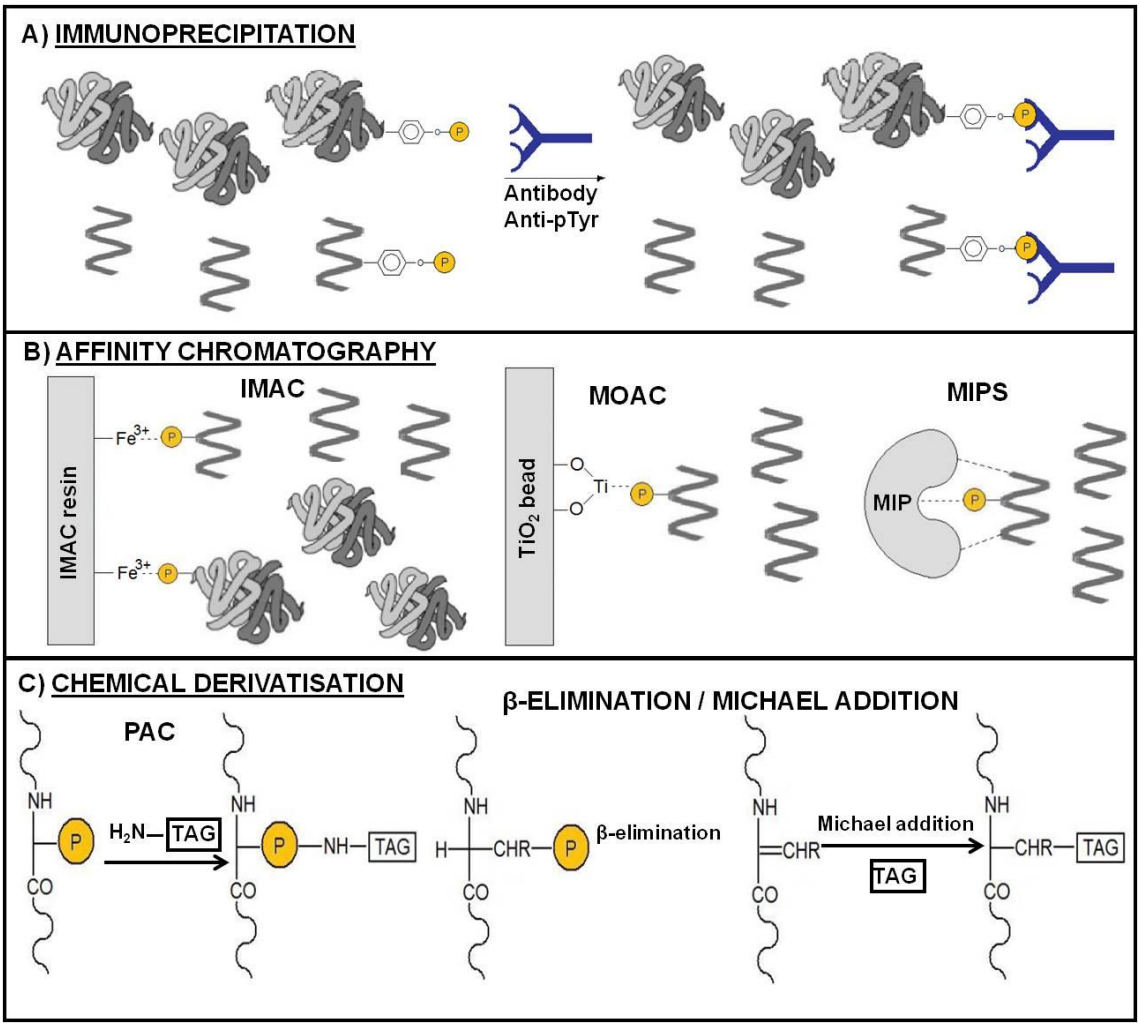

Fig. 2-1. Selective enrichment of phosphoproteins and phosphopeptides.

A) Immunoprecipitation: phosphoproteins or phosphopeptides are selectively precipitated through the use of appropriate anti-phospho antibodies; at the moment only the use of anti-pTyr antibodies has proven to be robust.

B) Affinity chromatography: a resin with immobilised chelated metal or TiO_2 can selectively bind the phosphoric group of peptides and also proteins in IMAC (Par. 2.3.4.2). A combined approach is SIMAC (IMAC + TiO_2). An alternative technique could be the use of Molecularly Imprinted Polymers (MIPs, Par. 2.3.4.10).

C) Chemical derivatisation: the phosphoric group reacts with the aminogroup of a tag in PAC or can be subjected to β-elimination and linking of a suitable tag through Michael addition (Par. 2.3.4.11).

2.3.4.1 Phosphoprotein enrichment by immunoprecipitation

Phospho-specific antibodies can be used to selectively immunoprecipitate phosphorylated proteins depending on the specificity of the antibody. As for Western blotting (see above) anti-phosphotyrosine antibodies are the most reliably and widely used in order to enrich tyrosine-phosphorylated proteins from complex mixtures.

After immunoprecipitation (IP) the phosphotyrosine enriched sample can be analysed with different analytical methods such as 1-DE and 2-DE (Stannard C, 2003).

Also in this case, variations of protein phosphorylation levels are very difficult to characterise except in combination with a particular protein labelling (Stable Isotope Labelling with Amino acids in Cell culture: SILAC, see Par. 2.3.6.1) using stable isotopes (^{13}C or ^{15}N) is used (Ong SE, 2002). This strategy allowed a quantitative and temporal investigation of tyrosine phosphorylation events of proteins involved in signalling pathways after stimulation with Epidermal Growth Factor (EGF) (Blagoev B, 2004).

2.3.4.2 Phosphopeptide and phosphoprotein enrichment using Immobilised Metal Affinity Chromatography (IMAC)

IMAC exploits the material formed through chelation of a di-, tri- or tetravalent metal by nitrilotriacetic acid (NTA), iminodiacetic acid (IDA) or Tris(carboxymethyl)ethylenediamine (TED) immobilised on a solid support, such as porous silica beads (Porath J, 1975). The most commonly used resins make use of Fe^{3+}, Ga^{3+} and Al^{3+}, even though Zn^{2+} and Zr^{4+} are used as well (Feng S, 2007).

This method is employed by routine in the enrichment of FPs prior to MS analysis, nevertheless it has some limititations; the most evident of which is its undesirable ability to bind acidic peptides. This limitation has been largely surpassed by the acidification of the medium (to protonate the carboxylic groups) (Posewitz MC, 1999) and esterification of the carboxylic moieties with methanolic HCl before the enrichment step, even if this method introduces complexity due to the variable yield of methylation.

A second limitation is the net bias of the method towards multiply phosphorylated peptides (Ficarro SB, 2002).

The method is particularly effective when used in combination with an enrichment step at the protein level. This operation can be carried out with methods such as IMAC itself, exploiting however a more suitable solid support, such as sepharose beads. Moreover, secondary interactions have to be reduced, e.g. with the use of denaturing conditions (6M urea). The detachment of the potentially many phosphate groups from the column imposes instead the use of a strong eluting buffer such as 0.1-0.2 M EDTA (Collins MO, 2005).

Other phosphoprotein enrichment methods are phosphotyrosine IP (Ficarro S, 2003), Strong Anion eXchange chromatography (SAX) (Trinidad JC, 2006), Strong Cation eXchange chromatography (SCX) (Nühse TS, 2003) and SDS-PAGE (Villen J, 2007).

2.3.4.3 Metal Oxide Affinity Chromatography (MOAC)

Metal oxide chromatography (MOAC) employs mainly Ti, Zr or Al oxides, in the form of solid or coated beads, as chromatographic media to sequestrate FPs. Many different crystalline forms and nanostructured materials have been devised (Leitner A, 2010).

The first report concerning the potential of these materials regarded the use of TiO_2-based columns to sequestrate phosphate ions from water (Ikeguchi Y, 2000).

In 2004, Pinkse et al. published a paper on the use of this material to bind FPs. They devised a 2D-LC-MS online strategy with TiO_2 beads (Titansphere) as the first dimension and RP as the second.

Acidic conditions (pH 2.9) promoted the adhesion of FPs to the first column, leaving the non-phosphorylated peptides to flow through and be analysed with nano-LC-RP- MS/MS. Basic conditions (pH 9.0) were used to elute FPs in a second step. The method was tested on a 153kDa homo-dimeric cGMP-dependent kinase, promoting the discovery a total of 8 phospho-sites, 2 of which were novel.

Larsen's group then devised an off-line strategy to bind FPs to a TiO_2 material. The use of additives such as 2,5-dihydroxybenzoic acid (DHB), phthalic acid or glycolic acid largely reduced the non-specific attachment of acidic peptides

(Jensen SS, 2007). This technique has been named HAMMOC, for hydroxy acid modified metal oxide chromatography.

A significant advantage of TiO_2 is its tolerance towards most buffers and salts used in biochemistry and cell biology laboratories. This is one of the reasons which made TiO_2 so common in large scale phosphoproteomics studies (Olsen JV, 2007). Not only has titanium oxide been employed for FPs enrichment. ZrO_2 microtips have recently been introduced as mean of FPs enrichment. This oxide shows a better performance in enriching singly phosphorylated FPs with respect to TiO_2 (Kweon HK, 2006). However, subsequent large-scale studies have also demonstrated a lower selectivity with regard to acidic peptides (Sugiyama N, 2008), suggesting the necessity for further improvements.

2.3.4.4 Sequential elution from IMAC (SIMAC)

The identification of multiply phosphorylated peptides has proven to be a hard task, mostly because of their difficult ionisation and subsequent low signal compared to singly- and non-FPs, so as to be not selected for subsequent fragmentation in the mass spectrometer.

To address this issue, in 2007 Martin Larsen's group presented an analytical strategy for sequential elution of mono- and multi-phosphorylated peptides. The sequential elution from IMAC (SIMAC) exploits the complementary characteristics of IMAC and TiO_2 in enriching the sample respectively in multiply and singly phosphorylated peptides (Thingholm TE, 2008).

In particular, the elution from IMAC in acidic conditions (pH 1.0) enriches the sample in mono-FPs, while the basic conditions (pH 11.3) elute subsequently the multi-FPs (Thingholm TE, 2008) A further enrichment with TiO_2 chromatography is needed only in the acidic fraction, because the basic one is sufficiently depleted of non-FPs.

The separation of singly and multiply FPs permits their analysis with $pdMS^3$ (phosphorylated directed fragmentation) in optimised settings for each group (Thingholm TE, 2008). This method was tested on a 120 µg whole-cell extract from human mesenchimal stem cells (hMSCs) and the results compared with those from TiO_2 enrichment alone. A total of 716 phospho-sites were identified with SIMAC, while the number was 350 with TiO_2. Moreover the number of

multiply phosphorylated peptides was also significantly increased (Thingholm TE, 2008).

Recently, an intriguing new method for the enrichment of multiply phosphorylated peptides, based on polyarginine-coated diamond nanoparticles was presented, however it has still to be tested on large scale samples and where a low amount of starting material (micrograms) is available (Chang Ck, 2008).

2.3.4.5 Magnetic beads

Starting from the TiO_2-based chemistry and with the idea of finding an easier way to perform the extraction of FPs, Chen and Chen (Chen CT, 2005) thought to conjugate the properties of magnetic materials with those of TiO_2, by coating Fe_3O_4 nanoparticles with TiO_2 through a silane bridge. The nanobeads were mixed with a tryptic digest, vortexed and captured with a magnet. The captured FPs were subsequently analysed through a laser desorption/ionisation from the inorganic particles and a run in MS. The method was named SALDI-MS, from Surface Assisted Laser Desorption/Ionisation Mass Spectrometry (Schürenberg M, 1999). There were subsequent improvements of the method, using for example Fe_3O_4@C@SnO_2 core-shell microspheres (the symbol @ means “coated by”), with which scientists were able to detect 77 phosphorylation sites in rat liver cells (Qi D, 2009).

2.3.4.6 Calcium phosphate precipitation (CPP)

In 1994, Reynolds et al. presented a strategy for FPs enrichment through Ca^{2+} ions and 50% ethanol precipitation. The precipitated peptides from a tryptic digest of casein mostly contained multiple phosphoserines (Reynolds EC, 1994).

Zhang et al. tested the strategy by using calcium chloride ($CaCl_2$), ammonia solution ($NH_3 \cdot H_2O$) and disodium phosphate (Na_2HPO_4) on a rice embryo preparation (Zhang X, 2007). The dissolved and desalted pellet was then enriched through IMAC. In total, 227 non-redundant phosphorylation sites were identified, of which 213 were on serine residues and 14 on threonine.

Through phosphate precipitation directly coupled to LC-MS/MS, Qiangwei Xia et al. identified 466 unique phosphorylation sites (379 on serine and 87 on

threonine) in post-mortem Alzheimer's disease brain tissue, 70% of which were not reported in the Phospho.ELM database (Xia QW, 2008).

In both studies no tyrosine phosphorylated peptides were identified: it is not clear if this is due to the low abundance of these residues or to the poor selectivity of the method. Anyway the method offers the advantage of being rather simple, column-free and straightforward.

Tab. 2-1. Comparison of enrichment and fractionation methods for phosphopeptides.

Method	Target	Sample type and amount	Strategy	Results	Reference	Comments
IMAC (Immobilised Metal Affinity Chromatography) IDA or NTA on a polymer matrix or magnetic beads with chelated Fe^{3+}, Ga^{3+}, Al^{3+} or other metal cations. Binding through electrostatic interaction between phosphate groups and metal cations.	protein, peptide	H1 stem cells proteins, 10 mg *D.melanogaster* lysate Kc167,10 mg	SCX-IMAC-RPLC-MS^2 (ETD-OT) SCX-IMAC-RPLC-MS^2 (LTQ-OT)	10844 phosphosites at 1% FDR 13720 phosphosites at 0.63% FDR	(Swinkels D, 2008) (Zhai B, 2008)	Proven to be effective in large scale analysis. Limited capacity and specificity, directed towards multiply phosphorylated peptides, affinity for acidic peptides
MOAC (Metal Oxide Affinity Chromatography) TiO_2, ZrO_2 or Nb_2O_5 as particles or layered on a Fe_3O_4 magnetic core. Bidentate binding between metal and phosphoric group oxygens.	peptide	HeLa lysate (amount not given) K562 lysate, 400 µg	SCX-TiO_2-RP-MS^2 &MS^3 (LIT-FT-ICR) SCX-TiO_2/Nb_2O_5-RP-MS^2 (MALDI-TOF)	6600 phosphosites, 2244 proteins at<1%FPR 622/642/834 phosphopeptides (Ti/Nb/all*) at 4%FPR	(Olsen JV, 2006) (Ficarro S, 2008)	Robust and chemically inert material, high capacity and fast absorption. Slow flow desorption, most effective for singly phosphorylated peptides.
SCX (Strong Cation Exchange) Ion Exchange Chromatography. Phosphopeptides less retained by stationary phase due to their higher negative charge	peptide	HeLa cell lysate, 300 µg HEK 293 cell lysate, 1 mg	SCX-RP-LC-MS^2&MS^3 (IT) SCX-RP-LC-MS^2 (ETD,LIT)	2002 phosphosites >5000 unique phosphopeptides 1%FDR	(Beausoleil SA, 2004) (Mohammed S, 2011)	Coelution with other acidic peptides. Useful as pre-enrichment technique

continue…

… continue

Method	Target	Sample type and amount	Strategy	Results	Reference	Comments
SAX (Strong Anion Exchange) Ion Exchange Chromatography. Phosphopeptides more retained by stationary phase due to their higher negative charge	peptide	Human liver protein digest, 100 µg *A.thaliana* membrane proteins digest, 500 µg	SAX-RPLC-MS2&MS3 (LTQ) SAX-IMAC-RPLC-MS^2 (Q-TOF)	274 Phosphosites at 0.96% FDR 299 Phosphopeptides	(Han G, 2008) (Nühse TS, 2003)	Useful for peptide fractionation. Useful as pre-enrichment technique
HILIC (Hydrophilic Interaction Chromatography) Phosphopeptides more retained by stationary phase due to their higher polarity	peptide	HeLa cell lysate, 1 mg *S.cerevisiae* total protein, 6 mg	HILIC-RP-MS & S2 (IT) IMAC-HILIC-RP-HPLC-MS^2 (LTQ)	1004 phosphosites 8764 unique phosphopeptides, 2278 proteins	(McNulty DE, 2008) (Albuquerque CP, 2008)	Coelution with other acidic peptides. Useful as pre-enrichment technique

***superimposition without redundancies of Ti and Zr detected phosphosites.**

Abbreviations: CID, Collision-Induced Dissociation; DHB, Dihydroxybenzoic acid; ECD, Electron Capture Dissociation; ETD, Electron Transfer Dissociation; FDR, False Discovery Rate; FPR, False positive rate; FT-ICR, Fourier Transform Ion Cyclotron Resonance; b-HPA, b-hydroxypropanoic acid; LIT, Linear Ion Trap; OT, Orbitrap; Q-TOF, Quadrupole-Time-Of-Flight; RP, Reversed Phase; SCX, Strong Cation Exchange; LTQ, Linear Trap Quadrupole; LCQ, Liquid Chromatography Quadrupole; IP, Immunoaffinity Purification.

2.3.4.7 Ion exchange chromatography (IC)

The simple enrichment of FPs with IMAC, TiO_2 or SIMAC has generally proven to be not productive when a deep knowledge of the phosphoproteome is required (Rigbolt KT, 2011).

A fractionation step is also needed. Chromatography techniques based on charge interaction, hydrophilic interaction or a combination of both has been employed for this purpose (Zarei M, 2011).

Anion exchange chromatography exploits the generally higher affinity of FPs for the positively charged stationary phase due to the intrinsic high negative charge carried by the phosphate group. Strong anion chromatography (SAX) has been employed both as a fractionating technique before a FPs enrichment step (e.g. with IMAC or TiO_2) (Zhang K, 2006) and also as sole fractionating technique before LC-MS/MS.

Nühse et al. for example identified more than 300 phosphorylation sites in the plasma membrane fractions of Arabidopsis thaliana using a SAX + IMAC approach (Nühse TS, 2004), while Han and co-workers identified 274 phosphorylation sites in human liver tissue extract without the enrichment step.

A drawback of this method has been reported by Thingholm et al. (Thingholm TE, 2009), who noted a strong attachment of FPs to the SAX resin, from which they are recovered with difficulty.

Its counterpart, strong cation chromatography (SCX), has been largely employed as a prefractionating technique for proteins and peptides. The pioneering work on FPs was carried out by Beausoleil et al. in 2004 (Beausoleil SA, 2004). Tryptic peptides were acidified at pH 2.7, where most of the peptides carry a +2 charge due to C-terminal lysine or arginine and the N-terminal amino group. FPs, instead, carry a reduced charge due to the phosphate group, e.g. +1 in monoFPs. The reduced affinity of the resin should therefore allow FPs to flow more easily through the column. This idea was confirmed by the results, which brought about the identification of 2000 phospho-sites in 8mg of nuclear extract of HeLa cells lysate.

Trinidad and co-workers evaluated the efficiency of SCX as a prefractionation method prior to IMAC compared to the efficiency of IMAC and SCX alone, finding a three-fold increase in FPs identified in the combined approach with respect to either single method (Trinidad JC, 2006).

The strength of SCX as a prefractionating system was further confirmed by Olsen et al., who identified 6600 phospho-sites in 2244 proteins in EGF-stimulated HeLa cells through SCX + TiO_2 (Olsen JV, 2006). In more recent reports 23000 and 36000 phosphorylation sites have been identified respectively with SCX followed by IMAC and TiO_2 respectively (Huttlin EL,

2010, Rigbolt KT, 2011). This remarkable increase in number of detected phospho-sites is mainly due to instrumental and software improvements (Zarei M, 2011).

It remains to be assessed whether the fractionation/enrichment approach can be suitable in samples where a small amount of starting material is available.

2.3.4.8 Hydrophilic Interaction Chromatography

Hydrophilic interaction chromatography (HILIC) is a separation technique for biomolecules (Alpert AJ, 1990). The method relies on the interaction of the analytes, e.g. peptides, with a neutral stationary phase through hydrogen bonding. They are eluted from the column with a mobile phase gradient, decreasing in organic content, according to their polarities (hydrophilicity).

McNulty and Annan introduced this method as a prefractionation step before IMAC (McNulty DE, 2008). They tested the FPs enrichment capacity of HILIC compared to SCX and IMAC alone, as well as the fractionation ability of HILIC before and after IMAC treatment. The analysis of 1 mg of tryptic digest of HeLa cells demonstrated the prefractionation ability of the method. The use of IMAC prior to HILIC in fact gave a high level of nonspecific binding due to non-FPs, while the reversed approach improved the selectivity towards FPs to more than 99%.

ERLIC (Electrostatic Repulsion - Hydrophilic Interaction Chromatography), or Ion Pair normal phase, is a newly developed chromatographic method able to enrich and fractionate FPs in a single step (Alpert AJ, 2008).

At pH 2.0 the C-termini and the carboxylic side chains of Asp and Glu are neutral, thus the peptides are generally positively charged and are not retained by a positively charged stationary phase. The presence of a phosphate group, however, reduces the net charge of FPs. This is not enough to overcome the overall repulsion for the stationary phase due to the basic residues, however an organic mobile phase, e.g. acetonitrile 70%, promotes their hydrophilic interaction within the column. The attraction for the column is enhanced in multiply phosphorylated peptides.

Zarei et al. showed a higher efficiency of ERLIC compared to SCX and HILIC in the fractionation of multiply phosphorylated peptides (Zarei M, 2011) more strongly retained by the stationary phase.

In a recent article (Chen X, 2011) Xi Chen et al. compared the FPs profiles obtained from a HeLa cell lysate by using 4 HPLC methods after a phosphor-enrichment with IMAC. Even though with any of the four methods (SCX, HILIC, ERLIC with volatile and non-volatile solvents) 4-5000 peptides could be identified, the combination of all the methods gave a total number of 9069 unique FPs, with a considerable amount of non-overlapping unique FPs. The four methods are thus complementary to fully cover the phosphoproteome.

2.3.4.9 Hydroxyapathite (HAP)

Firstly introduced by Tiselius and co-workers in 1956 (Tiselius A, 1956), hydroxyapathite (HAP) chromatography has been very popular until the 1980s, when new matrices were introduced. HAP is a crystalline form of calcium phosphate with the formula $Ca_{10}(PO_4)_6(OH)_2$, which binds FPs by virtue of both anionic and cationic interactions. In particular, Ca^{2+} binds phosphoric groups, and more strongly than it does other acidic groups. Binding to the matrix is thus proportional to the number of phosphor-groups on the peptides and can be exploited for their sequential elution according to their degree of phosphorylation. Mamone et al. (Mamone G, 2010) exploited this material to analyse a tryptic digest of standard proteins. The advantages of HAP are the low cost of the material and the possibility to elute stepwise the peptides according to the degree of phosphorylation. Yet the system has to be tested on more complex biological samples.

2.3.4.10 Molecularly Imprinted Polymers (MIPs)

Recently (Helling S, 2011), Sellergren's group has proposed a method for the depletion of phosphotyrosine containing peptides based on Molecularly Imprinted Polymers (MIPs). FP imprinting was performed using an epitope approach (Nishino H, 2006), i.e. using a part of the analyte of interest (in this case the N- and C-protected phosphotyrosine) as template to prepare a MIP able to fish for FPs. The Solid Phase Extraction analysis showed an 18-fold

preferential retention for phosphorylated angiotensin II with respect to the non-phosphorylated peptide, a preference not shown by the non-imprinted polymer. Moreover, the material showed a preference for a triply phosphorylated peptide over a monophosphorylated one, showing opposite behaviour comparing to TiO_2 material. Of course a more extensive analysis and improvements are needed in order to tackle more complex samples.

2.3.4.11 Chemical derivatisation strategies

Chemical derivatisation strategies exploit the typical properties of phosphate groups on peptides, such as the lability of the phosphoester bond and the subsequent easy substitution of phosphate with a nucleophilic tag.

A different widely used approach is the methyl esterification of the carboxylic groups, notoriously competitive with the phosphate groups due to their negative charge (Fig. 2-2).

2.3.4.11.1 Methyl esterification of carboxyl-groups

In the IMAC strategy carboxylic groups influence the elution of FPs, due to their charge being attracted by the positively charged metal of the resin. For this reason their esterification could prove useful. Ficarro et al. first applied this strategy for the analysis of the cell extract from *Saccharomyces cerevisiae* (Ficarro SB, 2002) through the IMAC approach: 383 sites of phosphorylation were detected with this method. Some characteristics of this approach have already been depicted in Par. 2.3.4.2 and not will be further analysed.

Methyl esterification can be also exploited as a mean of isotopic labelling (with CH_3OH and CD_3OH for two different cellular states) for quantification purposes (Ficarro S, 2003).

2.3.4.11.2 Biotin tagging by β-elimination and Michael addition

Many chemical derivatisation strategies have been devised to displace the phosphoryl group and bind a tag to the “naked” peptide. One of these methods (Jaffe H, 1998) relies on the β-elimination of the phosphate from phosphoserine and phosphothreonine producing dehydroanaline and β-aminobutyric acid respectively. These products can be directly detected using tandem MS or

derivatised, for example by Michael addition of a reactive thiol and subsequent binding of a tag.

One common tag is biotin, notoriously having great affinity for avidin, ideal for immobilisation to an affinity column (Oda Y, 2001).

This technique shows the limits of not being applicable to phosphotyrosine containing peptides and of the occurrence of side reactions such as tagging of non-phosphorylated serines.

Zhou et al. (Zhou H, 2001) proposed another method of derivatisation applicable to all residues, even if it involves many steps and has not been tested on complex samples yet.

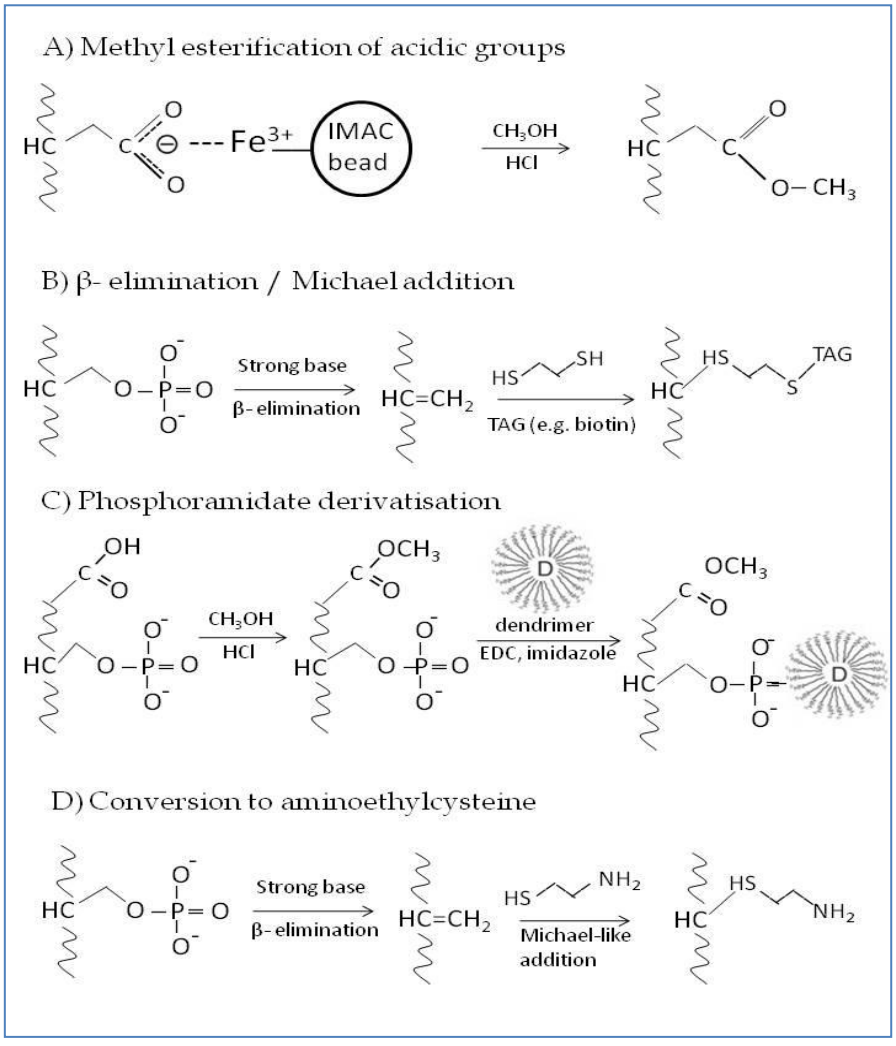

Fig. 2-2. Chemical derivatisation methods for phosphorylation capture and analysis.

A) IMAC suffers of not specific binding of acidic peptides to the resin. Esterification of carboxylic groups with Methanol/HCl is a strategy to overcome this problem.

B) In presence of a strong base the β-elimination at phosphoserine and phosphothreonine produces dehydroanaline and β-aminobutyric acid. These can be derivatised with a thiol through a Michael-like addition and a tag can be added. If the tag is biotin, its affinity with avidin can be exploited.

C) FPs can be derivatised to phosphoramidates after esterification of carboxylic groups. If a dendrimer is employed the derivatised peptides can be separated through size-selective methods.

D) β-elimination and Michael-like addition of cysteamine converts phosphoserine and phosphothreonine in lysine analogues that specific enzymes leave in the C-terminus.

2.3.4.11.3 Phosphoramidate conversion

In 2005 Aebersold's group proposed a derivatisation procedure based on the carboxyl protection through methyl esterification followed by conjugation to a soluble polymer with phosphoramidate chemistry (PAC) (Tao WA, 2005).

The mixture of peptides is first converted to the corresponding methyl esters. In this step two cellular states can also be differentially labelled for quantitative analysis. Subsequently, the methylated peptides are combined and allowed to react with EDC, imidazole and a polyamine dendrimer. Phosphopeptides are converted into the corresponding phosphoramidates, easily separated from the non-FPs through size selective methods. FPs are recovered with a brief acid hydrolysis and sent to MS analysis.

When coupled with pervanadate stimulation and an initial antiphosphotyrosine protein precipitation step, this method allowed the identification and quantification of all known, plus previously unknown phosphorylation sites in 97 tyrosine proteins in Jurkat T cells.

A modification of this method was proposed (Bodenmiller B, 2007), exploiting the reaction of the phosphate groups with cystamine and a reducing agent instead of the dendrimer. The –SH group of cystamine react with maleimide-activated glass beads, immobilizing the FPs on a solid phase. This method

allowed the identification of 229 FPs in the cytosolic proteome of *Drosophila melanogaster* Kc167 cells without any pre-enrichment step.

2.3.4.11.4 Conversion to aminoethylcysteine

Even after a good preconcentration step it is difficult to exactly assign a phosphorylation site, due to the lability of the phosphate group, often lost during the backbone fragmentation in a MS collision, and to the intrinsic low abundance of phosphorylated peptides.

To address this problem, Knight et al. (Knight ZA, 2003) devised a derivatisation method based on β-elimination and Michael addition of cysteamine to convert phosphoserine and phosphothreonine into aminoethylcysteine (Aec) and β-methylaminoethylcysteine respectively. Due to the resemblance of Aec to lysine, the use of proteases that recognise this amino acid (e.g. Lys-C and lysyl endopeptidase) cleaves proteins leaving it at the C-terminus. The system works also with β-methylaminoethylcysteine and permits the identification of the exact site of phosphorylation.

The limitation of the method is racemisation in the addition step, converting only 50% of the phosphoamino acids in the appropriate enzyme substrate. In the case of multiply phosphorylated peptides this fact greatly increases the complexity of the peptidic mix arising from the protein.

2.3.4.12 Comparison of enrichment methods

From this survey of enrichment methods it is evident that no single technique is able to tackle the entire phosphoproteome. Some methods work in the direction of enriching only some species, such as the antibodies for phosphotyrosine or the combination β-elimination/ Michael addition selective for phosphoserine and phosphothreonine. Other methods, such as calcium precipitation, SAX, SCX and HILIC, work better as pre-separation techniques to reduce sample complexity before more specific enrichment methods such as IMAC, MOAC, SIMAC and PAC.

Every enrichment technique presents advantages and disadvantages, but also different specificities. Usually, MOAC is more specific for monophosphorylated peptides, due to the strong affinity for multiply phosphorylated ones, and their lack of elution. On the contrary, IMAC is more specific for multiply

phosphorylated peptides, but has a lower capacity and selectivity when used with highly complex samples. The combined approaches, such as SIMAC, seem to be promising but reveal the necessity of a pre-enrichment step (Han G, 2008).

A systematic comparison of methods was made by Bodenmiller and co-workers (Fig. 2-3). They examined the reproducibility, specificity and efficiency of IMAC, PAC and two protocols for TiO_2 chromatography: $pTiO_2$ (phthalic acid in the loading buffer to quench nonspecific binding) and $dhbTiO_2$ (2,5-dihydrobenzoic acid, quencher too) (Bodenmiller B, 2007). Each method was tested through the injection of 1.5 mg of tryptic digest from cytosolic fractions from *Drosophila melanogaster* cells. The authors found very good reproducibility for all the methods, making them suitable for quantitative analysis. Moreover, none of the methods was able to reveal the entire phosphoproteome, but they showed partially overlapping results between each other.

In general a simple and straightforward strategy is desired, with few preparation steps and little sample handling in order to avoid loss of FPs. It is of course true that the amount of starting material and the expertise of the people performing the extractions are also critical factors. For this reason detailed protocols are needed (Goto H, 2007, Thingholm TE, 2009).

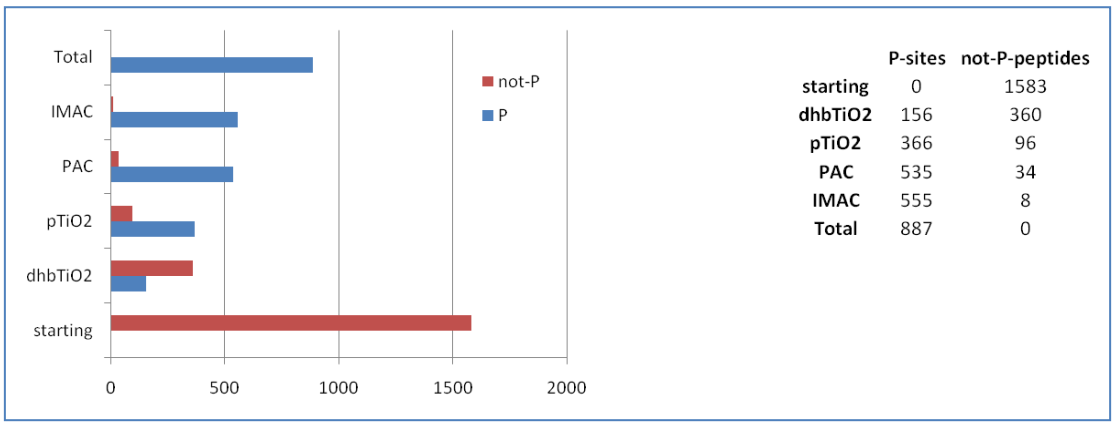

	P-sites	not-P-peptides
starting	0	1583
dhbTiO2	156	360
pTiO2	366	96
PAC	535	34
IMAC	555	8
Total	887	0

Fig. 2-3. Comparison of phosphorylation enrichment methods. The graph shows the efficiency and selectivity of IMAC, PAC and TiO_2, applied on a tryptic digest of a cytosolic protein extract of *D. melanogaster* cells (Bodenmiller B, 2007). In the starting material no FPs were detected, while the best selectivity in terms of P vs. not-P sites was IMAC.

2.3.5 MS-based strategies for phosphoproteome analysis

Mass spectrometry has become the preferential method for peptide and protein identification following the separation steps, also in the PTM analysis (Domon RB, 2006).

The first step of a typical MS analysis consists of the cleavage of a single protein or a protein mixture by a dedicated enzyme, usually trypsin, which preferentially cleaves the peptide bonds after arginine or lysine. Moreover, the tryptic fragments' weights are in the range 700-3500 Da, a size suitable for MS analysis.

The peptides are thus separated by nanoLC and vaporised/ionised through an ESI source. Their mass is evaluated and a second fragmentation, generating MS/MS spectra, permits to evaluate also their amino acid sequence. This is possible because of the higher lability of the bonds between amino acids. Depending on the position of the cleavage along the peptide chain, the MS/MS fragments are classified in a,b,c (starting from the N-terminal) or x,y,z (starting from the C-terminal) according to Roepstorff and Fohlman (Biemann K, 1988, Roepstorff P, 1984) (Fig. 2-4). Only the highest abundance peptides are submitted to MS/MS. This creates a hurdle in phosphoproteomics, because of the lower abundance and difficult ionisation of FPs compared to the co-present non-FPs, thus introducing the need for an enrichment step, as explained in Par. 2.3.4.

The information about the peptide sequence is submitted to database-digging software such as MASCOT (Perkins DN, 1999) or SEQUEST (Ducret A, 1998), which explore protein databases to find a sequence match with previously annotated proteins and rank the correlations through a probability score.

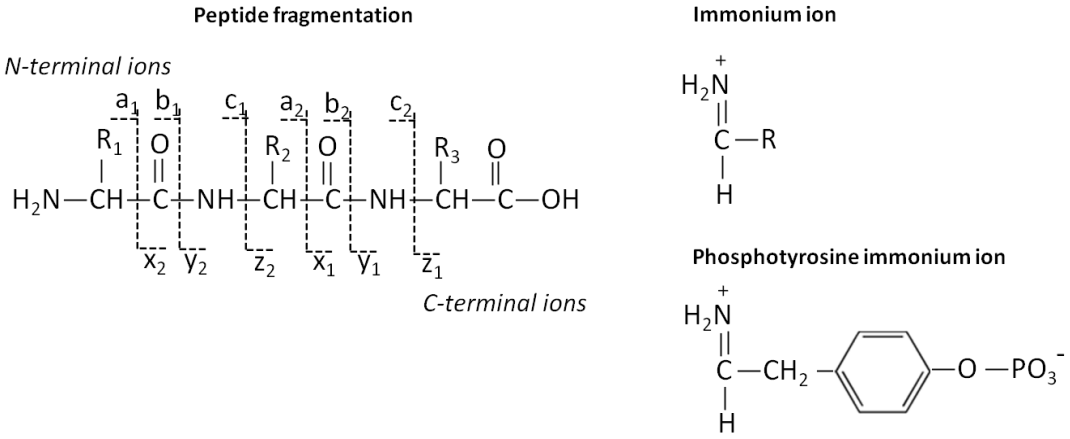

Fig. 2-4. Common nomenclature of peptide fragment ions. The peptide fragmentation in MS/MS mostly breaks the inter-residue bonds to generate fragment series. CID generates preferentially y and b ions, while mostly z and c ions are originated by ECD and ETD. Phosphotyrosine immonium ion is diagnostic of tyrosine phosphorylation.

2.3.5.1 Collision Induced Dissociation (CID)

The most established method to induce a secondary fragmentation in peptides is the collision induced dissociation (CID). Basically, the peptide ion collides with an atom of an inert gas (He or Ar) which transfers its kinetic energy, subsequently redistributed between the atoms bringing about the breaking of bonds. When a phosphoserine or phosphothreonine is present in the peptide sequence, the phosphoester bond is by far the most labile, thus a neutral loss of phosphoric acid H_3PO_4 (98 Da) takes place, generating dehydroalanine or dehydroaminobutiric acid respectively. Given that most of the energy is employed to break the phosphoester bond, far less energy is available for the subsequent fragmentation of the peptide chain (Larsen MR, 2005).

This drains information when the identification of the phosphate group position is needed: only the bare presence or absence of a phosphate is assessed.

To overcome this issue several strategies have been applied. The first one is the introduction of a tertiary fragmentation, specifically directed towards peptides where the loss of phosphate is detected. This strategy is named pdMS^3 (phosphorylation directed MS^3) (Reinders J, 2005). The information due to the alternative fragmentations of the precursor ion are lost in this case, but they can be retained through another approach, named Multi-Stage Activation

(MSA) (Steen H, 2001). In this case the ion trap, filled with the selected ion coming from neutral loss, is filled again with the original peptide and both are fragmented at the same time, giving rise to a more information-rich superimposed MS^2 / MS^3 spectrum.

Partial neutral loss also happens at phosphotyrosine residues, which lose a HPO_3 group (80Da) resulting in a characteristic phosphotyrosine immonium ion at m/z 216 (Fig. 2-4). The phosphoester bond is however more stable in this case, thus the information collection is not compromised. Steen et al., for example, used the diagnostic fragment at m/z 216 for the selective detection of phosphotyrosine-containing peptides in chicken ovalbumin and murine MAP-kinase 2 (Steen H, 2001).

2.3.5.2 Electron capture dissociation (ECD)

The limitation of poor fragmentation of the peptide backbone in the presence of a phosphate group was overcome in 1998 with by the use of a new fragmentation strategy. Electron Capture Dissociation (ECD) is a method developed by Zubarev and colleagues to improve the fragmentation of multiply charged protein and peptide ions (Zubarev RA, 1998). These ions readily capture a thermal electron (<0.2 eV), which induces a non-ergodic fragmentation, i.e. without vibrational energy redistribution such as in CID. The result is fragmentation occurring mostly at S-S and N-C_α backbone bonds, leaving the PTM bonds intact. The generated ions are c and z type (Fig. 2-4) (Kleinnijenhuis AJ, 2007). The method has some drawbacks, such as a greater affinity for disulphide bonds and difficult fragmentation of N-terminal proline residues, which have two bonds to break. Moreover it can only be carried only with expensive FT-ICR instruments (costing around 1$ million) to generate the static magnetic field for the electrons, which reduces the wide-scale adoption of the technique.

2.3.5.3 Electron transfer dissociation (ETD)

The effort to find an ECD-like method without the need for expensive instruments brought about the advent of ETD (Electron Transfer Dissociation). In this approach the electron is transferred to multiply charged peptides (charge >2+) through a radical anion with low electron affinity, such as anthracene or

azobenzene (Schroeder MJ, 2005). The method can be implemented on linear quadrupole ITs, with their inherent drawbacks of reduced resolution and accuracy (Syka JE, 2004). Molina et al. (Molina H, 2007) carried out a large scale analysis of human embryonic kidney 293T cells, identifying 1435 phospho-sites, 80% of which were novel. Moreover, they identified 60% more FPs with ETD compared to CID, mainly due to the 40% more fragment ions. It has to be remarked the little overlap between the two fragmentation techniques, that was exploited to develop an integrated approach. Since ETD works better with high charge peptides, Lys-C was thought to give better results than trypsin, cleaving the peptides only at C-terminal lysine. Surprisingly the results did not match expectations, probably due to the higher number of missed cleavages in the tryptic lysate (Molina H, 2007). Another way to generate highly charged peptides was attempted by Larsen et al, who added 0.1% m-nitrobenzyl alcohol (m-NBA) to the LC-MS solvent (Kjeldsen F, 2007). This approach increased the predominant charge from 2+ to 3+, improving the ETD results. The approach is currently being tested on more complex samples. Another fact to remark is the evolution of the software, born for the CID approach, in the direction of meeting the features of spectra generated by new enzymes and fragmentations (Kim S, 2010), (http://www.matrixscience.com).

Tab. 2-2. Comparison of fragmentation methods. All the methods show good results with a class of peptides, suggesting that an integrated approach CID/ECD or CID/ETD could be more effective (Molina H, 2007).

	Fragmentation agent	Generated ions	Instruments	Pros	Cons
CID	Inert gas (He, Ar)	y, b	ESI-MS	Better fragmentation of low charge peptides (2+)	Fragmentation mostly at the phosphogroup
ECD	Thermal electron	z, c	FT-ICR	Fragmentation only along the peptide bond	Need of expensive FT-ICR

ETD	Low electron affinity anion (e.g.anthracene)	z, c	IT, Q-TOF	Fragmentation only along the peptide bond	Less sensitive than CID

2.3.6 Quantitative approaches for phosphoproteome analysis

In order to take a dynamic picture of the phosphorylation events in a particular pathway, it is desirable to monitor which sites are phosphorylated and to which extent following a stimulus. To achieve this goal some quantification methods are available and can be classified on the basis of the analysis step in which the quantitative information is generated: a differential isotopic label can be introduced in the cell culture, e.g. with labelled amino acids (SILAC), in the protein mixture (ICAT), in the enzymatic digestion (^{18}O labelled water), or in the peptide mixture (iTRAQ), otherwise, in label-free experiments, the quantitative information is extracted at the MS level (Fig.7). A thorough review about quantitation strategies has been published by Bantscheff et al. (Bantscheff M, 2007).

		LEVEL			
		CELL	PROTEINS	PEPTIDES	MS
METHOD	**SILAC**	**X**			
	^{18}O		**X**		
	ICAT		**X**	**X**	
	iTRAQ			**X**	
	LABEL-free				**X**

Fig. 2-5. Strategies for quantitative analysis of protein phosphorylation. An isotopic label can be introduced in different moments of the analysis or not at all, in label-free experiments.

2.3.6.1 Metabolic labelling

Metabolic labelling was first described in 1999 (Oda Y, 1999). In 2002 Mann and co-workers introduced the term Stable Isotope Labelling by Amino acids in Cell culture (SILAC) and used it for quantitative analysis of protein

phosphorylation in 2003 (Ibarrola N, 2003). The typical experiment consists of growing a cell population in a medium containing an essential amino acid labelled with a stable isotope (^{15}N or ^{13}C), and growing in parallel another cell population in a medium on non-labelled amino acid. Usually labelled arginine and lysine are used, in order to ensure that every peptide from one culture contains a label after tryptic digestion. After several doublings, the cells are harvested from both cultures, and the protein extracts mixed together. After proteolysis, peptides can be analysed by MS and differences in the abundance of a peptide in the two cell extracts are shown through the different heights of two mass shifted peaks.

Recently, with this method Olsen et al.(Olsen JV, 2006) reported the most comprehensive analysis of the effects of EGF stimulation on phosphoproteome dynamics in HeLa cells. This strategy has allowed the drawing of some detailed maps of time-resolved signalling pathways (Goss VL, 2006, Olsen JV, 2010). The major limitation of SILAC stays in the cost of labelled amino acids.

2.3.6.2 Protein and peptide labelling

Post-biosynthetic labelling of proteins and peptides is performed by chemical or enzymatic derivatisation *in vitro*.

Enzymatic labelling exploits the incorporation of ^{18}O atoms from isotopically-enriched water during protein digestion. Trypsin and Glu-C introduce two heavy oxygen atoms, resulting in a 4 Da mass shift, generally sufficient for the differentiation of isotopomers. This method has been applied for quantitative proteomic purposes (Dengjel J, 2007), but complete labelling is difficult to obtain.

Chemical modification can be carried out at the protein or peptide level by introducing a tag on a chemically reactive side chain of an amino acid (Ong et al., 2005), in practice only cysteine and lysine are used for this purpose. A group of labelling reagents targets the N-terminus and the ε-aminogroup in the lysine side chain. They mostly exploit N-hydroxysuccinimide (NHS) chemistry or other active esters and acid anhydrides, such as in the Isotope-Coded Protein Label (ICPL) (Schmidt A, 2005), isotope Tags for Relative and Absolute

Quantification (iTRAQ) (Ross PL, 2005), Tandem Mass Tags (TMT) (Thompson A, 2003) and acetic/succinic anhydride (Zhang X, 2002).

iTRAQ is a commercially available reagent, allowing the evolution of biological systems to be followed over multiple time points. It was used, for example, to quantify 222 tyrosine phosphorylation sites across seven time points following EGF stimulation (Wolf-Yadlin A, 2007).

Carboxylic groups of side chains of aspartic and glutamic acid as well as of the C-termini of peptidic chains can be isotopically labelled by esterification using deuterated alcohols, for example d_0 and d_3 methanolic HCl (Goodlett DR, 2001). This reaction is particularly interesting, since methylation is also a step used in the IMAC enrichment method to reduce non-specific binding of acidic peptides to the resin (Par. 2.3.4.2).

General drawbacks of the chemical derivatisation methods are the production of undesired side products that negatively influence the quantification results and the cost of some of the reagents.

2.3.6.3 Absolute quantification using internal standards

The use of isotope-labelled internal standards in the field of proteomics is known with the name AQUA: Absolute QUAntification of proteins (Gerber SA, 2003).

The simplest protocol requires adding a known amount of a stable isotope-labelled peptide to the protein digest and a comparison of its signal in the mass spectrum with respect the areas of other peaks (Pan S, 2005).

There are some drawbacks with this approach. Firstly the high dynamic range of concentrations of peptides makes finding an appropriate concentration of standard for every analyte a difficult task; secondly, it is likely that a peptide isobaric with the standard will be found in the peptide mixture, therefore limiting its specificity. These problems, however, have been addressed with the approach called Multiple Reaction Monitoring (MRM) (Kirkpatrick DS, 2005), in which the triple quadrupole MS monitors the masses of both the peptide and its fragments during the experiment. The combination of retention time, peptide mass and fragment mass practically eliminates ambiguities, extending the dynamic range to 4-5 orders of magnitude (Bondarenko PV, 2002). The real

values determined by quantification through the AQUA approach are naturally biased by the manipulation of sample before adding the standard: the amount of protein determined may not therefore reflect its actual expression level in the cell.

2.3.6.4 Label-free quantification

There are two approaches for label-free quantification of proteins. The first one relies on the measurement of the area of an MS peak of a peptide related to a protein: the increase of this area means also an increased amount of the protein. This approach is called eXtracted Ion Chromatogram (XIC), because a single ion peak area is extracted from a plot of signal intensities against time in the chromatogram (Wang G, 2006). Signal intensities of the same peptide in different experiments is then compared to extract quantitative information, for example the stoichiometry of phosphorylation (Steen H, 2005).

The other approach measures the amount of peptides generated from a protein: the greater the amount of protein the more are the tandem-MS generated peptides. Relative quantification is thus achieved by comparing the number of spectra generated from a protein in different experiments. It is necessary to perform a normalisation, for example depending on the protein mass, therefore creating Protein Abundance Indexes (PAIs) (Rappsilber J, 2002). The relationship between the number of peptides observed and the amount of protein has been found to be logarithmic in nature (emPAI) (Lu P, 2007).

2.3.7 Non-MS approaches to elucidate cellular signalling networks

2.3.7.1 Antibody-based approaches

In order to monitor previously identified phosphorylation sites, arrays employing phosphospecific antibodies have been used to investigate dozens of phosphorylation sites simultaneously (Belluco C, 2005). The general hurdle to overcome with these techniques is the limited availability of dedicated antibodies, however further improvements could extend the use of microarray technology in phosphoprotein studies (Schmelzle K, 2006).

Methods were developed to monitor the phosphorylation status of tyrosine (Gembitsky DS, 2004) and the kinetics of phosphorylation (Khan IH, 2006) proteins in a multiplex format.

In order to evaluate the phosphorylation dynamics on a cellular scale, flow cytometry approaches have also been devised to monitor up to 11 phosphorylation events in parallel (Sachs K, 2005). Again, the main limitation of this approach is the availability of suitable fluorescently-labelled antibodies.

2.3.7.2 Interaction of phosphoproteins and phosphorylated sites

The phosphorylation-related events include also protein-protein interactions in the cell signalling network. To investigate these phenomena, Jones et al. (Jones RB, 2006) devised a protein array to study the binary interactions between 61 fluorescent-labelled, tyrosine phosphorylated peptides from EGFR receptors with approximately 150 SH2 and PTB domains. By measuring the fluorescence at different titration points they determined the K_D values for every peptide-receptor couple.

Another approach was followed by Yaoi et al. (Yaoi T, 2006), who immobilised SH2 domains on microspheres to extract interacting proteins and phosphoproteins from a complex mixture of different cell lines.

Both approaches revealed new insights in the cellular signalling networks.

2.3.7.3 Kinase screening in peptide and protein arrays

Peptide microarrays consist of synthetic peptide sequences deposited onto glass slides or attached to a derivatised surface, usually in triplicate, with peptides having substitutions in the phosphorylation sites as controls. The *in vitro* phosphorylation reaction is performed in the presence of radiolabelled ATP, the array exposed to a film and the image captured. The method assumes that phosphorylation of peptides should be in most cases similar to that of the same sequence in the intact protein, due to the fact that many phosphorylation sites are in accessible and flexible regions of the protein structure (Nühse TS, 2004). Collins et al. used this approach to investigate the phosphorylation of synaptic proteins, finding 28 unique phosphorylation sites (Collins MO, 2005).

Phosphorylation *in vitro* will naturally differ from that observed *in vivo*, but the screening can select and give priority to some phosphorylation sites for further investigation.

The same approach can be used for immobilised proteins or protein domains.

Ptacek et al. (Ptacek J, 2005) immobilised yeast proteins in high density arrays (4400 proteins in duplicate) on glass slides. They screened 87 kinases, finding that each kinase recognised up to 256 substrates, with an average of 47 substrates per kinase. These data allowed the construction of a global kinase-substrate interaction network. There is of course a concern about non-specific phosphorylation, but also the perspective of a high throughput analysis for mapping phosphorylation networks.

2.3.8 Bioinformatics

The knowledge discovery process in proteomics has been greatly boosted in recent years by the introduction of new bioinformatics tools.

Widely used phosphoproteomics databases are, for example: PhosphoSite (Hornbeck PV, 2004) containing around 100,000 non-redundant phosphorylation sites (as well as other modifications, given that the cell signalling is not exclusively phosphocentric), and Phosida (Gnad F, 2007), containing temporal phosphorylation data from cell stimulation in time-course experiments.

These databases not only permit mining of the data, but also the interpretation of data in the context of biological regulation, diseases, tissues, subcellular localisation, protein domains, sequences, motifs, etc. (http://www.phosphosite.org)

2.3.9 Conclusion about phosphoproteomics

Phosphoproteomics is a rapidly growing field, owing its evolution to the importance of protein phosphorylation in many biological processes and its alteration in many diseases.

The analysis is usually performed with MS-based methods, supported by enrichment steps at the protein or peptide level. The improvements in MS have

been enormous, with increases in resolution, mass accuracy, greater dynamic range, sensitivity and speed, driving progress in this field.

Of course the evolution of bioinformatics methods must also be mentioned, with the development of suitable software for literature mining, prediction algorithms, post-analysis annotation and so on. The aim of phosphoproteomics is not only to find phosphorylation sites, but also to monitor the dynamics of phosphorylation following stimuli to characterise completely signalling networks.

Nowadays the phosphoproteome of highly complex samples has been tackled (Trinidad JC, 2006, Villen J, 2007), but further development of the methods, including bioinformatics tools capable of integrating complex databases, is needed for a more thorough knowledge of the mechanisms of phosphorylation networks.

2.4 Molecularly Imprinted Polymers

A relatively recent technique to develop affinity receptors that could find interesting applications in pre-fractionation is the molecular imprinting of polymers (MIPs). MIP permits the synthesis of materials with designed recognition properties, by exploiting a “template” mediated synthesis, where the “template” is a molecule of interest. During the polymerisation, functional monomers assemble around the template either via reversible covalent bonds (Wulff G, 1991). or via non-covalent interactions such as hydrogen bonds, ionic bonds, hydrophobic interactions, van der Waals forces, etc. (Sellergren B, 1989, Mosbach K, 1994).

The pre-assembly is locked-in by crosslinking, forming a polymer with embedded molecular depressions, or clefts, complementary to the template in size, shape and functionality.

Molecular imprinting of small molecules such as herbicides, metal ions or amino acids has been successfully accomplished and numerous papers express the potential of such materials as sensors (Mosbach M, 2001, Piletsky SA, 2001), chromatography beds (Cormack PAG, 2007, Kempe M, 1994), synthetic antibodies (Ye L, 2001, Vlatakis G, 1993), synthetic enzymes (Leonhardt A, 1987, Wulff G, 2002) or systems for controlled drug release (Sellergren B, 2005,

Cunliffe D, 2005). These studies demonstrate that imprinted materials might exhibit very high selectivity and even enantioselectivity (Leonhardt A, 1987).

2.4.1 MIPs for proteins and peptides

A particular challenge concerns the development of MIPs to recognise large target molecules such as peptides and proteins. The complexity of such a process has been attributed to several reasons (Bossi A, 2007). Firstly, large molecules are not able to diffuse through the polymeric network, limiting the use of crosslinking that proved to be successful in preserving the imprints. Secondly, the relative non-rigidity of proteins and the ease of unfolding may lead to the formation of poorly-defined recognition sites. Thirdly, the poor solubility of most proteins in most organic solvents limits the synthesis conditions.

In addition, large molecules possess a number of potential binding groups and the choice of the functional monomers plays a crucial role in determining the quality of the imprints. In the case of large biomolecules, it was suggested to exploit the biochemical information on the natural receptors of the target proteins, as a starting point in the decision process towards the definition of the monomer composition (Cecìlia A, 2005).

To overcome the limitations posed by the complexity of protein structure, it has been proposed to imprint only part of the protein. The short peptide sequences selected are called epitopes (Rachkov A, 2001).

Regarding peptides imprinting, Kempe and Mosbach (Kempe M, 1995) demonstrated chiral separation of small peptide sequences with highly cross-linked MIPs. In another study, Kempe (Kempe M, 2000) developed a MIP able to recognise Z-oxytocin peptide, despite the selectivity of rebinding not being remarkable. In a more systematic study, carried out by Klein et al. (Klein JU, 1999), imprinting of tripeptide sequences was assayed, with specific binding of approximately 30% for the print sequence and much lower binding of other similar sequences. Finally, Hart and Shea (Hart BR, 2001) proposed metal affinity (Ni^{2+}) to histidine terminal groups and obtained a quite successful peptide imprinting.

A different strategy to address the issue of protein imprinting consists of surface aided imprinting, which attempts to produce successful imprints by depositing the proteins onto a support, thus taking advantage; 1) of the orientation of the template, and 2) of the problems linked to template entrapment. Proteins have been at first deposited on/immobilised to a solid surface and subsequently the polymer has been grown (Shi HQ, 1999, Bossi A, 2001, Shiomi T, 2005).

A wide choice of supports and materials have been used: polysiloxanes in the very early study of Glad et al. (Glad M, 1985) who demonstrated the successful imprinting of the glycoprotein transferrin and later Lulka et al. (Lulka MF, 2000) created a MIP for ricin over silica particles. Fluoro-polymer films were prepared by Ratner and co-workers (Valdes TI, 2008) by radio frequency glow discharge plasma deposition to form films around proteins deposited on a mica surface previously coated with disaccharide molecules. Bossi et al. (Bossi A, 2000) coated polystyrene microtiter plates with a thin layer of a stable conjugated polymer (aminophenyl boronic acid) polymerised in the presence of various protein templates. Rick and Chou (Rick J, 2006) imprinted proteins in thin layers of aminophenylboronic acid and used micro-calorimetry measurements to assess the enthalpy changes associated with the rebinding and the imprinting efficiency.

To address the issue of the non-compatibility of proteins with organic solvents, some research groups have been working with imprinting in aqueous conditions, thus with water compatible polymers, which ensures solubility and conformational stability of the proteins. Despite these advantages, the results are still limited. Hjerten and co-workers (Hjertén S, 1989) pioneered the use of lightly crosslinked polyacrylamide hydrogels as the polymeric matrix. Hirayama et al. (Chao GT, 2008) incorporated charged functional groups (either positive or negative) in polyacrylamide gels in an attempt to achieve a better recognition. Ou et al. (Ou SH, 2004) combined polyacrylamide simultaneously with two functional monomers, methacrylic acid and 2-(dimethylamino)ethyl methacrylate.

A drawback of hydrogel protein imprinting is the amount of protein template that remains entrapped in the MIP is generally high, due to diffusional limitations and

the collapse of local polymeric environments. In an attempt to ameliorate the rigidity of the hydrogel architecture, Gou et al. (Zhu WP, 2008) developed a composite material, by insertion of imprinted polyacrylamide gel into the pores of chitosan or modified chitosan beads. The results achieved with protein and peptide imprinting still needs to be improved, if the final goal of these materials is to compete with natural receptor systems. MIP methods for the selective recognition of specific peptide sequences and/or proteins remain a significant challenge.

2.4.2 MIPs for proteome with particular attention to phosphopeptides

Of particular interest in the proteome era is the use of MIPs for phosphopeptide (FP) enrichment prior to proteomic MS analysis.

The works published deal quite exclusively with the preparation of MIPs for inorganic phosphates, and are mostly targeted to agricultural/waste water subjects (Kugimiya A, 2008, Yamazaki T, 2001). Sellergren's group tried to develop MIP-based method for FP enrichment, achieving a positive indication of its feasibility, but still showing limited success (Emgenbroich M, 2008). Most of the papers dealing with phospho-groups converge in assessing the effectiveness of urea and thiourea monomers for the capture (Helling H, 2011).

2.5 Synthesis and characterisation of MIP nanoparticles selective for peptides containing phosphotyrosine

The purpose of this research line is to develop a selective material for pTyr-containing peptides. The application of such material will be primarily as an alternative to antibodies, largely employed in phosphoproteome analysis to selectively enrich phosphoproteins and/or phosphopeptides present in a protein or peptide mixture. The advantage of MIPs "plastic antibodies" with respect to their natural counterparts is the potentially much lower cost of their production plus resistance to harsh conditions (pressure, temperature, basic or acidic pH) and in general a higher stability: they can also be used in both aqueous and organic solvents (Ye L, 2008). In perspective, the nano size of MIPs (nanoMIPs) further points out their use *in vivo* to selectively target a phosphorylated epitope, for which a suitable plastic antibody has been devised. This opens the exciting

scenario of diagnostic and therapeutic molecules specifically tailored to the target by using itself as a model template. What stands as a remarkable example of biomimicry is the recent report of Kenneth Shea and colleagues, who devised a plastic antibody specifically directed against the peptide mellitin, a component of bee venom. These MIP nanoparticles worked *in vivo,* by removing a lethal amount of toxin from the circulation of mice and significantly reduced their mortality (Hoshino Y, 2010).

The first step of the nanoMIP synthesis process consists of optimisation of the production method for nanoparticles, which should be of suitable size and polydispersity. Their use *in vivo* requires for example a size ideally less than 100nm (similar in size to viruses) to penetrate living cells and translocate within the body (Perrault SD, 2009) moreover a Polydispersity Index, associated with a homogeneous population (see next paragraph), should be ideally less than 0.2 (Müller RH, 1993), (www.malvern.com). It should be noted that the definitions of Polydispersity Index (PdI) used in Dynamic Light Scattering theory (see next paragraph) and in polymer science are different, moreover in the latter the values of PdI are equal to or greater than 1. A particle size similar to the size of proteins greatly facilitates the diffusion of the protein itself through the matrix, reducing the time of analysis (Wulff G, 2012, Ye L, 2001). The same method of synthesis is subsequently used in the presence of the template molecule to create its print in the nanoparticle. The molecule is then removed and the remaining cavities maintain the ability to rebind the same molecule due to their size and chemistry (functional groups of monomers oriented to compatible groups of the template during the polymer synthesis). The imprinted and non-imprinted nanoparticles are then tested for specificity, selectivity and capacity (see Par. 2.5.4).

Between the different ways of nanoparticles synthesis, photopolymerisation seemed to be a valuable choice. This method employs a starter triad composed of a coloured antenna, a reducer and an oxidiser, that in this case were methylene blue (MB), toluenesulphinic acid (TSIA) and diphenyliodonium chloride (DPIC), as suggested by Righetti et al. (Lyubimova T, 1993) (Fig. 2-6). The described mechanism employs MB, activated by light, to form an excimer

with TSIA, by which it is reduced. TSIA radical is an active one, while MB radical is passive, thus terminates the polymerisation chain reaction. The purpose of DPI is to boost the reaction through $MB^{\cdot}$ oxidation to form an active radical $Ph^{\cdot}$ while regenerating MB* (Fig. 2-6) (Kim D, 2004). This method permits control to be exerted over the polymer growth through a light-switch-like mechanism.

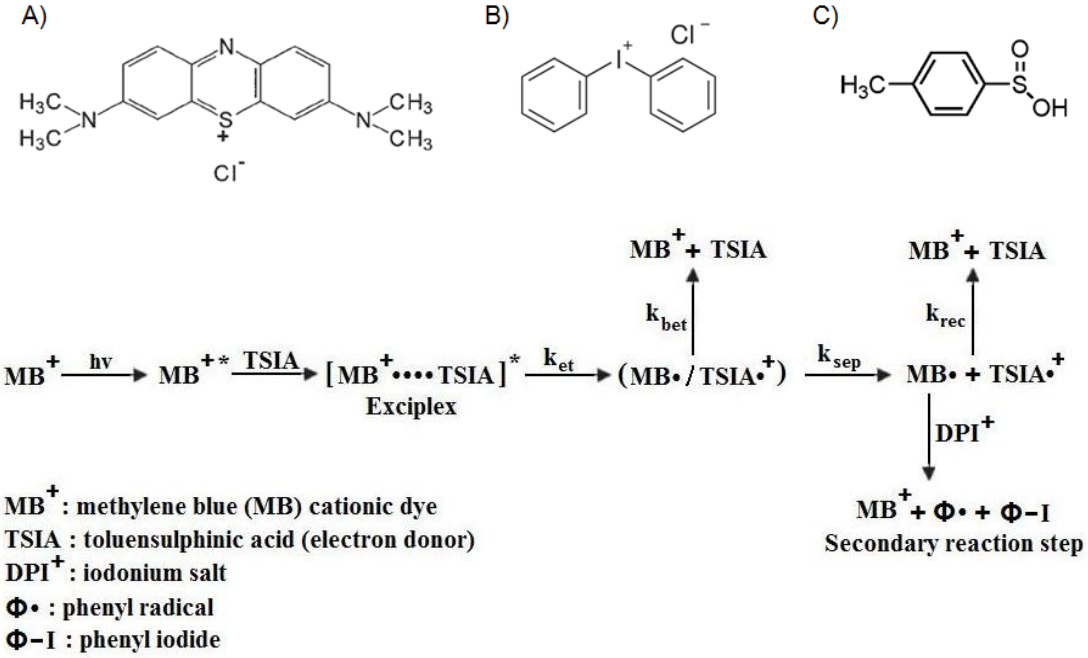

Fig. 2-6. Chemical structures of the three compounds employed as starter triad for the photopolymerisation process: A) Methylene blue (MB), B) Diphenyliodonium chloride (DPI), C) Toluenesulphinic acid (TSIA), plus the mechanism of activation: a visible-light-induced electron transfer initiation process (Kim D, 2004).

2.5.1 Techniques for nanoparticles physical characterisation

The physical characterisation of the nanoparticles can be made with a variety of different techniques, addressed to understand and control their synthesis and applications. Some widely used techniques are Transmission Electron Microscopy (TEM), Scanning Electron Microscopy (SEM) and Atomic Force Microscopy (AFM), mainly devoted to visualise the particles and thus explore their morphology plus other characteristics such as aggregation. Other techniques such as X-ray Photoelectron Spectroscopy (XPS) evaluate instead

surface characteristics such as chemical composition or electronic state (Rudenberg HG, 2010). Dynamic Light Scattering (DLS) is another widely used technique that allows an assessment of particle size, particle number and tendency to aggregation to be made (Berne BJ, 2000). In this project AFM and DLS were used.

2.5.1.1 Dynamic Light Scattering

Dynamic Light Scattering (DLS) is a physical technique employed to determine size distribution of particles in solution. The physical phenomenon at its basis is Rayleigh scattering, i.e. the diffusion of light in all the directions from particles smaller than the wavelength of light used (Chu B, 1992). When the light is coherent and monochromatic, such as that from a laser, constructive and destructive interference occurs between the light emitted by the scatterers. This interference changes continuously with time due to Brownian motion of the particles. By detecting the light intensity at a certain angle (usually 173° respect to the light source) an intensity fluctuation can thus be observed. This fluctuation is faster for fast-moving particles, thus depends on the size of the particles, on their shape and on the temperature and viscosity of the medium. The fluctuation is mathematically expressed by the autocorrelation function (Eq. 2-1):

$$g^2(q;\tau) = \frac{\langle I(t)I(t+\tau)\rangle}{\langle I(t)\rangle^2}$$

Eq. 2-1.

where $g^2(q;\tau)$ is the autocorrelation function at a particular wave vector q, and delay time τ, and I is the intensity. At short time delays τ the correlation is high, meaning that intensity changed very little due to the little motion of the particles. At longer time delays the correlation between intensities instead decreases exponentially and depends essentially on the diffusion coefficient of the particles (Fig. 2-7).

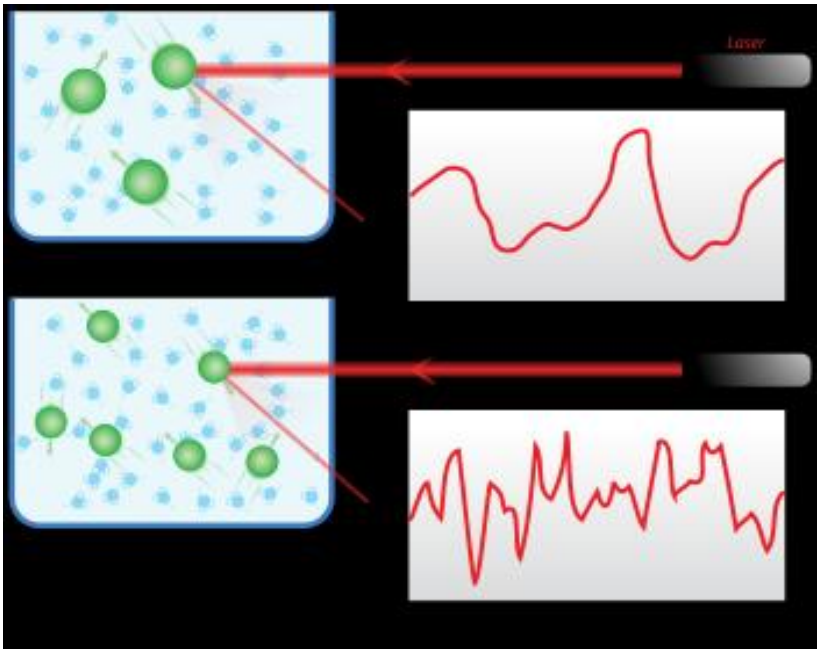

Fig. 2-7. Representation of the principle of Dynamic Light Scattering. Smaller particles give quicker fluctuations of a scattered laser light, as evidenced by the correlation function (picture taken from: Wikipedia).

Information about the particles can be extracted by fitting the decay of the autocorrelation function. Numerical methods are employed for the purpose and they are essentially based on an assumed size distribution. For example, if the sample is monodisperse the decay is fitted well by a simple exponential (Eq. 2-2):

$$g^1(q;\tau) = \exp(-\Gamma\tau)$$

Eq. 2-2.

where Γ is the decay rate. The translational diffusion coefficient can be derived from the wave vector *q* and Γ according to Eq. 2-3:

$$\Gamma = q^2 D$$

Eq. 2-3.

where q is (Eq. 2-4):

$$q = \frac{4\pi n_0}{\lambda} \sin\left(\frac{\theta}{2}\right)$$

Eq. 2-4.

where λ is the incident laser wavelength, n_0 is the refractive index of the sample and θ is the angle at which the detector is positioned respect to the light source. Through the Stokes-Einstein equation (Eq. 2-5) is therefore possible to derive the hydrodynamic radius of the particles:

$$D = \frac{k_B T}{6\pi\,\eta\, r}$$

Eq. 2-5.

In this equation D is the diffusion coefficient, k_B the Boltzmann's constant, T the temperature, η the viscosity of the medium and r the radius of the spherical particle.

In most cases, however, the sample is polydisperse and the autocorrelation function is the sum of exponential decays of all the species in solution (Eq. 2-6):

$$g^1(q;\tau) = \sum_{i=1}^{n} G_i(\Gamma_i)\exp(-\Gamma_i\tau) = \int G(\Gamma)\exp(-\Gamma\tau)\,d\Gamma$$

Eq. 2-6.

In this case a commonly used mathematical model to describe the system is the cumulant method. This model introduces the variance of the system as Polydispersity Index (Eq. 2-7):

$$g^1(q,\tau) = \exp\left(-\bar{\Gamma}\tau\right)\left(1 + \frac{\mu_2}{2!}\tau^2 - \frac{\mu_3}{3!}\tau^3 + \cdots\right)$$

Eq. 2-7.

where $\bar{\Gamma}$ is the average decay rate and $\mu_2/\bar{\Gamma}^2$ is the second order Polydispersity Index.

It should be noted that DLS gives information on the hydrodynamic diameter of spherical particles, meaning that it models the behaviour of irregularly shaped

objects as if they were spheres. Moreover the measured size considers also the layer of solvent or ions around the particles. This information is therefore generally different from what can be measured for example with electronic microscopy such as TEM, that “sees” the naked particles (Egerton R, 2005).

2.5.1.2 Atomic Force Microscopy

The Atomic Force Microscope (AFM) is an instrument belonging to the class of the Scanning Probe Microscopes (SPM). Its spatial resolution is of the order of nanometres making it particularly useful in the study of nanoparticles, including both their morphology and their interactions with partners.

The AFM consists of a silicon or silicon nitride cantilever, with a tip of the radius of curvature of the order of nanometres (Fig. 2-8). The tip moves along the surface to sample all the relief and depressions. Interactions of the probe with the surface are: mechanical contact force, van der Waals forces, capillary forces, chemical bonding, electrostatic forces, magnetic forces, Casimir forces, solvation forces, etc (Giessibl FJ, 2003).

The area scanned is typically of the order of microns in the x and y-dimensions. A laser beam impinges on the upper surface of the cantilever, the light being reflected and detected by a diode microarray. The detected ray of light gives rise to an electric signal which is digitised, elaborated and transformed in a reconstructed image of the surface (topography) by dedicated software.

There are basically three ways of profiling a surface: contact mode, non-contact mode and tapping mode.

In contact mode the tip passes close to the surface keeping the interaction between them constant. The force must be repulsive in this case, in order to avoid snapping of the tip.

In non-contact mode there is no contact between the surface and the tip: the cantilever oscillates at a frequency slightly higher than its resonance frequency with an amplitude of few nanometres (< 10 nm). The interaction with the surface tends to decrease the frequency of oscillation, but a feedback loop system keeps it constant by modifying the average distance between tip and surface.

In intermittent contact, or tapping mode, the oscillation has a greater amplitude (100-200nm) and the tip intermittently touches the surface. This technique is well suited for soft matter, such as lipid bilayers.

With AFM it is also possible to evaluate interaction forces by binding a ligand to the tip and scanning its interaction with a receptor immobilised to the surface (Butt H, 2005).

AFM measurements in liquid samples are also possible, thus preserving the nature of labile molecules such as proteins (Hinterdorfer P, 2006).

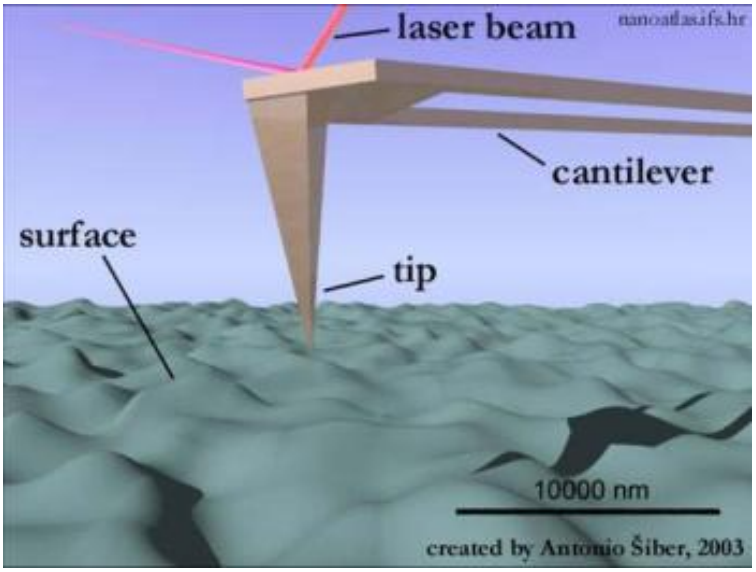

Fig. 2-8. Representation of how Atomic Force Microscopy works. A nanometric size tip moves along a surface surveying relieves and depressions. A laser beam is reflected by the upper part of a cantilever that bears the tip and impinges to a detector. This information is interpreted by a software that reconstructs the surface topology (picture taken from: http://www.nanoatlas.ifs.hr).

2.5.2 Nanoparticle synthesis

Different recipes were followed to find the best approach to produce nanoparticles of suitable size (diameter ideally less than 100nm) with low PDI and high yield in their production.

A Fmoc-protected phosphotyrosine (Fmoc-pTyr) was used as template, as suggested by Sellergren et al. (Emgenbroich M, 2008).

Regarding the choice of functional monomers, positively charged monomers could be thought of as effective for the phosphate group. Their choice is

however not advisable because of the bias introduced in imprinting: charged monomers are attracted by the charges independently of the molecule structure, i.e. the sequence of amino acids in the case of peptides and/or proteins (Emgenbroich M, 2008).

Instead, the functional monomers chosen were 2-hydroxyethyl methacrylate (HEMA) and 1,3-diallylurea (DAU), while cross-linkers were *N*,*N*'-methylene-bis-acrylamide (BIS) and 1,4-bis(acryloyl)piperazine (BAP).

HEMA showed good properties in producing hydrogels, and is extensively used in commercial products, such as contact lenses, for its swelling properties (Karlgard CCS, 2003). The production of a soft polymer such as a hydrogel is necessary when working with proteins, to permit their internalisation in the polymer matrix (Brahima S, 2002). Diallylurea has similar properties to the suggested monomers for phosphotyrosine imprinting, as recently reported by Sellergren et al. (Emgenbroich M, 2008). BIS is a commonly used cross-linker for protein/peptide imprinting and for gel electrophoresis matrixes (Kryscio DR, 2012, Righetti PG, 2005). BAP shows instead better mechanical characteristics (keeping the shape) respect to BIS, and this is the reason for its choice in protein imprinting (Kirat KE, 2009). The synthesis was carried out in two solvents. The aqueous solvent was 100mM, pH 8.20 Tris buffer, that does not show interference with the binding with pTyr (like a more "physiological" PBS) but at the same time is largely employed in proteomics (Rabilloud T, 2010).

2.5.3 Bulk synthesis

Finally, the bulk synthesis (Tamayo FG, 2007) out of two recipes, chosen according to AFM and DLS results, was carried out. Rebinding experiments were performed on this material in order to collect preliminary information in standardised conditions before using nanoparticles. The method consists of the preparation of a solid polymer subsequently crushed and sieved to give micron-sized particles.

2.5.4 Functional characterisation of MIPs

Functional characterisation of MIPs consists of an assessment of the following characteristics:

capacity: amount of template that can be bound by 1 mg of polymer;

specificity: affinity of the template for MIP, expressed by the equilibrium dissociation constant K_D;

selectivity: ability of MIP to discriminate between the template and other substrates;

imprinting factor: ratio between the amount of substrate bound from MIP and from its non-imprinted counterpart (Non-Imprinted Polymer, NIP).

MIPs ability to rebind the template from its solutions can be evaluated as follows. A fixed amount of MIP and of NIP is put in contact with increasing concentrations of template molecule. After incubation the amount of free substrate [A] is evaluated in solution, therefore assessing its amount bound to the resin [AB] by subtracting it from the initial amount of substrate [A]i (Eq. 2-11). A graph of substrate bound [AB] respect to the ratio [AB]/[A] (Scatchard plot, Fig. 2-9) permits an evaluation of the affinity constant (K_D) of the substrate for the polymer (Eq. 2-9) and the maximum amount of guest bound (the capacity, or the apparent maximum number of binding sites [B]max) given respectively by the slope and the intercept of the Scatchard equation (Eq. 2-10). In an ideal 1:1 interaction between substrate and homogeneous binding sites of the polymer (Eq. 2-8), K_D is defined as follows:

$$A + B \rightleftharpoons AB$$

Eq. 2-8.

$$K_D = \frac{[A]\,[B]}{[AB]}$$

Eq. 2-9.

$$\frac{[AB]}{[A]} = \frac{[B]_{max} - [AB]}{K_D}$$

Eq. 2-10.

$$[A] = [A]_i - [AB]$$

Eq. 2-11.

The nature of the binding sites is never uniform and more kinds of guest-binding sites exist (Matsui J, 1995). This characteristic is evidenced by a non-linear graph such as Fig. 2-9, whose slopes give the value of two K_Ds.

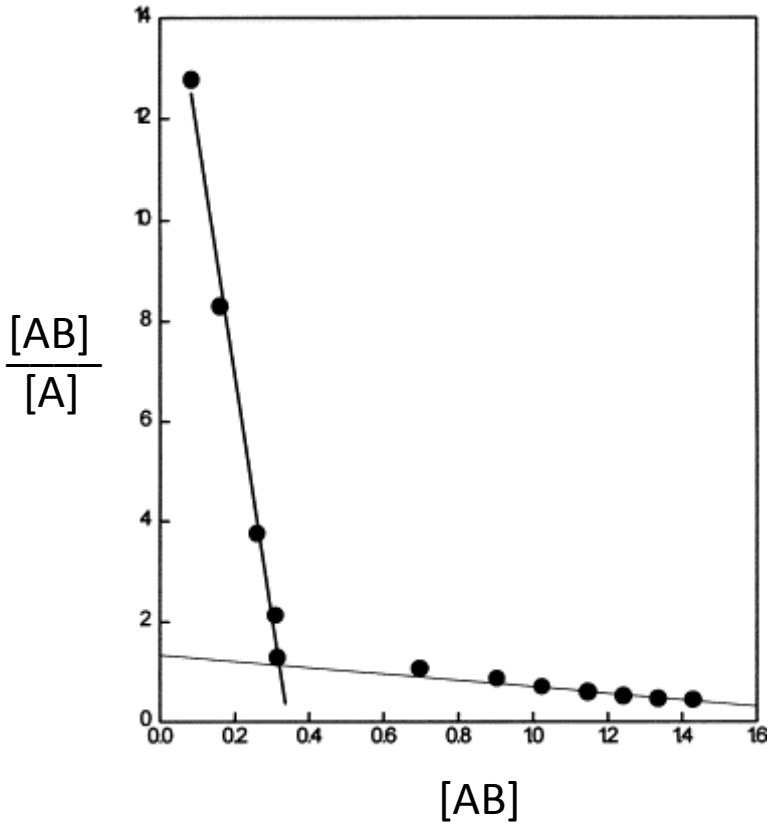

Fig. 2-9. Scatchard plot to estimate the binding nature of the polymer. Two kinds of binding sites are evidenced by two different slopes in the graph.

2.5.5 Materials and methods

2.5.5.1 Materials

Reagents 2-hydroxyethyl methacrylate (HEMA), 1,4-bis(acryloyl)piperazine (BAP), toluensulphinic acid (TSIA), diphenyliodonium chloride (DPI) and methylene blue (MB) were purchased by Fluka (Steinheim, DE); 1,3 diallylurea (DAU) was an Aldrich product obtained from Sigma-Aldrich (St.Louis, MO,

USA); *N*,*N*'-methylene-bis-acrylamide (BIS) was a BioRad product (Hercules, CA, USA).

2.5.5.2 Small-scale synthesis of the nanoparticles

The list of recipes related to the synthesised polymers is reported in Tab. 2-5 (Par. 2.5.6.1). Fmoc-protected phosphotyrosine was added in some samples at the ratio 1:2 with respect to the functional monomer, as suggested by Sellergren et al. (Emgenbroich M, 2008).

Synthesis was carried out either in 100mM Tris buffer pH 8.20 or in acetonitrile/water 9:1 v/v. All syntheses were made in a final volume of 3 mL and in 6 mL HPLC vials with silicon reversible cap. Samples were treated with an argon flow for 10 min prior to illumination. Irradiation was performed with a VIS transilluminator lamp (40W).

2.5.5.3 Dialysis of the nanoparticles

After the synthesis samples were dialysed straightaway by using a dialysis tubing cellulose membrane (Sigma) with cut-off 12000 Da. MilliQ water was used as receptor medium. Dialysis took place for 48h with 3 changes of solvent. The sample volume/receptor medium ratio was 1:400.

2.5.5.4 Size analysis of the nanoparticles

The size of the synthesised nanoparticles was determined by the Dynamic Light Scattering (DLS) technique on a Zetasizer Nano ZS instrument equipped with 633nm laser and DTS Ver. 4.10 software package (Malvern Instruments Ltd., Worcestershire, UK). All samples were sonicated for 20 min prior to analysis and filtered on a 0.45 µm filter to eliminate large sedimenting particles. A 180 sec equilibration time was needed for the sample to reach ambient temperature (25 °C) after sonication. The mean value of the particle size was calculated from the results of three measurements on each sample. The light was collected at an angle of 173° with respect to the incident laser light. Size measurement results are reported in Tab. 2-6.

2.5.5.5 Yield of the nanoparticles

The yields of the syntheses were calculated for the samples, as reported in Tab.2.3. Ten ml of solution containing nanoparticles were dialysed and freeze

dried in pre-weighed Falcon polypropylene tubes. Yields were calculated with respect to the initial amount of monomers.

2.5.5.6 Atomic force microscopy of the nanoparticles

AFM measurements were made on four samples produced with four different recipes, chosen according to DLS measurements. The best for size and PdI recipes were chosen, considering however to not exclude monomers, cross-linkers or solvents that could furnish interesting morphological or aggregation characteristics. The instrument was an NT-MDT Solver P47H-PRO AFM. Mica dishes (Ted Pella) were freshly peeled with sticky tape before sample deposition. Samples (not dialysed) were sonicated for 5 min, diluted 1:1 (v:v) with ethanol and 50 µl of the mixture was deposited on mica dishes. After 5 min the dishes were washed by dipping into 0.20 µm filtered MilliQ water and dried for 20 sec with an air flow. Images were collected at room temperature (20 °C) in semi-contact mode using NT-MDT NSG11 silicon cantilevers with Au backside coating, with a minimal applied force at a scan frequency of 0.5-2 Hz with 512 pixel resolution.

2.5.5.7 Large-scale synthesis of the nanoparticles

Eight recipes were produced on a larger scale. The recipes were chosen according to DLS measurements as explained in Par. 2.5.5.6. Moreover a choice of a variety of monomers, cross-linkers and solvents could offer interesting characteristics of rebinding. The recipes chosen are listed in Tab. 2-3. The reactions were carried out in borosilicate glass bottles in a final volume of 100 mL after argon bubbling for 10 min. Irradiation was performed with a VIS transilluminator lamp (40W) under gentle stirring (250rpm).

Tab. 2-3. Samples produced on large scale (W=Tris 100mM, pH8.2; A/W=ACN/Water 9:1 v/v).

Recipe	Monomers	% T	% Cm	Time polym.	mmol (mg) Cross linker	mmol (mg) monomer	mmol (mg) Fmoc-pTyr	solvent
F	HEMA/BIS	1	80	5'	6.30 (974)	1.58 (206)		W
F+pTyr	HEMA/BIS	1	80	5'	6.30 (974)	1.58 (206)	0.79 (382)	W
H1	HEMA/BAP	1	67	5'	4.55 (884)	2.27 (148)		W
H1+pTyr	HEMA/BAP	1	67	5'	4.55 (884)	2.27 (148)	1.13 (532)	W
L3	HEMA/BIS	0.2	80	18h	1.26 (195)	0.32 (41)		A/W
L3+pTyr	HEMA/BIS	0.2	80	18h	1.26 (195)	0.32 (41)	0.16 (77)	A/W
M3	DAU/BIS	0.2	80	18h	1.26 (195)	0.32 (45)		A/W
M3+pTyr	DAU/BIS	0.2	80	18h	1.26 (195)	0.32 (45)	0.16 (77)	A/W

2.5.5.8 Dialysis of the nanoparticles

After synthesis the samples were dialysed straightaway by using a dialysis tubing cellulose membrane (Sigma) with cut-off 12000 Da. MilliQ water was used as dialysate. Dialysis took place for 96 hours with 12 changes of solvent. The sample volume/dialysate ratio was 1:50.

2.5.5.9 Electrodialysis of the nanoparticles

Dialysed nanoparticles were electrodialysed for 4h with a set current of 500 V, 5.0 mA, 1 W. Samples were put in a 3500 KDa cut-off SpectraPor membrane with addition of 10mM histidine (Sigma). Anodic buffer was 1 L of a 10 mM histidine solution. After electrodialysis samples were dialysed again for 4 h against 1 L of MilliQ water with the same membrane.

2.5.5.10 Concentration of the nanoparticles

Electrodialysed samples were concentrated with Centriprep YM30 centrifugal filter devices (30 kDa cut-off, Millipore). The applied centrifugal force was 1500 x g for 15 min, according to manufacturers' instructions. An initial volume of 100 mL was reduced to 10 mL.

2.5.5.11 Yield evaluation of the nanoparticles

One mL of every concentrated solution, corresponding to 10 mL of initial nanoparticles solution, was put in previously weighed 6 mL HPLC vials to quantify the presence of particles. Samples were freeze-dried for 24h and the weight measured with a Ohaus Explorer balance.

2.5.5.12 Standard bulk synthesis

Two recipes were chosen to produce bulk polymers and perform rebinding experiments. This operation was made to gain an idea of the binding properties of the material under standardised conditions.

Solvents: acetonitrile, methanol and hydrochloric acid, used to clean the synthesised polymers from Fmoc-pTyr, unreacted species and pTyr after rebinding, were purchased from Carlo Erba (Milano, Italy).

A 500 mg of HEMA/BIS 80%C and DAU/BIS 80%C were dissolved in 8 mL Tris buffer 20 mM, pH 8.20 (final total monomers content 6%T) and divided in two 6mL HPLC vials to prepare the non-imprinted polymers (NIPs, controls).

In a second aliquot Fmoc-pTyr was added with a molar ratio 1:2 with respect to the functional monomer to prepare the molecularly imprinted polymers (MIPs, see Tab. 2-4). Methylene blue, diphenyliodonium chloride and toluenesulphinic acid were subsequently added to all the aliquots to achieve a final concentration of 100µM, 50µM and 1 mM respectively before being treated with an argon flow for 5 min prior to illumination. Irradiation was performed with a VIS transilluminator lamp (40W). Aluminium foil was used to wrap the reaction environment and thus illuminate the reactor from every direction. The illumination duration was 4h for HEMA/BIS and 16h for DAU/BIS. The recipes were as follows:

Tab. 2-4. Recipes of the synthesised bulk polymers.

Recipe	Monomer (mg / µmol)	Cross-linker (mg / µmol)	Fmoc-pTyr (mg / µmol)
HEMA/BIS (NIP)	87 / 668	413 / 2679	
HEMA/BIS + Fmoc-pTyr (MIP)	87 / 668	413 / 2679	161 / 334
DAU/BIS (NIP)	93 / 663	407 /2641	
DAU/BIS + Fmoc-pTyr (MIP)	93 / 663	407 / 2641	160 / 331

2.5.5.13 Polymer cleaning and drying

After the synthesis the polymer samples were cleaned through a series of washing steps to remove the unreacted monomers, initiators and Fmoc-pTyr. The solvent used were in order: acetonitrile/water 1:1 v/v, acetonitrile, methanol/HCl 0.1M 1:1 v/v.

The synthesised HEMA/BIS NIP and MIP were put in 50 mL Falcon tubes and a volume of solvent 4 times the amount of polymer was added, mixed on an orbital rotor and centrifuged at 3000 x g for 20 mins, at 25°C. The synthesised DAU/BIS NIP and MIP, after the solvent addition, were divided into aliquots in 2 mL Eppendorf tubes, mixed on the orbital rotor for and centrifuged at 10000 x g for 20 minutes, at 25°C. This different treatment was needed because DAU/BIS MIP would not sediment at low speed. The supernatants were then drained, analysed with UV-VIS spectrometry and replaced with fresh solvent. The graphs of the cleaning steps are reported in Fig. 2-43 and Fig. 2-44. Absorbance was measured with an Unicam UV2 UV-VIS spectrometer, at wavelength λ = 214 nm in quartz cuvettes, to evaluate the presence of double bonds (unreacted monomers).

After cleaning, samples were spread on cellulose paper and left at ambient temperature (25 °C) for 72 h until dryness. The weights of the dry polymers are reported in Tab. 2-10. Yields were calculated respect to the initial amount of monomers.

2.5.5.14 pTyr calibration curve

In order to evaluate the presence of pTyr in rebinding experiments two calibration curves were made. Firstly pTyr (Sigma) was dissolved in PBS buffer + 0.02% Tween-20 at increasing concentrations. The first curve was produced with an Unicam UV2 UV-VIS spectrometer, at wavelength λ = 272 nm in quartz cuvettes. The second one was obtained with a Jasco FP8200 spectrofluorimeter, in quartz cuvettes, at λ_{exc} = 265 nm and λ_{em} = 297 nm. All the measurements were made in triplicate.

2.5.5.15 Rebinding experiments

After extensive cleaning the polymers were subjected to rebinding experiments to evaluate capacity (μg substrate bound by 1mg of polymer) and affinity (K_D). Due to the limited amount of DAU/BIS polymer, only HEMA/BIS polymer was subjected to these measurements.

Ten mg aliquots of HEMA/BIS NIP and MIP were put in contact with 2 ml of increasing concentrations of pTyr and gently shaken on an orbital rotor for 4 hours. Then the solutions were centrifuged at 10000 x g for 20 min at 25°C. The supernatant was drained and filtered through a 0.22 μm cellulose membrane to eliminate material in suspension. The pTyr concentration was evaluated on the initial solutions and on the drained solutions with a Jasco FP8200 spectrofluorimeter, in quartz cuvettes, at λ_{exc} = 272 nm and λ_{em} = 297 nm. Absorbance data from the initial solutions were used to produce a calibration curve, from which concentrations could be calculated. The difference between the concentration of the initial solutions and of the same solutions left in contact with the polymer gives the amount of pTyr bound to the polymer. Then the pTyr bound per mg of polymer was calculated and the maximum capacity estimated.

2.5.5.16 Cleaning after rebinding

Polymers subjected to rebinding experiments were cleaned through a series of passages in Methanol/HCl 0.1M 1:1 solution in ratio 20:1 with respect to the polymer amount. The presence of pTyr was evaluated through absorbance measurements at wavelength 272 nm.

Cleaning passages were repeated until an absorbance < 0.01 was detectable (Tab 2-11, Fig. 2-47).

2.5.6 Results and discussion

2.5.6.1 Recipes

Nanoparticles were synthesised modifying the following parameters: type of monomers and cross-linkers, polymerisation time, initiators amount, stirring, molar cross-linker percentage (%C_m), presence of template.

The samples were synthesised in triplets. Thirty-five different conditions were explored, and they are listed in Tab. 2-5.

Tab. 2-5. List of polymerisation nanoparticles recipes. W= TRIS buffer 100mM, pH8.2; A/W=Acetonitrile/Water 9:1 v/v.

Recipe	Monomers	% T	%C_m	µM MB	mM TSIA	µM DPI	Time Polym.	Stirring	Solvent	Fmoc-pTyr
A1	HEMA/BIS	1	46	100	1	50	5'	y	W	
A2	HEMA/BIS	1	46	100	1	50	10'	y	W	
A3	HEMA/BIS	1	46	100	1	50	30'	y	W	
A4	HEMA/BIS	1	46	100	1	50	60'	y	W	
C	HEMA/BIS	1	46	10	1	50	10'	y	W	
D	HEMA/BIS	1	46	10	0.1	5	10'	y	W	
B1	HEMA/BIS	1	46	100	1	50	5'	n	W	
B2	HEMA/BIS	1	46	100	1	50	10'	n	W	
G	HEMA/BAP	1	40	100	1	50	5'	y	W	
E1	HEMA/BIS	1	72	100	1	50	5'	y	W	
E2	HEMA/BIS	1	72	100	1	50	10'	y	W	
H1	HEMA/BAP	1	67	100	1	50	5'	y	W	
H2	HEMA/BAP	1	67	100	1	50	10'	y	W	
F	HEMA/BIS	1	80	100	1	50	5'	y	W	
P	HEMA/BIS	1	80	100	1	50	5'	y	W	y
L1	HEMA/BIS	0.2	80	100	1	50	10'	y	A/W	
L2	HEMA/BIS	0.2	80	100	1	50	60'	y	A/W	
L3	HEMA/BIS	0.2	80	100	1	50	18h	y	A/W	
M1	DAU/BIS	0.2	80	100	1	50	10'	y	A/W	
M2	DAU/BIS	0.2	80	100	1	50	60'	y	A/W	
M3	DAU/BIS	0.2	80	100	1	50	18h	y	A/W	
I1	HEMA/BIS	0.2	80	100	1	50	5'	y	W	

continue...

...continue

I2	HEMA/BIS	0.2	80	100	1	50	60'	y	W	
J	DAU/BIS	0.2	80	100	1	50	5'	y	W	
S	HEMA/BIS	0.2	80	100	1	50	60'	y	A/W	y
T	DAU/BIS	0.2	80	100	1	50	60'	y	A/W	y
Q	HEMA/BIS	0.2	80	100	1	50	5'	y	W	y
R	DAU/BIS	0.2	80	100	1	50	5'	y	W	y
N	HEMA/BIS	0.1	80	100	1	50	60'	y	A/W	
O	DAU/BIS	0.1	80	100	1	50	60'	y	A/W	
K	DAU/BIS	0.1	80	100	1	50	5'	y	W	
U	HEMA/BIS	0.1	80	100	1	50	60'	y	A/W	y
V	DAU/BIS	0.1	80	100	1	50	60'	y	A/W	y

2.5.6.2 Dynamic Light Scattering analysis

DLS analysis was performed on the synthesised samples. Results are reported in Tab. 2-6:

Tab. 2-6. DLS results for size (Z average ± standard deviation) and Polydispersion Index (PdI).

Recipe	Monomers	% T	%C m	Time polym	Solvent	Fmoc-pTyr	Zave nm	PdI
A1	HEMA/BIS	1	46	5'	W		72 ± 65	0.9
A2	HEMA/BIS	1	46	10'	W		167 ± 35	0.4
A3	HEMA/BIS	1	46	30'	W		684 ± 100	0.2
A4	HEMA/BIS	1	46	60'	W		313 ± 150	0.3
C	HEMA/BIS	1	46	10'	W		174 ± 14	0.4
D	HEMA/BIS	1	46	10'	W		105 ± 44	0.6
B1	HEMA/BIS	1	46	5'	W		194 ± 52	0.6
B2	HEMA/BIS	1	46	10'	W		145 ± 47	0.8
G	HEMA/BAP	1	40	5'	W		232 ± 43	0.6
E1	HEMA/BIS	1	72	5'	W		155 ± 10	0.7
E2	HEMA/BIS	1	72	10'	W		187 ± 54	0.7
H1	HEMA/BAP	1	67	5'	W		79 ± 29	0.7
H2	HEMA/BAP	1	67	10'	W		113 ± 19	0.4
F	HEMA/BIS	1	80	5'	W		163 ± 15	0.3
P	HEMA/BIS	1	80	5'	W	y	153 ± 12	0.2
L1	HEMA/BIS	0.2	80	10'	A/W		110 ± 7	0.2
L2	HEMA/BIS	0.2	80	60'	A/W		147 ± 2	0.2
L3	HEMA/BIS	0.2	80	18h	A/W		121 ± 2	0.2
M1	DAU/BIS	0.2	80	10'	A/W		211 ± 18	0.3
M2	DAU/BIS	0.2	80	60'	A/W		164 ± 15	0.2
M3	DAU/BIS	0.2	80	18h	A/W		129 ± 4	0.2
I1	HEMA/BIS	0.2	80	5'	W		172 ± 18	0.2
I2	HEMA/BIS	0.2	80	60'	W		192 ± 10	0.3
J	DAU/BIS	0.2	80	5'	W		180 ± 62	0.4
S	HEMA/BIS	0.2	80	60'	A/W	y	174 ± 3	0.1
T	DAU/BIS	0.2	80	60'	A/W	y	120 ± 10	0.4

continue…

…continue

Recipe	Monomers	% T	%C m	Time polym	Solvent	Fmoc-pTyr	Zave nm	PdI
Q	HEMA/BIS	0.2	80	5'	W	y	131 ± 11	0.4
R	DAU/BIS	0.2	80	5'	W	y	183 ± 17	0.3
N	HEMA/BIS	0.1	80	60'	A/W		208 ± 32	0.2
O	DAU/BIS	0.1	80	60'	A/W		239 ± 10	0.2
K	DAU/BIS	0.1	80	5'	W		219 ± 24	0.3
U	HEMA/BIS	0.1	80	60'	A/W	y	245 ± 18	0.2
V	DAU/BIS	0.1	80	60'	A/W	y	301 ± 10	0.2

Here following the systematic evaluation of the effect of the variation of conditions explored in nanoparticles production.

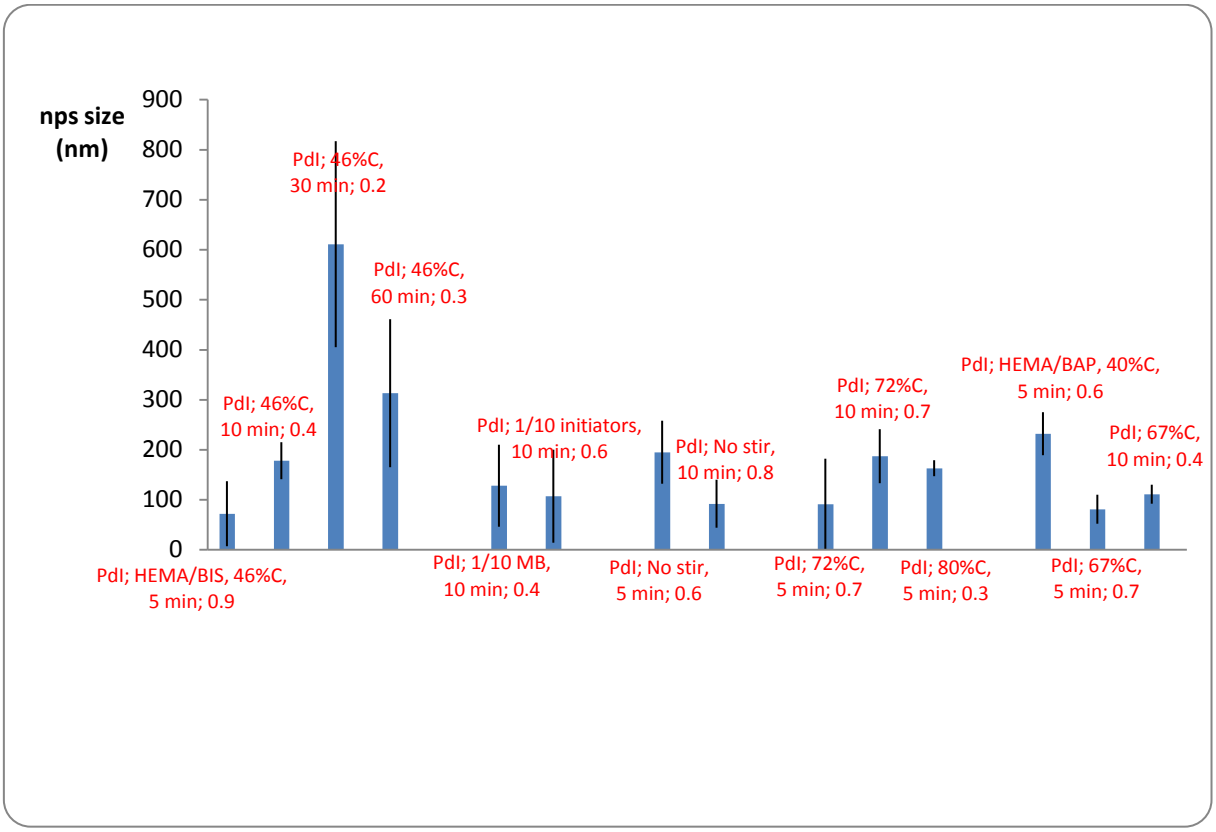

Fig. 2-10. nps size modification due to different experimental conditions in recipes containing 1% of total monomers (1%T). PdI values are the red numbers above the bars.

Fig. 2-10 shows the tendency of the size of nps to increase with a longer polymerisation times in Tris buffer (first four bars).

Reducing the initiators content increases the standard deviation and the polydispersity of the sample.

Avoiding stirring also had an effect on the standard deviation and on polydispersity; moreover, turbidity of the reaction mixture appeared sooner when the sample was not stirred (20 mins instead of 25). The turbidity means the size has increased above 1 micron, thus it can be seen with the naked eye.

The use of a higher cross-linker percentage does not induce size shrinkage or enlargement on HEMA/BIS nps, but it clearly shrinks HEMA/BAP ones, probably due to different mechanical properties. Bis-acryloyl piperazine was also shown to provide slightly larger pores in gels (Hochstrasser DF, 1988). In general a higher cross-linker amount helps MIP cavities to retain their shape by making the structure more rigid and the use of an 80%C composition gave good results both for size and polydispersity.

Even though HEMA/BAP particles were smaller than those of HEMA/BIS, they had a higher PdI and batch to batch synthesis was less reproducible.

Literature reports a controlled size increase through the “post dilution method”, by which dilution of the reaction mixture is made just before the gelation point to reach a %T lower than critical concentration (Wulff G, 2012). This method could be mimicked by using low %T from the beginning or a worse solvent, in which particles can precipitate when they reach a size large enough to not stay in suspension.

The initial recipe modified for cross-linker percentage (80%C instead of 46%C) was thus subjected to the following experimental variations: lower %T, solvent change and functional monomer change.

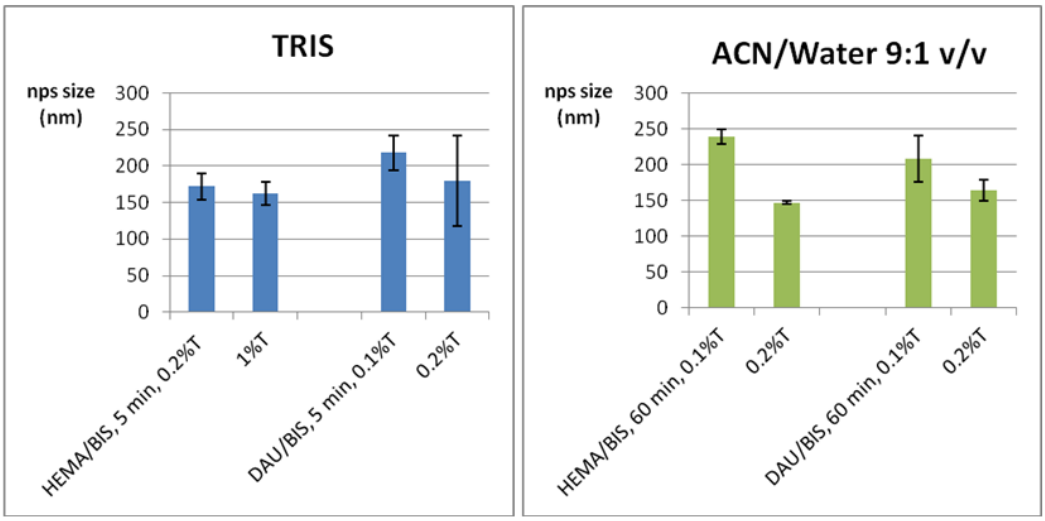

Fig. 2-11. nps size modification due to the variation of total monomers content %T.

In Fig. 2-11 the effect of total monomers content on nps size is shown. The first part of the Figure (blue bars) reports results obtained in Tris buffer at low polymerisation time, while the second part (green bars) concerns experiments made in ACN/W at higher polymerisation time. No extended polymerisation time was available for synthesis in Tris buffer because solutions became turbid for the same monomer composition, indicating the presence of micron-size particles.

Raising the amount of monomers had a slightly shrinking effect on the nps. The most interesting effect of using a lower monomer content is however the low PdI of the samples, resulting above 0.3 only in 3 recipes on 18 with %T≤0.2 (Tab. 2-6). This fact was already observed by Wulff et al., who reported a higher molecular weight and polydispersity for hydrogels produced with high crosslinking and higher amounts of monomers (Wulff G, 2012). This significant improvement suggests the use of a low monomer amount in the progress of the analysis, and polydispersity issues will be not further considered.

The effect of the solvent was subsequently explored (Fig. 2-12). ACN/Water 9:1 v/v was chosen as dispersing media. In order to facilitate the dissolution of the reagents, these were firstly added of 1 volume of water, then diluted with 9 volumes of acetonitrile.

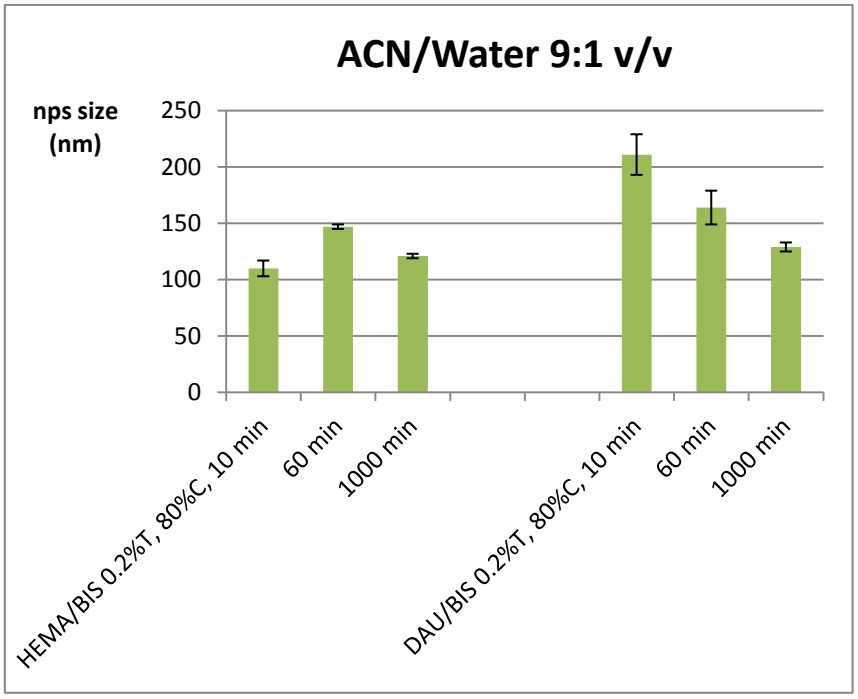

Fig. 2-12. Effect of the solvent on nps size.

The most interesting effect of the use of ACN/Water 9:1 v/v is its property of keeping the size of the particles in the nano range, without generating turbidity (thus allowing particles to grow to the micro range) as happens in Tris buffer, at least at low total monomer amount (less than 1%T). This can be possibly a result of its poor solubilizing properties with respect to the growing particle, that cannot grow too much in solution before precipitation (Wulff G, 2012). This is evidenced by the clear aspect of the solutions after 18h (1000 min) of reaction and by the stopped nps growth in 10 min, 60 min and 18h of reaction (Fig. 2-12). A decrease in nps size for longer polymerisation time was also observed with the use of DAU monomer. This fact can be explained with the faster kinetics of DAU in being incorporated in the growing particles: an initial fast production of particles consumes the monomers, that remain in lower concentration in solution but still in presence of an excess of initiators. The next step was thus the exploration of the effect of monomer substitution from HEMA to DAU.

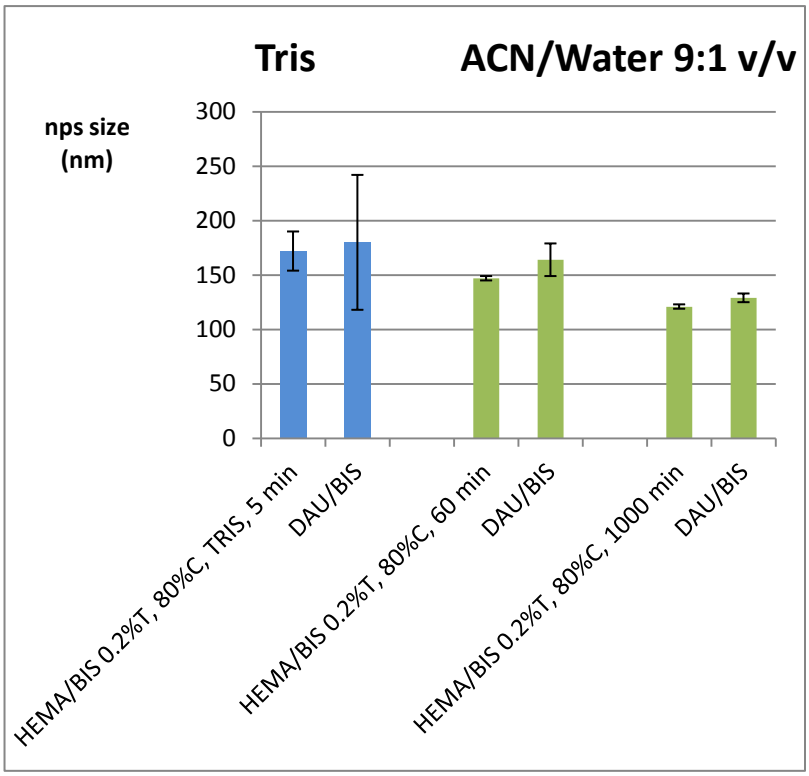

Fig. 2-13. Comparison of different functional monomers.

There was not a high size variation nanoparticle between the use of HEMA and DAU, both in Tris buffer and ACN/W for short and long polymerisation times (Fig. 2-13). Anyway DAU shows a faster polymerisation kinetics than HEMA, with a turbidity point (visible particles in the reaction mixture) of 3min at 1%T and 15 min at 0.2% in TRIS buffer (HEMA gives turbidity in 20 min with the first recipe and remains transparent for longer than 60 min with the second). Literature generally reports a different kinetics of the different monomers in being included in the growing polymer, as well as a different solubility of the nanoparticles made with different monomers (Piletska EV, 2008).

The following step was the study of the effect of the template in the polymerisation mixture. The tested recipes are reported in Tab. 2-7 and the results in Fig. 2-14.

Tab. 2-7. Evaluation of template effect on the size of the nanoparticles. Samples F-O (left side of the table) were produced without the template, while samples P-Q (right side of the table) were produced by following the same recipes plus the addition of template.

Recipe	Monomers	% T	% Cm	Time polymerisation	µmol cross-linker	µmol monomer	Solvent	Zave nm	PdI	Recipe	µmol pTyr	Zave nm	PdI
F	HEMA/BIS	1	80	5'	630	160	W	163 ± 15	0.3	P	80	153 ± 12	0.2
I1	HEMA/BIS	0.2	80	5'	126	32	W	172 ± 18	0.2	Q	16	131 ± 11	0.4
J	DAU/BIS	0.2	80	5'	126	32	W	180 ± 62	0.4	R	16	183 ± 17	0.3
L2	HEMA/BIS	0.2	80	60'	126	32	ACN/W	147 ± 2	0.2	S	16	174 ± 3	0.1
M2	DAU/BIS	0.2	80	60'	126	32	ACN/W	164 ± 15	0.2	T	16	120 ± 10	0.4
N	HEMA/BIS	0.1	80	60'	63	16	ACN/W	208 ± 32	0.2	U	8	245 ± 18	0.2
O	DAU/BIS	0.1	80	60'	63	16	ACN/W	239 ± 10	0.2	V	8	301 ± 10	0.2

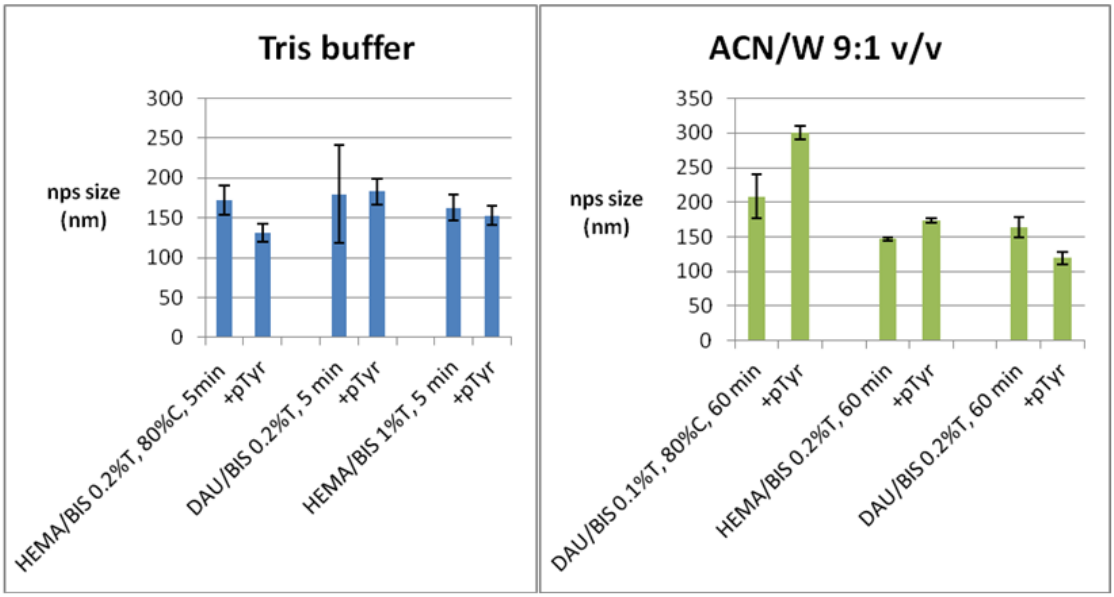

Fig. 2-14. nps size modification due to the addition of Fmoc-pTyr in molar ratio 1:2 with respect to the functional monomer.

The presence of pTyr in the polymerizing mixture does not change significantly the dimensions of the nanoparticles. This “template effect” is instead reported in some other literature examples (Yoshimatsu K, 2012).

2.5.6.3 Yield evaluation of small-scale synthesised nanoparticles

Reaction yield was measured for some recipes (Tab. 2-8). The choice was made depending on the size of the nanoparticles and the Polydispersity Index.

Tab. 2-8. Yield of reaction for some chosen recipes. The lyophilised volume corresponds to 10ml of the initial solution.

Recipe	Monomers	% T	$\%C_m$	Time polymerisation	Solvent	Amount (mg)	Yield %
H1	HEMA/BAP	1	67	5'	W	2.8	2.8
F	HEMA/BIS	1	80	5'	W	2.3	2.3
L1	HEMA/BIS	0.2	80	10'	A/W	0.1	0.5
L2	HEMA/BIS	0.2	80	60'	A/W	0.5	2.5
L3	HEMA/BIS	0.2	80	18h	A/W	1	5
M1	DAU/BIS	0.2	80	10'	A/W	0.9	4.5
M2	DAU/BIS	0.2	80	60'	A/W	0.6	3
M3	DAU/BIS	0.2	80	18h	A/W	1.1	5.5
I1	HEMA/BIS	0.2	80	5'	W	4.1	20.5
I2	HEMA/BIS	0.2	80	60'	W	0.5	2.5
J	DAU/BIS	0.2	80	5'	W	0.4	2
N	HEMA/BIS	0.1	80	60'	A/W	0.1	0.5
O	DAU/BIS	0.1	80	60'	A/W	0.1	1
K	DAU/BIS	0.1	80	5'	W	0.1	1

The yields were in the range between 0.5% and 5.5%, with no significant difference between preparations made with different monomers (Tab. 2-3). The evaluation of the variation in the product amount gave a ±1.0mg of uncertainty. Recipes H1, F, L3 and M3, shown in Tab. 2-4

Tab. 2-4, seemed to be the most promising to proceed with a large-scale synthesis, with the intention of not excluding the use of any monomer or solvent. Recipes I2 and J, even though seemly promising, would have required a huge amount of starting material to produce enough polymer. Recipe I1 seems to be an experimental deviation (error in the synthesis step, because weight measurement on another part of the solution gave the same result), in fact a longer polymerisation time gave a lower amount of product.

2.5.6.4 AFM images

The four samples chosen to be produced on a larger scale and thus subjected to rebinding experiments were analysed by AFM. Images were taken for non-dialysed samples. Dialysed samples did not show the presence of any particles on the mica surface both with the same immobilisation method used for non-dialysed samples and by doubling the contact time from 5 to 10 min.

The next pictures represent AFM images of a sample prepared with the recipe “F” through the procedure explained in the section “materials and methods”. The bar on the right side of the pictures is the height of the objects expressed in nanometers.

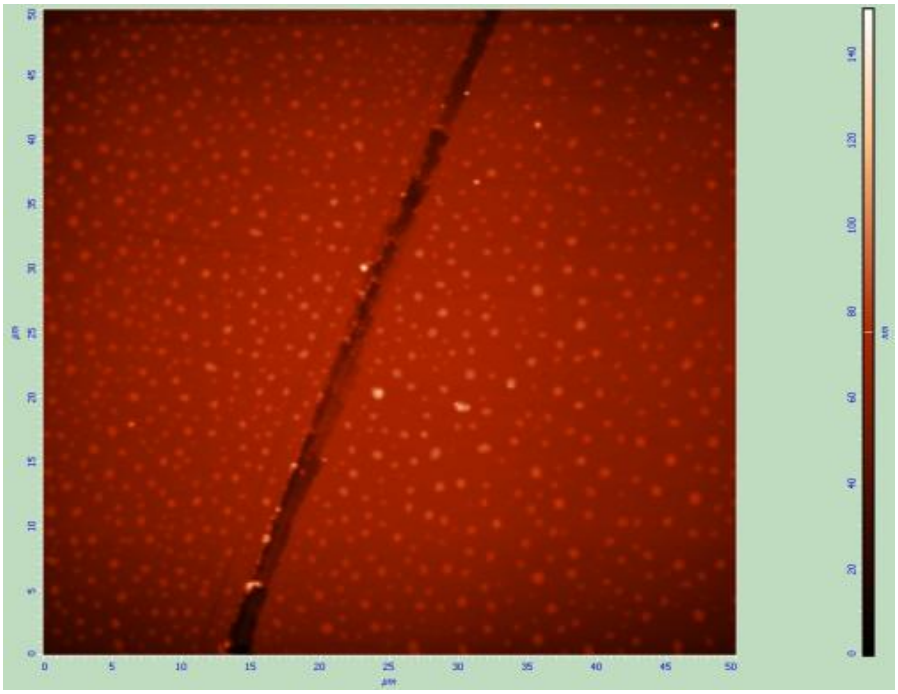

Fig. 2-15. A 50 µm x 50 µm image of sample “F” (HEMA/BIS 1%T, 80%C, 5 min of polymerisation in water).

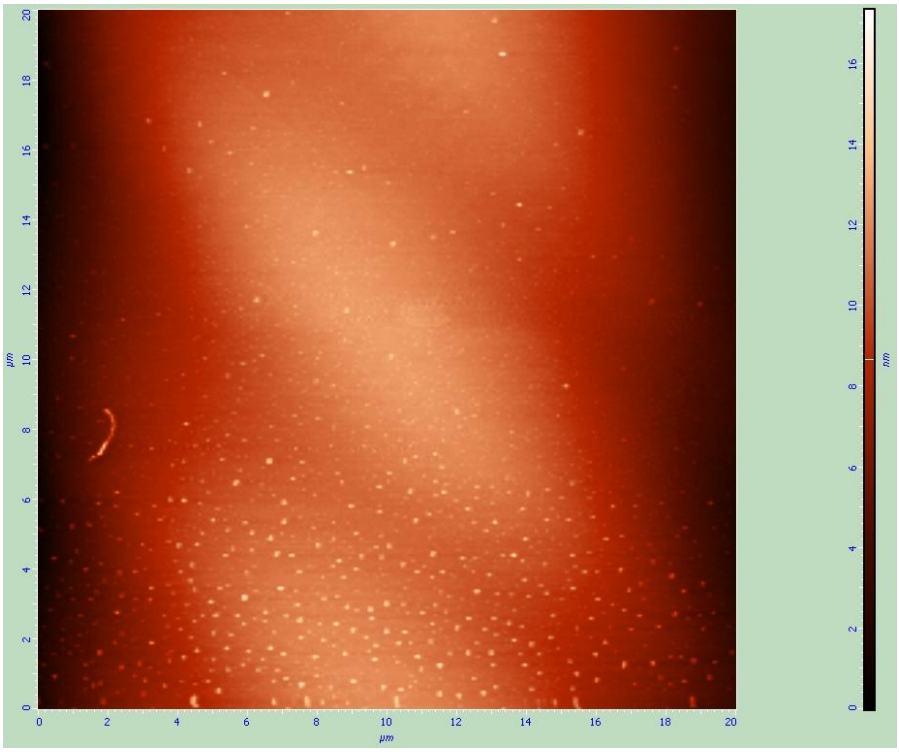

Fig. 2-16. A 20 µm x 20 µm image of sample “F”.

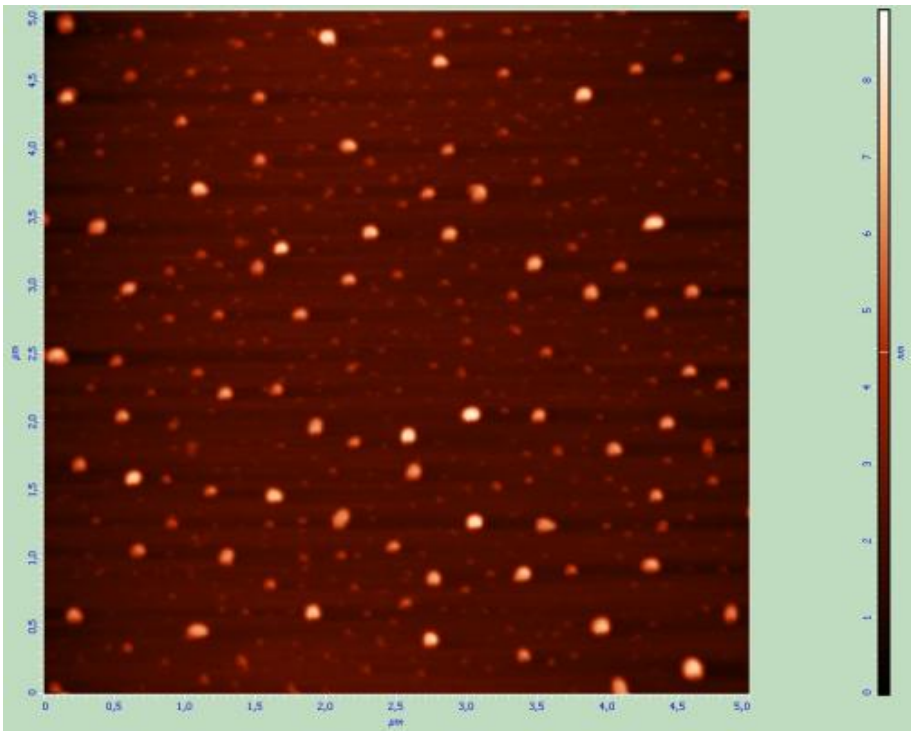

Fig. 2-17. A 5 µm x 5 µm image of sample “F”.

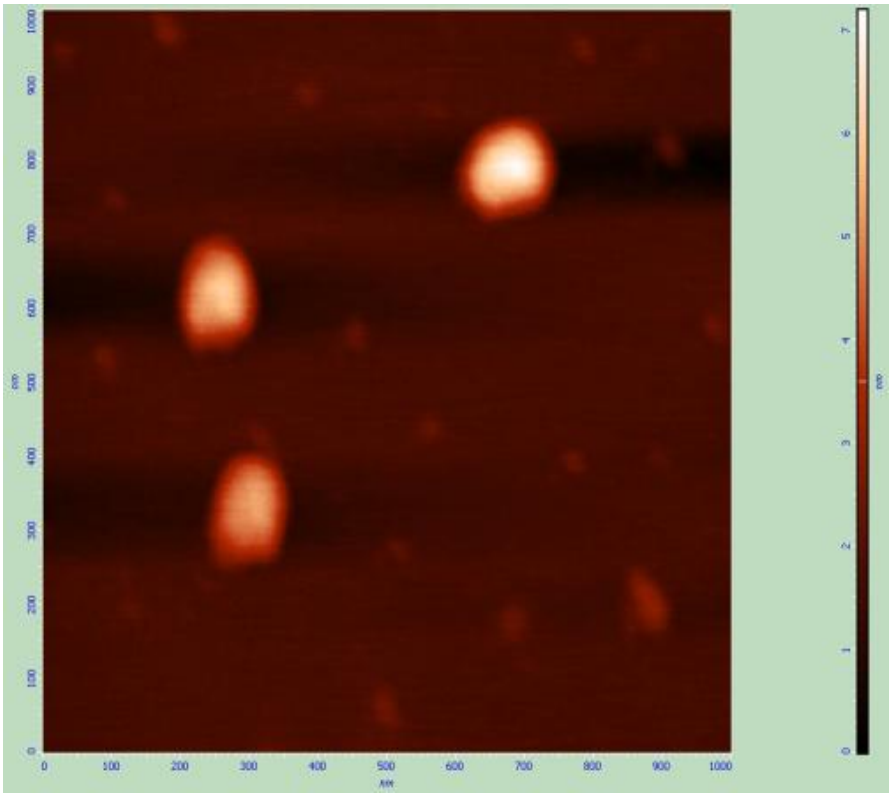

Fig. 2-18. A 1 µm x 1 µm image of sample "F".

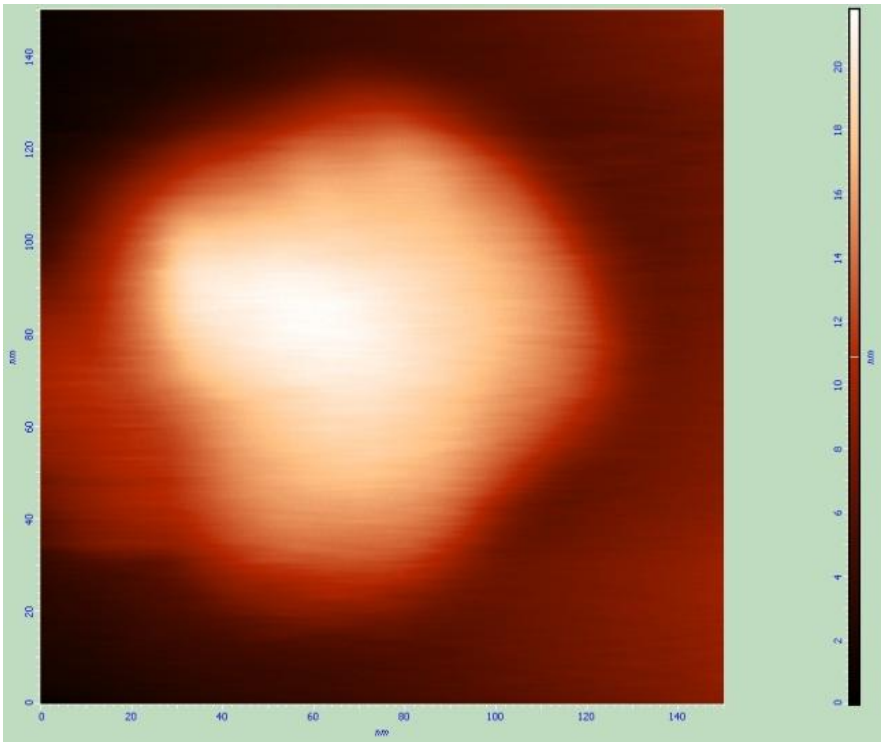

Fig. 2-19. A 150 nm x 150 nm image of sample "F".

The particles show a flat, irregular shape, with few aggregates present. The size range is approximately from 20 nm x 2 nm (width x height) to 200 nm x 20 nm. Another immobilisation method was tried on the same sample, employing $NaHCO_3$ buffer (200mM pH 9.0) 1:1 v/v instead of ethanol. The results are visualised in the following pictures.

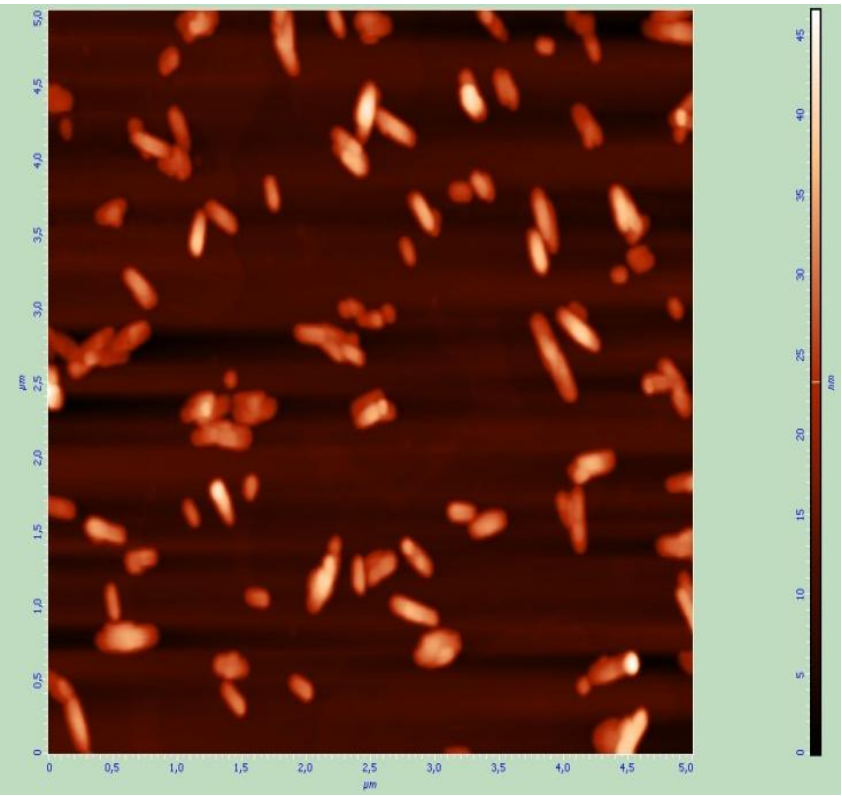

Fig. 2-20. A 5 µm x 5 µm image of sample "F" immobilised on the mica dish with a $NaHCO_3$ buffer.

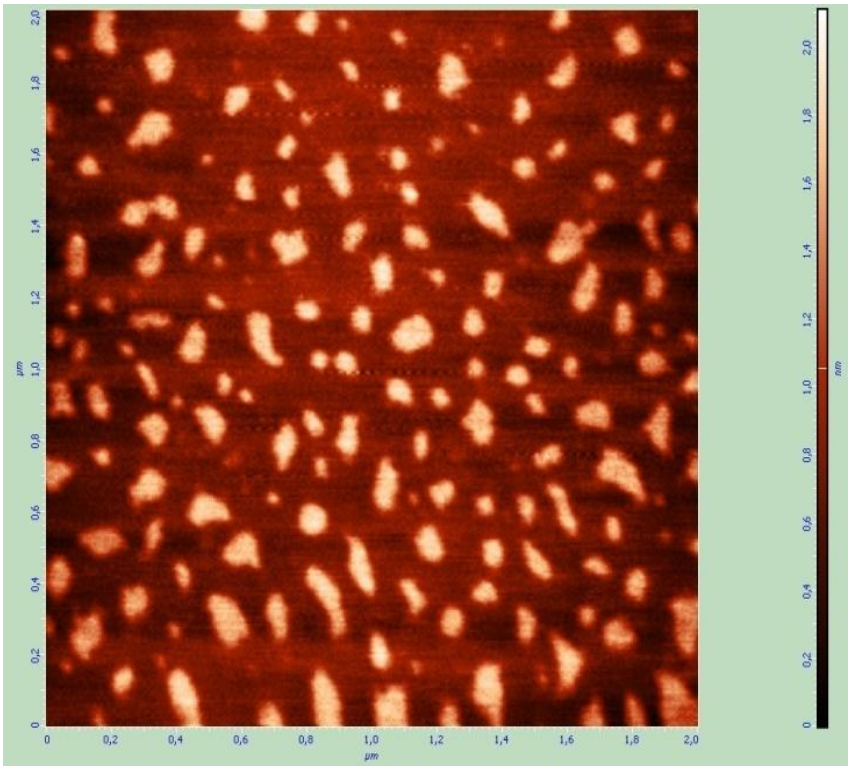

Fig. 2-21. A 2 µm x 2 µm image of sample "F" immobilised on the mica dish with a $NaHCO_3$ buffer.

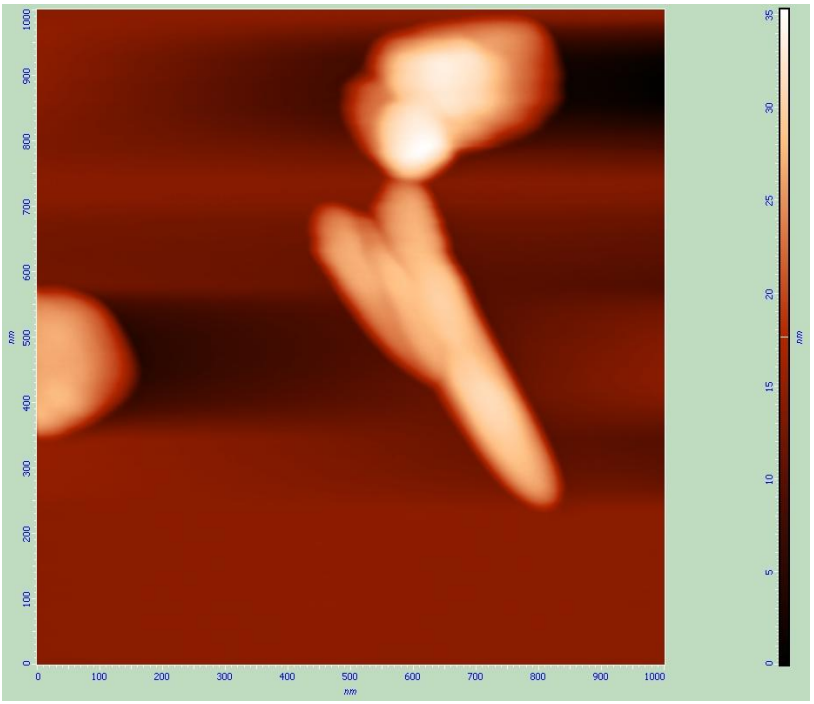

Fig. 2-22. A 1 µm x 1 µm image of sample "F" immobilised on the mica dish with a $NaHCO_3$ buffer.

A comparison of the two immobilisation methods shows a tendency to aggregation with the use of the basic buffer instead of ethanol. The other samples were therefore analysed through immobilisation after a 1:1 v/v dilution with ethanol.

The next pictures represent AFM images of a sample prepared with the recipe “H1” through the procedure explained in the section “materials and methods”.

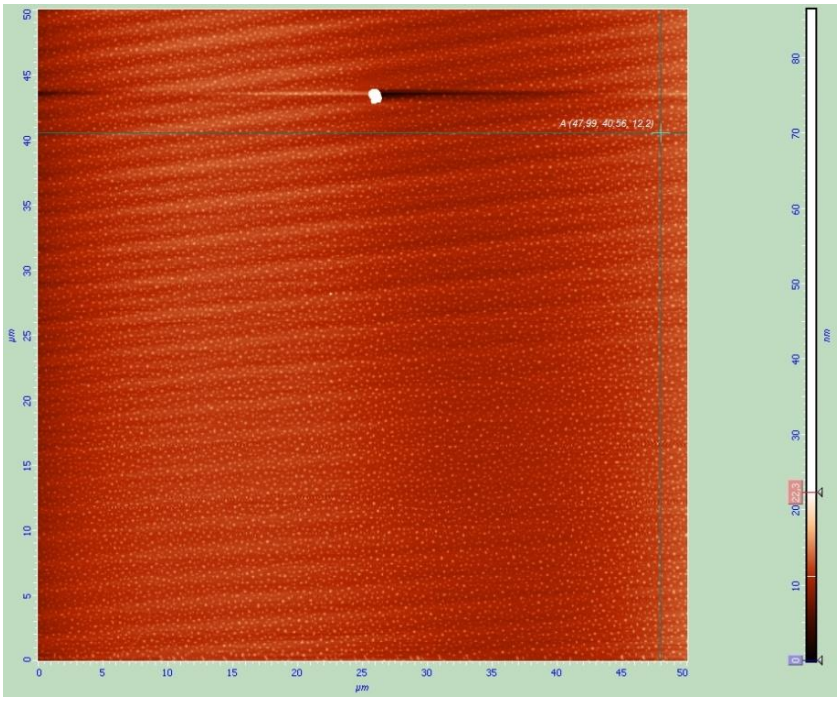

Fig. 2-23. A 50 µm x 50 µm image of sample “H1” (HEMA/BAP 1%T, 67%C, 5 min of polymerisation in water).

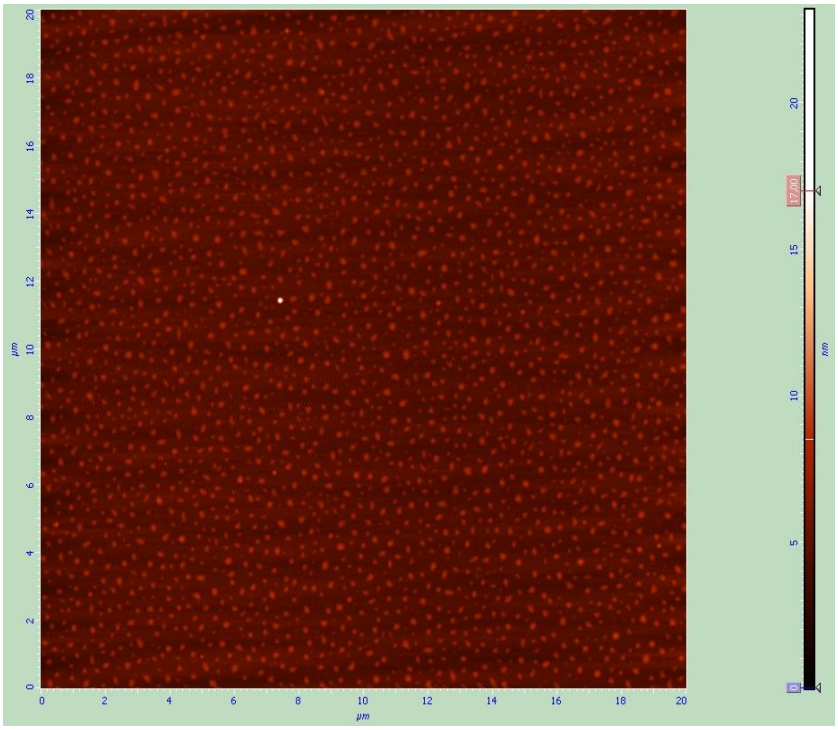

Fig. 2-24. A 20 µm x 20 µm image of sample “H1”.

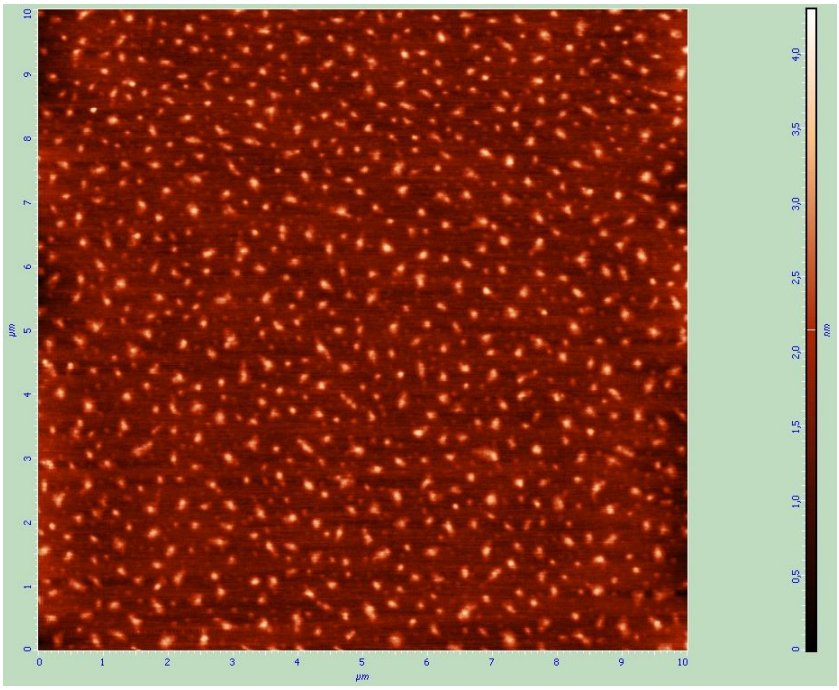

Fig. 2-25. A 10 µm x 10 µm image of sample “H1”.

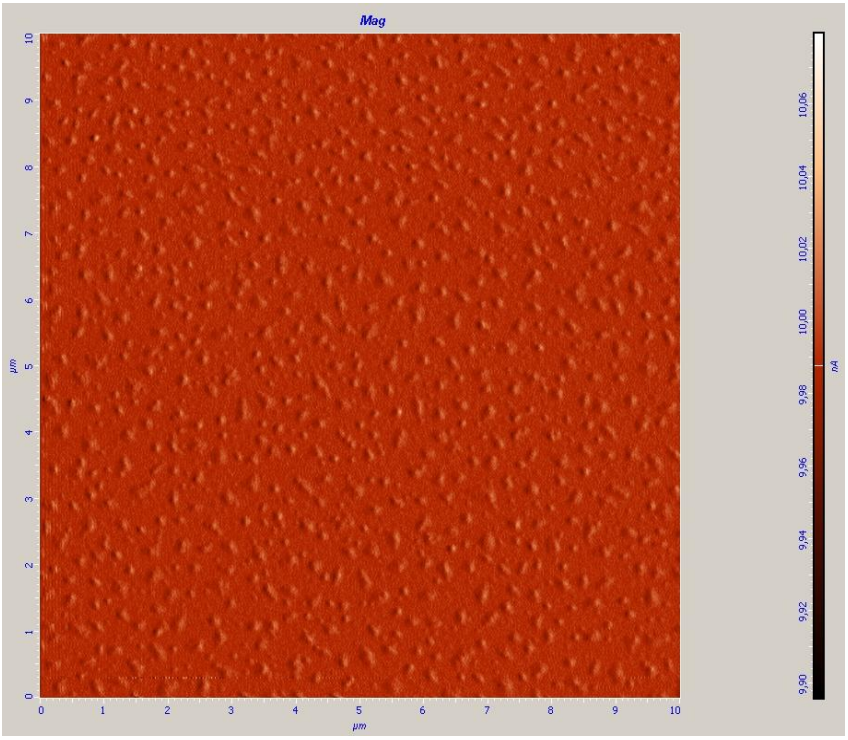

Fig. 2-26. A 10 µm x10 µm image of sample "H1" with semi-contact error mode acquisition, to put in evidence changes in height.

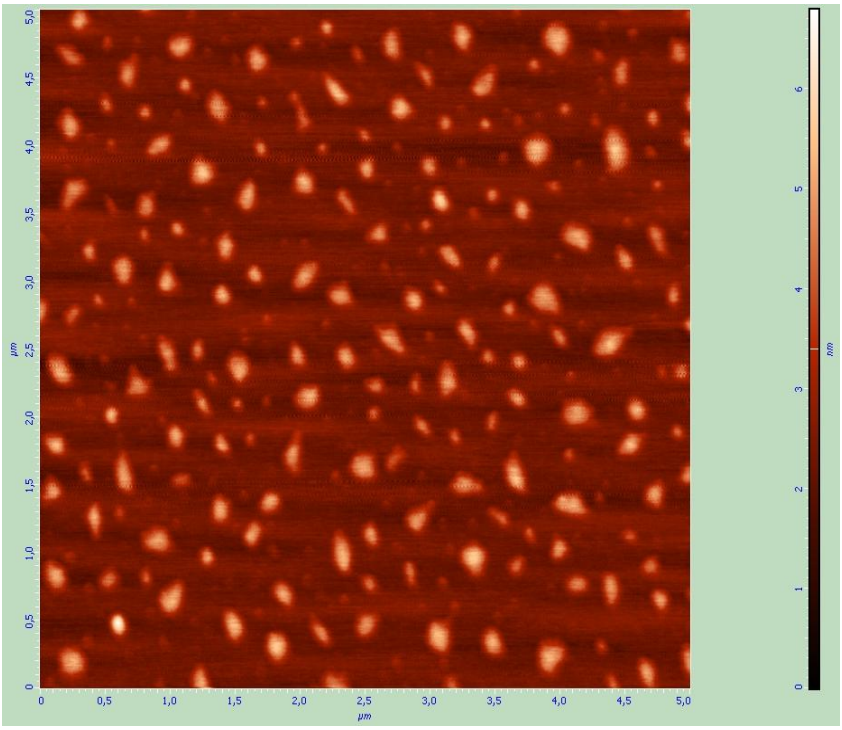

Fig. 2-27. A 5 µm x 5 µm image of sample "H1".

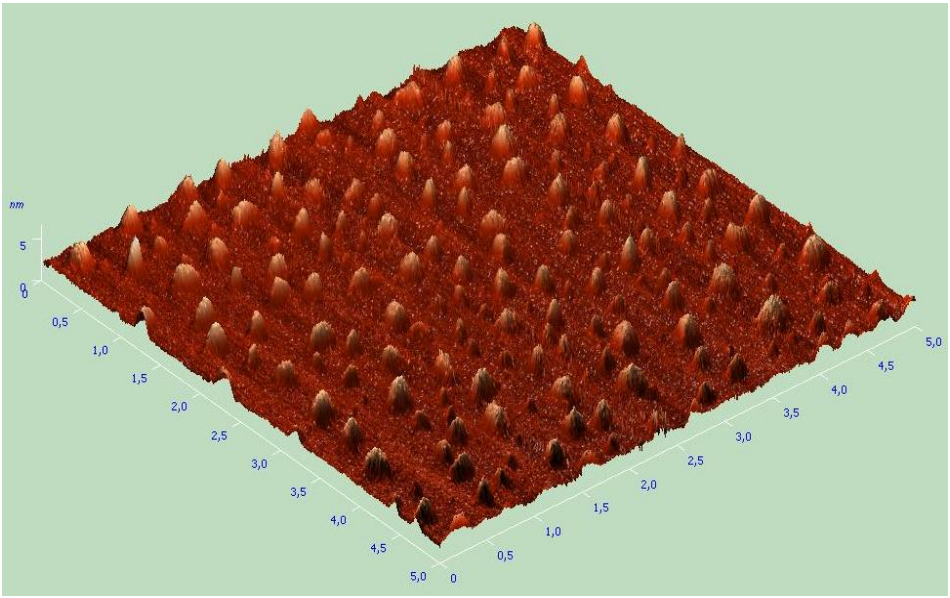

Fig. 2-28. A 5 µm x 5 µm image of sample "H1" with 3D image elaboration.

The particles show a flat shape, with regular distribution on the surface.

The next pictures represent AFM images of a sample prepared with the recipe "L3" through the procedure explained in the section "materials and methods".

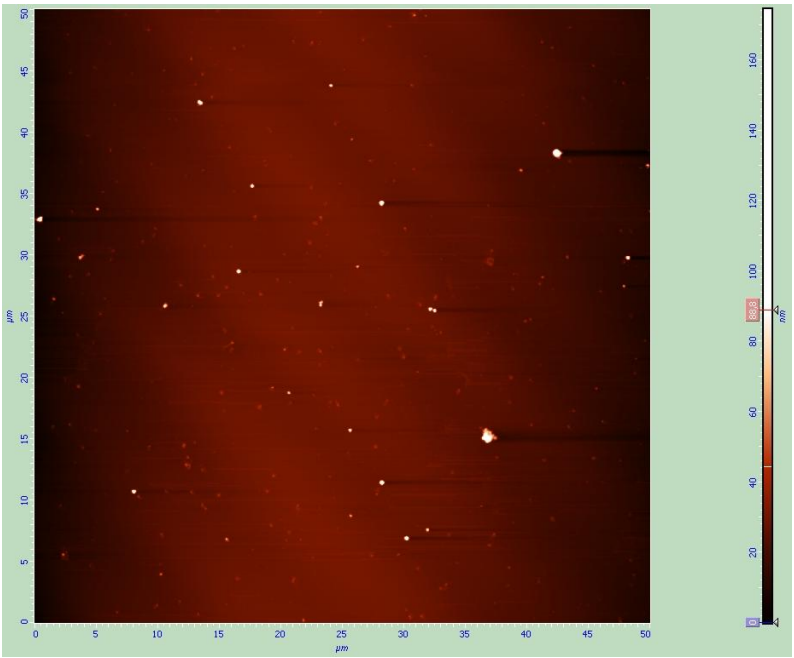

Fig. 2-29. A 50 µm x 50 µm image of sample "L3" (HEMA/BIS 0.2%T, 80%C, 18 hours of polymerisation in ACN/water 9:1 v/v).

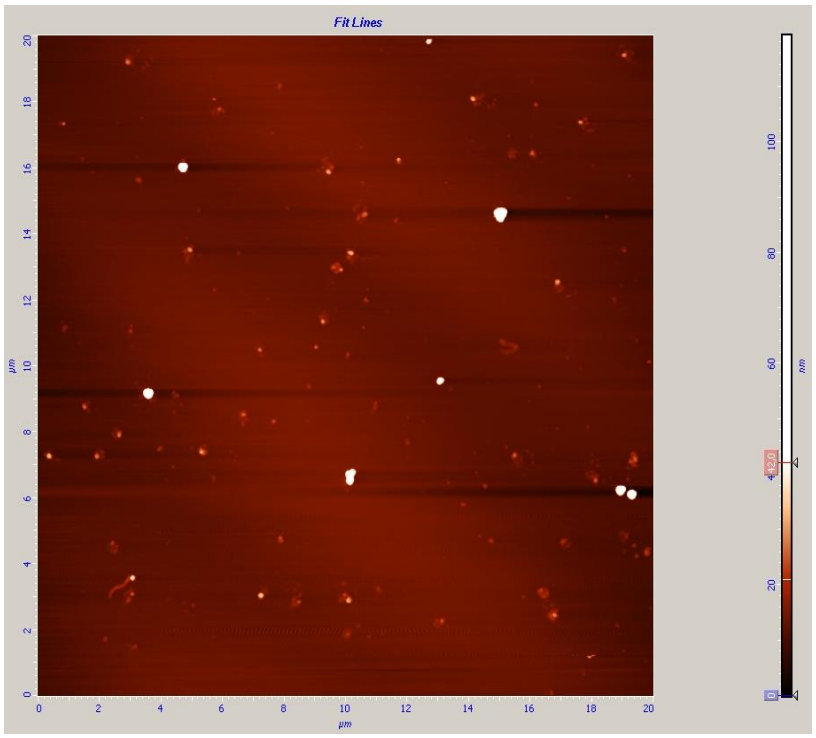

Fig. 2-30. A 20 µm x 20 µm image of sample “L3”.

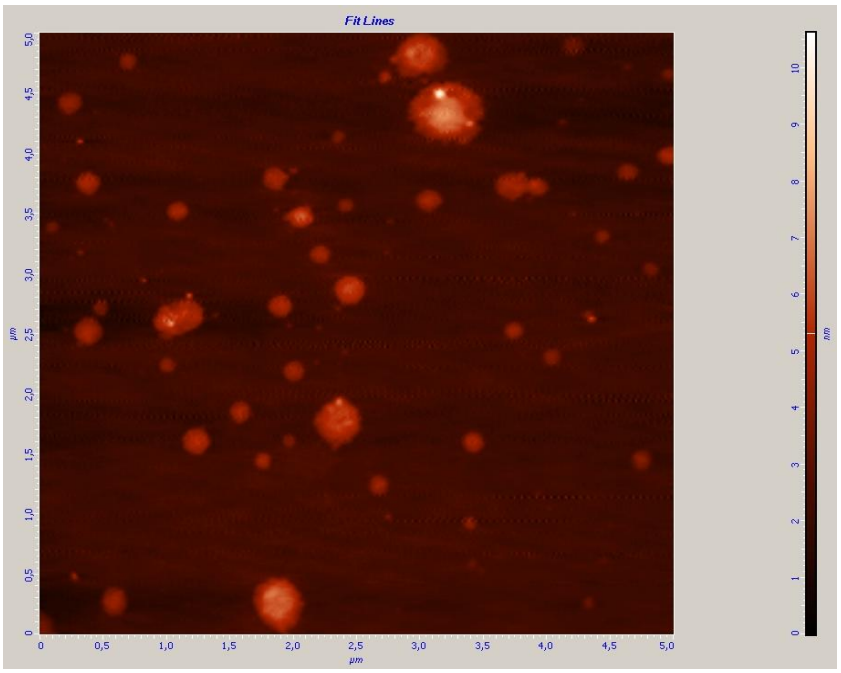

Fig. 2-31. A 5 µm x 5 µm image of sample “L3”.

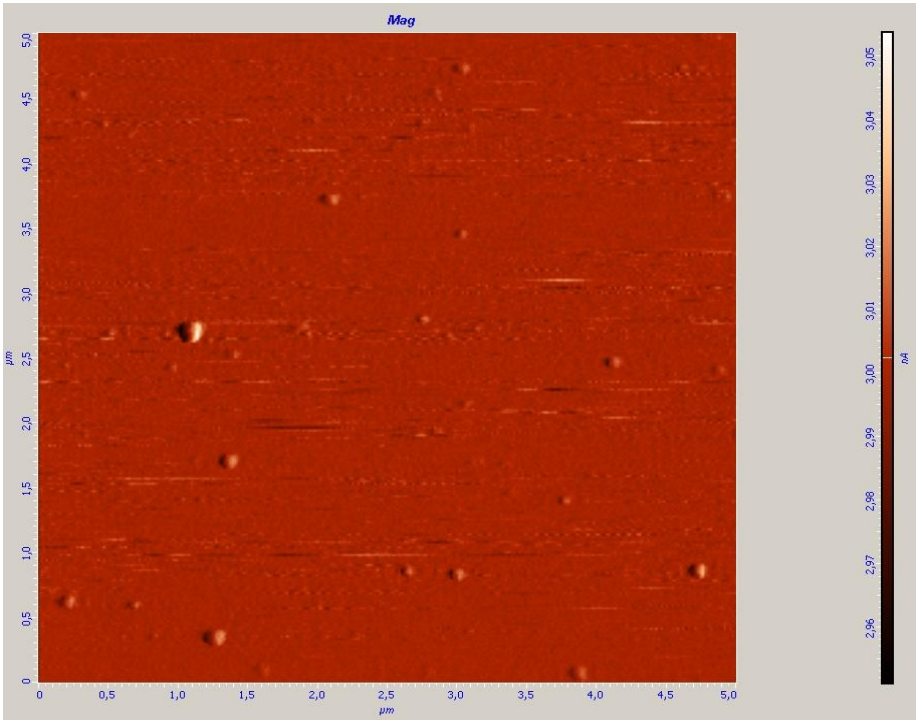

Fig. 2-32. A 5 µm x 5 µm image of sample "L3" with semicontact error acquisition, to put in evidence changes in height.

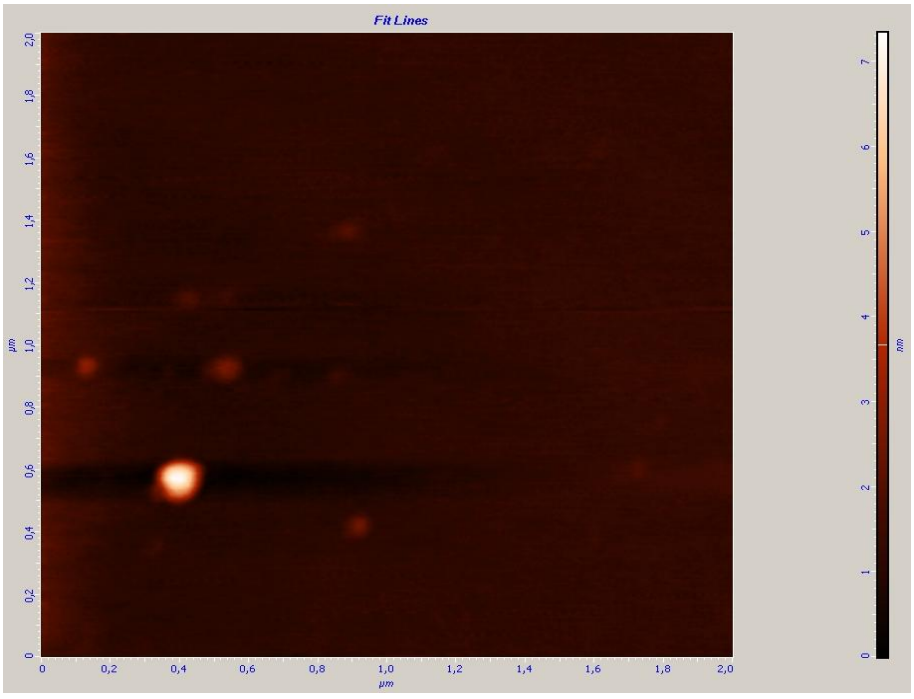

Fig. 2-32. A 2 µm x 2 µm image of sample "L3".

The particles show a flat shape, with more aggregates than the samples prepared in Tris buffer. Moreover, fewer particles are present, probably due to

the fact that the particles were initially immersed in ACN/W instead of Tris buffer. This could have hampered the adsorption of the particles onto the mica surface.

The next pictures represent AFM images of a sample prepared with the recipe “M3” through the procedure explained in the section “materials and methods”.

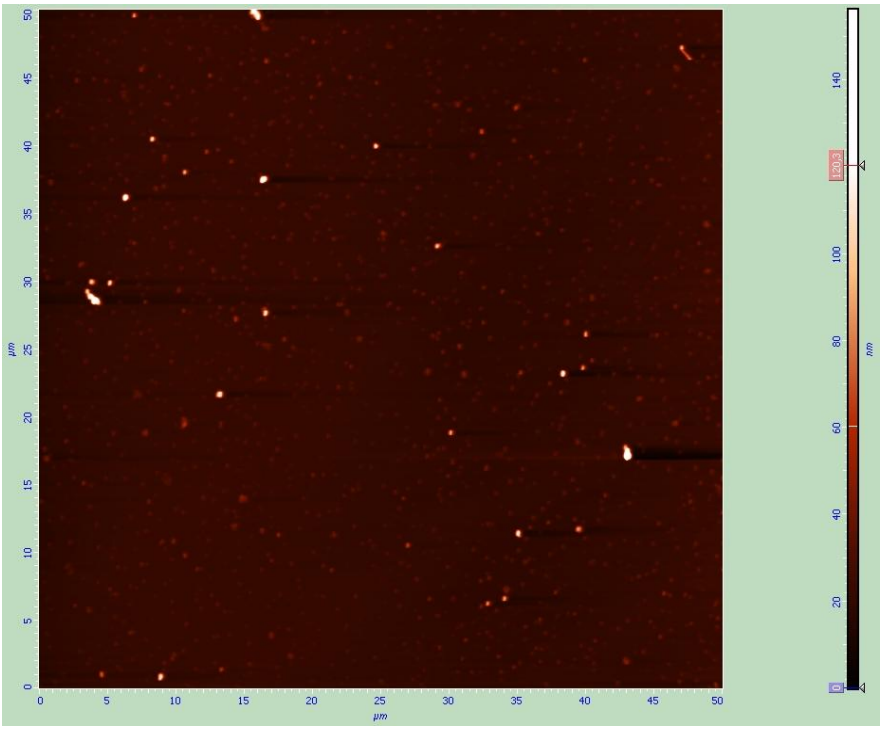

Fig. 2-33. A 50 µm x 50 µm image of sample “M3” (DAU/BIS 0.2%T, 80%C, polymerisation of 18 hours in ACN/water 9:1 v/v).

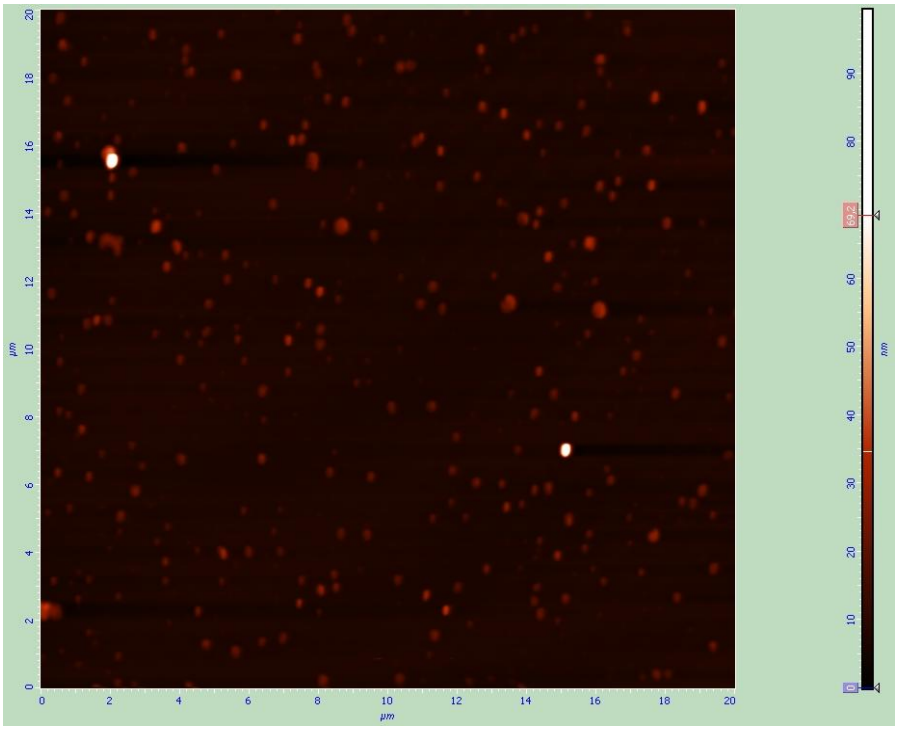

Fig. 2-34. A 20 µm x 20 µm image of sample “L3”.

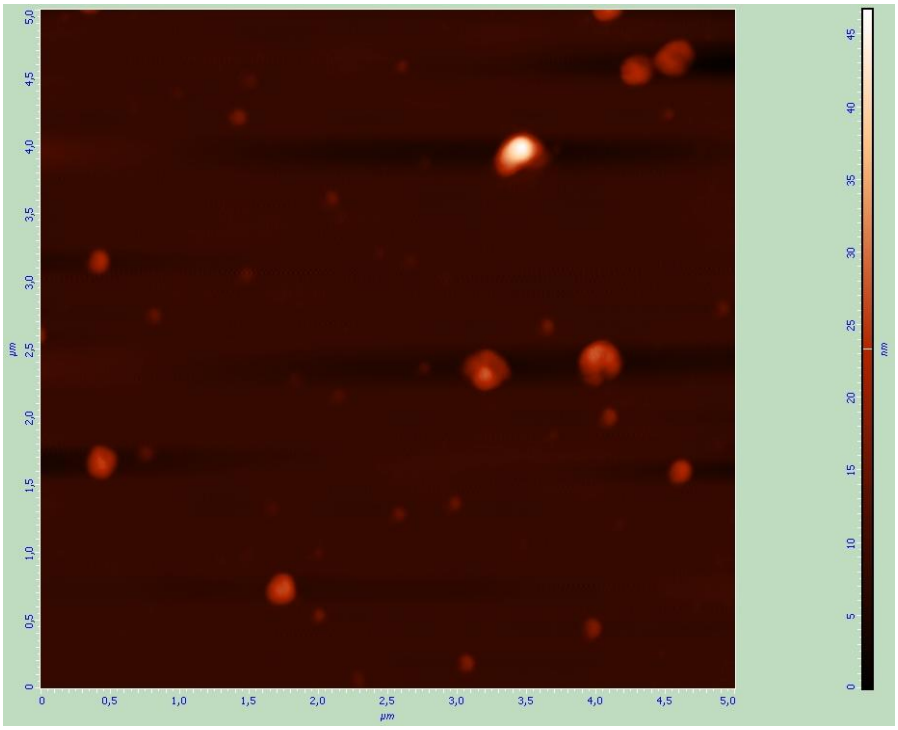

Fig. 2-35. A 5 µm x 5 µm image of sample “L3”.

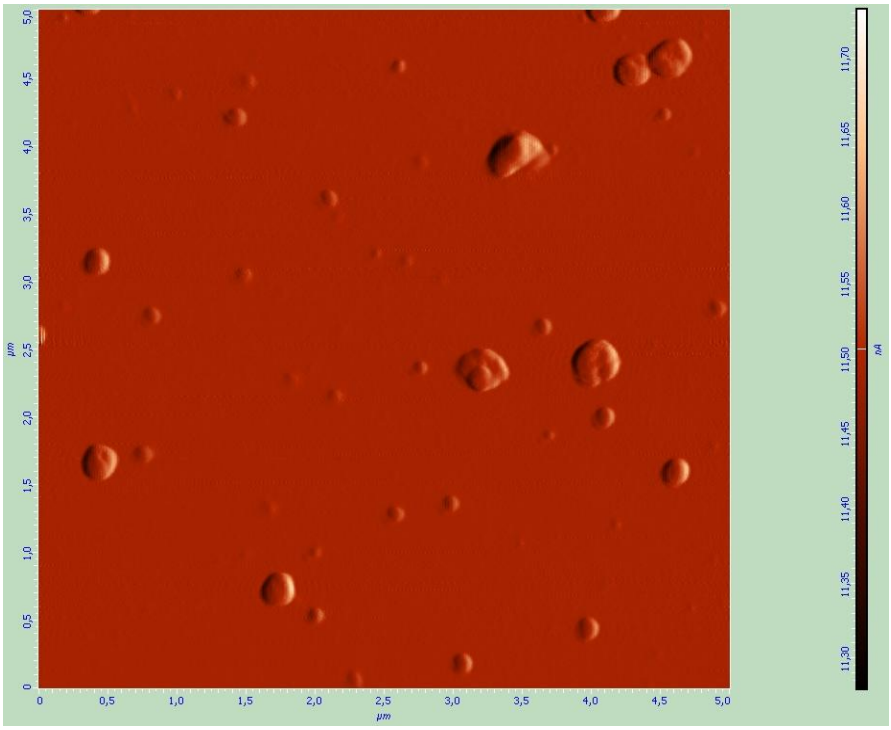

Fig. 2-36. A 5 µm x 5 µm image of sample "L3" with semicontact error-mode acquisition, to put in evidence changes in height.

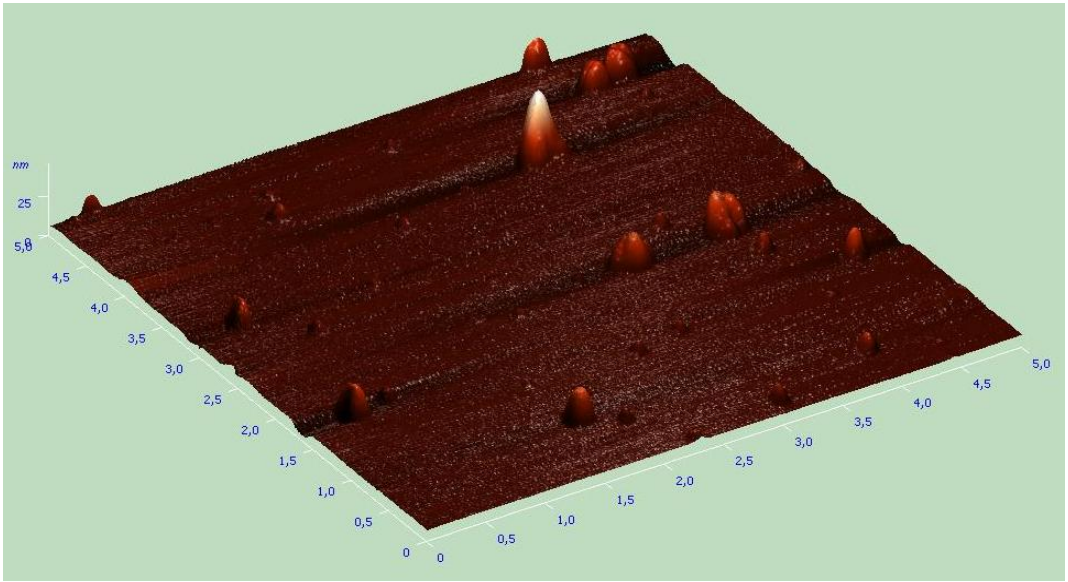

Fig. 2-37. A 5 µm x 5 µm image of sample "L3" with 3D image elaboration.

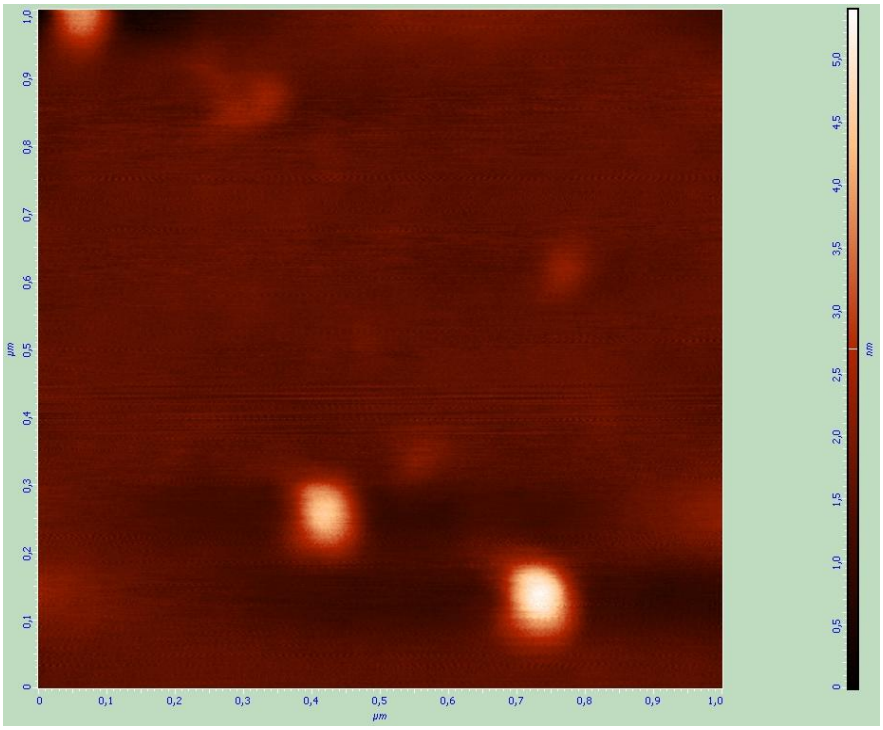

Fig. 2-38. A 1 µm x 1 µm image of sample “L3”.

The particles show a flat shape, similar to what can be observed in the sample prepared with recipe “L3”. Few particles are actually present, probably due to the fact that the particles were initially immersed in ACN/W instead of Tris buffer. This could have hampered the adsorption of the particles onto the mica surface.

The next flanked pictures represent the comparison of images of the four samples at different magnifications.

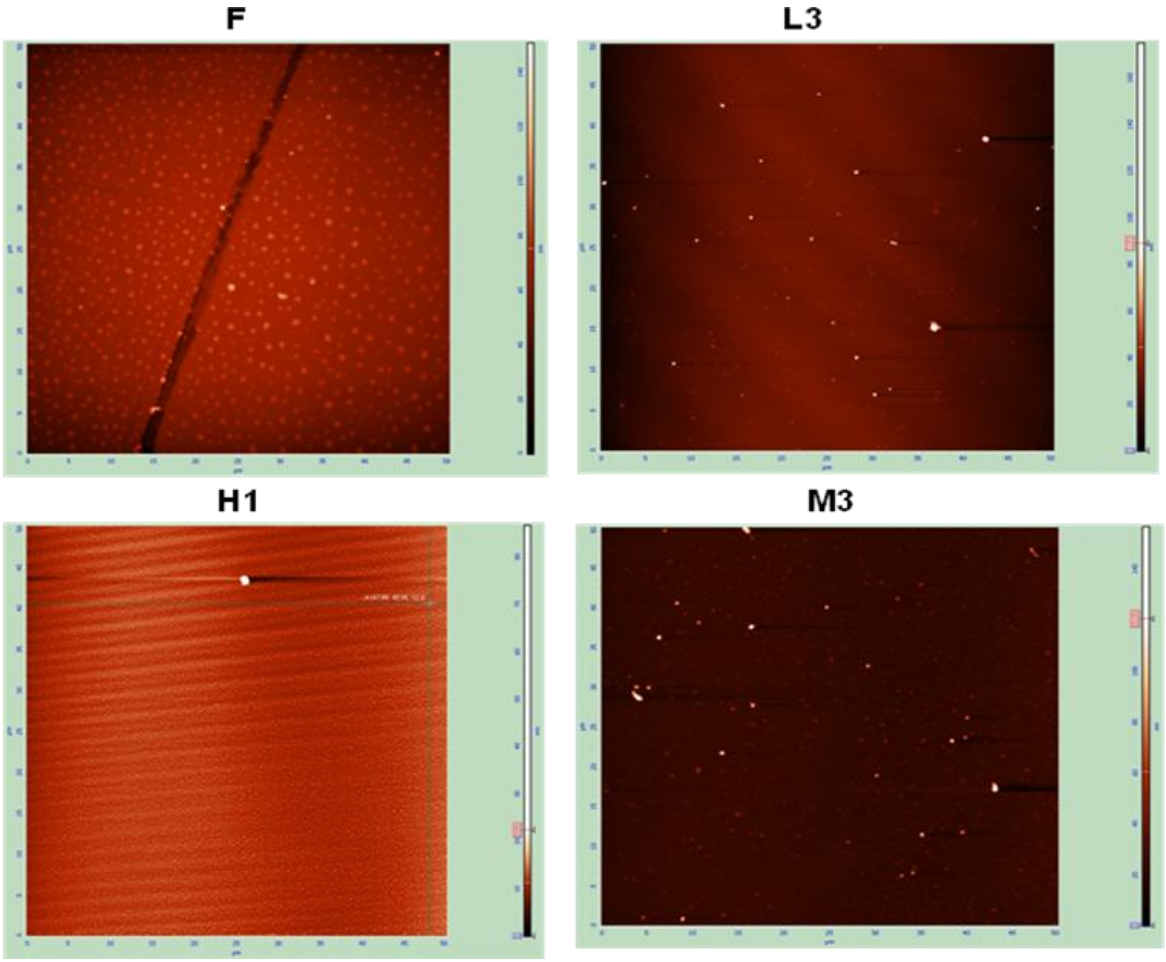

Fig. 2-39. Comparison of the 50 μm x 50 μm magnification images of the four samples.

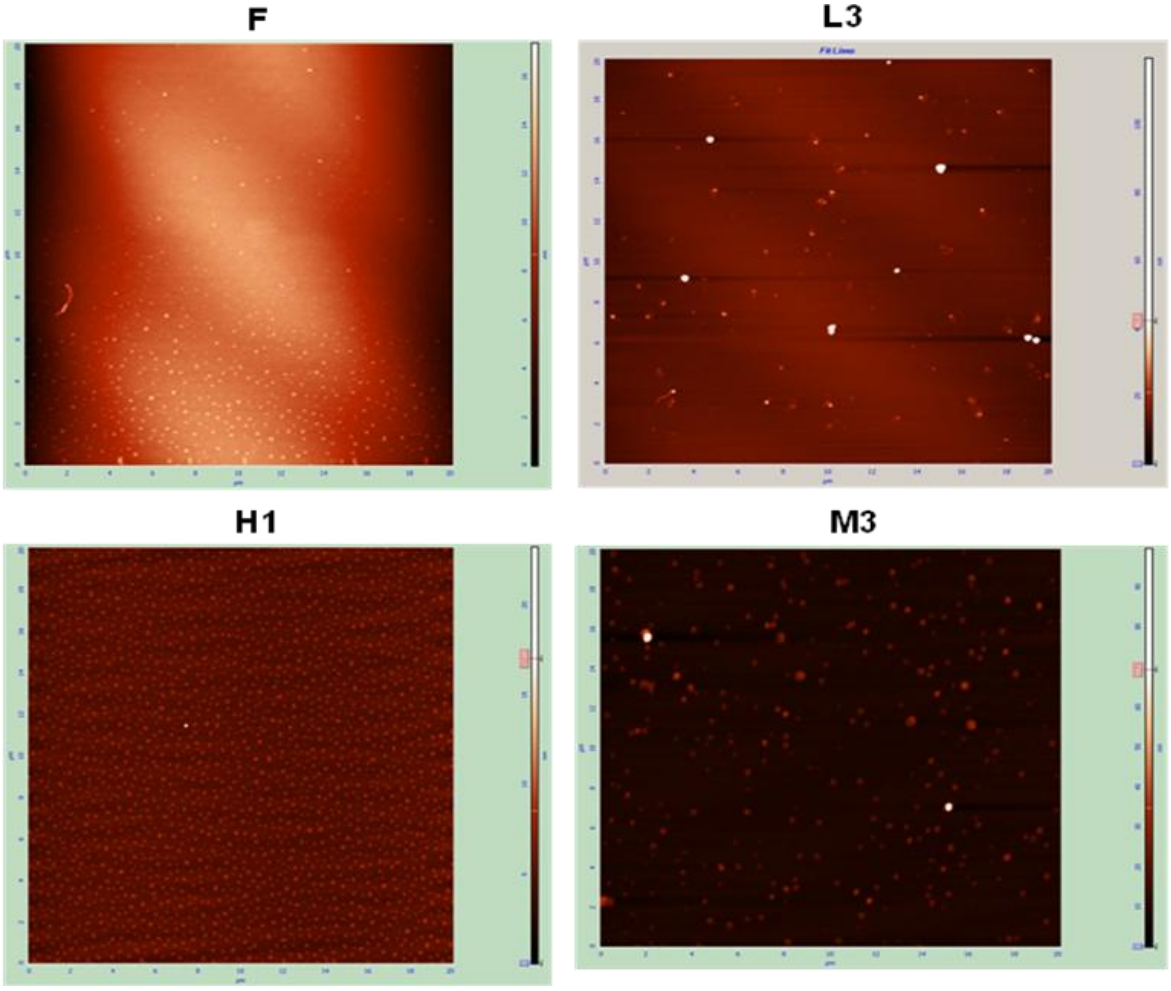

Fig. 2-40. Comparison of the 20 μm x 20 μm magnification images of the four samples.

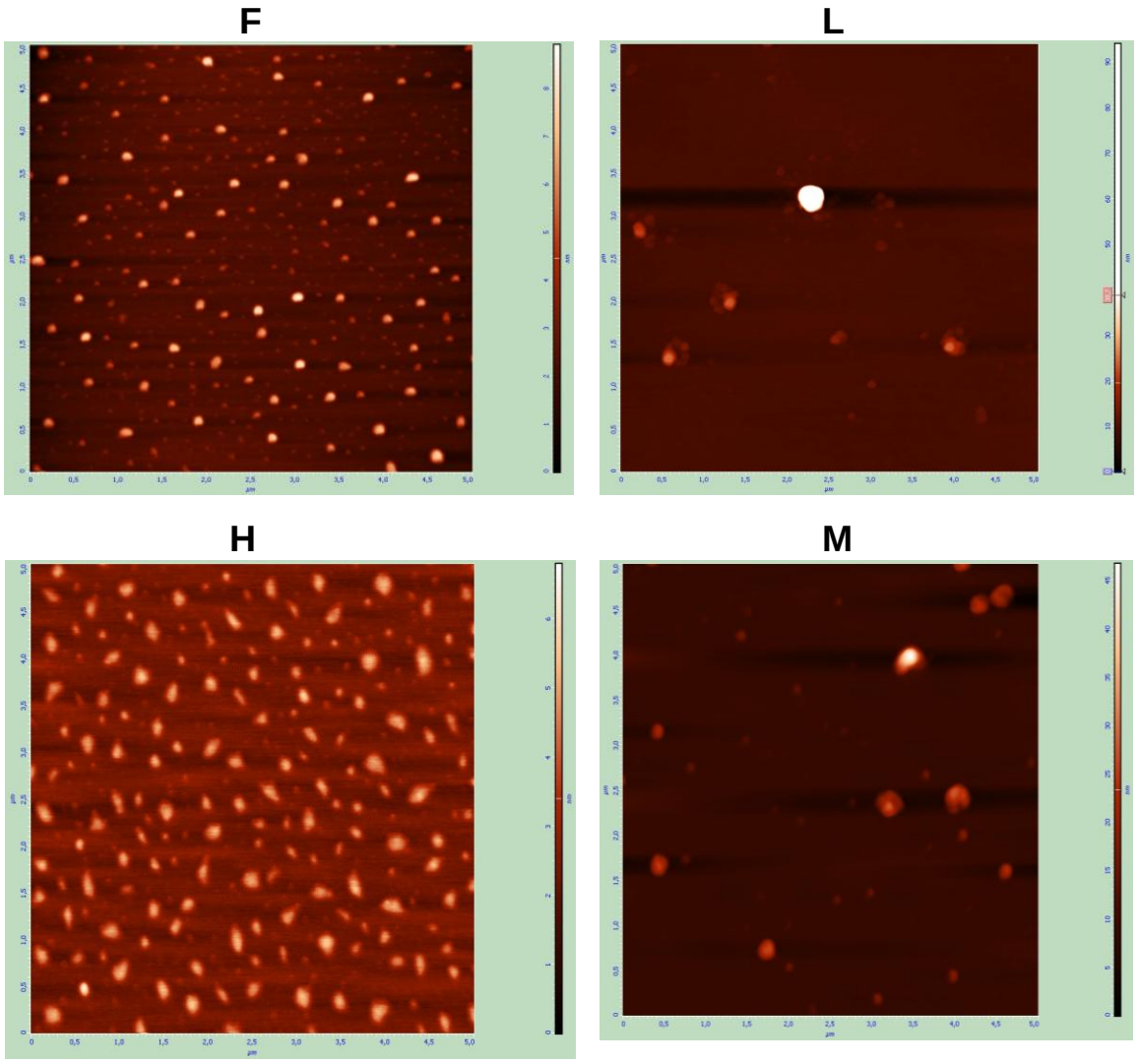

Fig. 2-41. Comparison of the 5 µm x 5 µm magnification images of the four samples.

The general appearance of the nanoparticles is flat, with height 1/10 of the width. The size range is approximately from 20nm x 2nm (width x height) to 200nm x 20nm.

There is a higher density of particles for samples produced with recipes “F” and “H1”. One possible explanation can be the solvent: they are dissolved in Tris buffer, while samples “L3” and “M3” in ACN/Water 9:1 v/v. This fact could

hamper the attachment of the particles onto the mica surface. More aggregates are present in samples prepared in ACN/W.

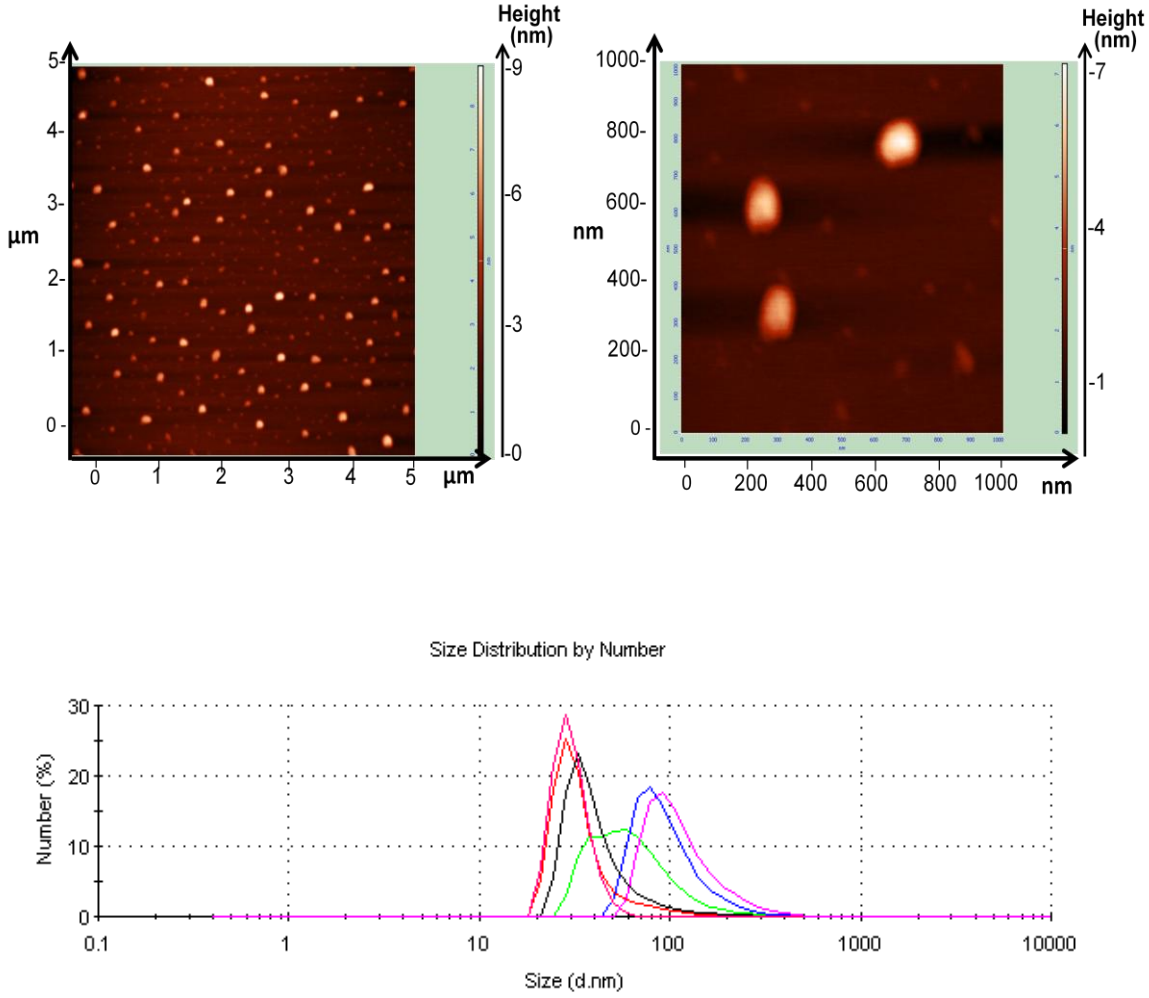

Fig. 2-42. Comparison of AFM and DLS data on a sample prepared with recipe "F" (HEMA/BIS 1%T, 80%C, 5 min of polymerisation in water). The six peaks represent the size distribution by number of particles measured by the instrument at different times. Measurements are typically made every 3 minutes.

There is a seemingly comparable size pattern between AFM and DLS data: AFM pictures show a general pattern of bigger, evident nanoparticles with dimension around 100 nm x 7 nm (width x height) on a layer of smaller particles with dimension around 20 nm x 5 nm. A similar pattern seems to emerge from DLS data, with a detected population apparently split into two parts: the first having a hydrodynamic diameter of approximately 20 nm and the second of 80 nm.

2.5.6.5 Yield evaluation of large-scale synthesised nanoparticles

Here following the assessment of particles presence in concentrated samples. The amount of monomer, cross-linker and pTyr indicated in the table are the theoretically present in 1mL of sample if all the starting material was converted to nanoparticles. The cross-linker content was 80%C (mol/mol) for all the recipes.

Tab. 2-9. Weight of particles in large-scale synthesised samples.

Recipe	Monomers	% T	mg cross-linker	mg monomer	mg Fmoc-pTyr	Solvent	Amount (mg)
F	HEMA/BIS	1	97.4	20.6		W	1.0
F + Fmoc-pTyr	HEMA/BIS	1	97.4	20.6	38.2	W	0.0
H1	HEMA/BAP	1	88.4	29.6		W	0.3
H1+ Fmoc-pTyr	HEMA/BAP	1	88.4	29.6	53.2	W	0.5
L3	HEMA/BIS	0.2	19.5	4.1		A/W	0.0
L3+ Fmoc-pTyr	HEMA/BIS	0.2	19.5	4.1	7.7	A/W	0.9
M3	DAU/BIS	0.2	19.5	4.5		A/W	0.2
M3+ Fmoc-pTyr	DAU/BIS	0.2	19.5	4.5	7.7	A/W	0.3

The results show a proportionally lower amount of material produced on a large scale with respect to the amount prepared on a small scale (from 2 to 10 times less). This reduced efficiency could be due to the reduced amount of light that reaches the reagents. The glass of a bottle is in fact thicker than the glass of a vial and the reagents are in media less exposed to the light due to the greater volume of liquid.

2.5.6.6 Cleaning of polymers prepared with standard bulk synthesis

Only HEMA/BIS and DAU/BIS in Tris buffer were prepared with a standard synthesis method to evaluate binding properties. Here following the graphs of the cleaning of the polymers. The cleaning proceeded until there was no further decrease of the signal (Abs< 0.05).

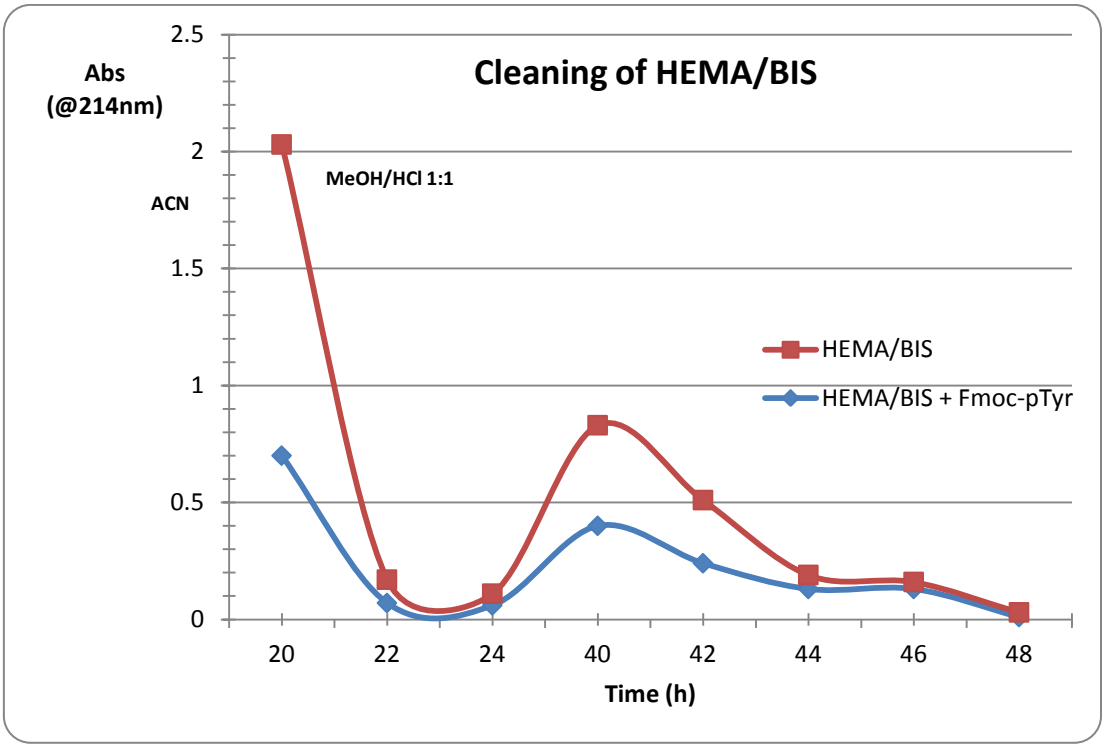

Fig. 2-43. Cleaning of HEMA/BIS NIP and MIP.

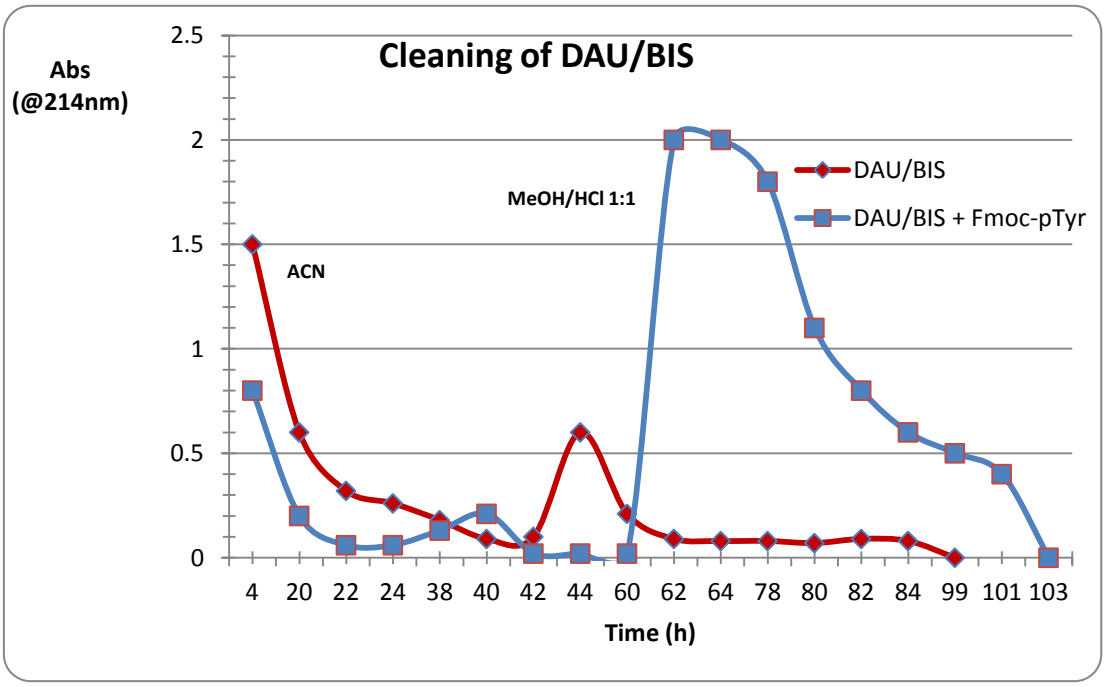

Fig. 2-44. Cleaning of DAU/BIS NIP and MIP.

After cleaning the samples were dried on a cellulose filter paper for 72h. The amount of polymer is reported in Tab. 2-10 with the corresponding yields:

Tab. 2-10. Amount and yield of the polymers prepared with standard bulk synthesis.

	HEMA/BIS MIP	HEMA/BIS NIP	DAU/BIS MIP	DAU/BIS NIP
Amount (mg)	216	143	43	118
Yield %	43	29	9	24

The amount of DAU/BIS MIP was not sufficient to perform rebinding experiments, which were therefore only carried out on HEMA/BIS polymers. An optimisation of the synthesis conditions has to be made in order to produce a greater amount of material.

2.5.6.7 Rebinding experiments

Results of testing presented here present the calibration curve for pTyr and the graph showing the evaluation of pTyr binding properties of HEMA/BIS NIP and MIP. The measurements were made in triplicate.

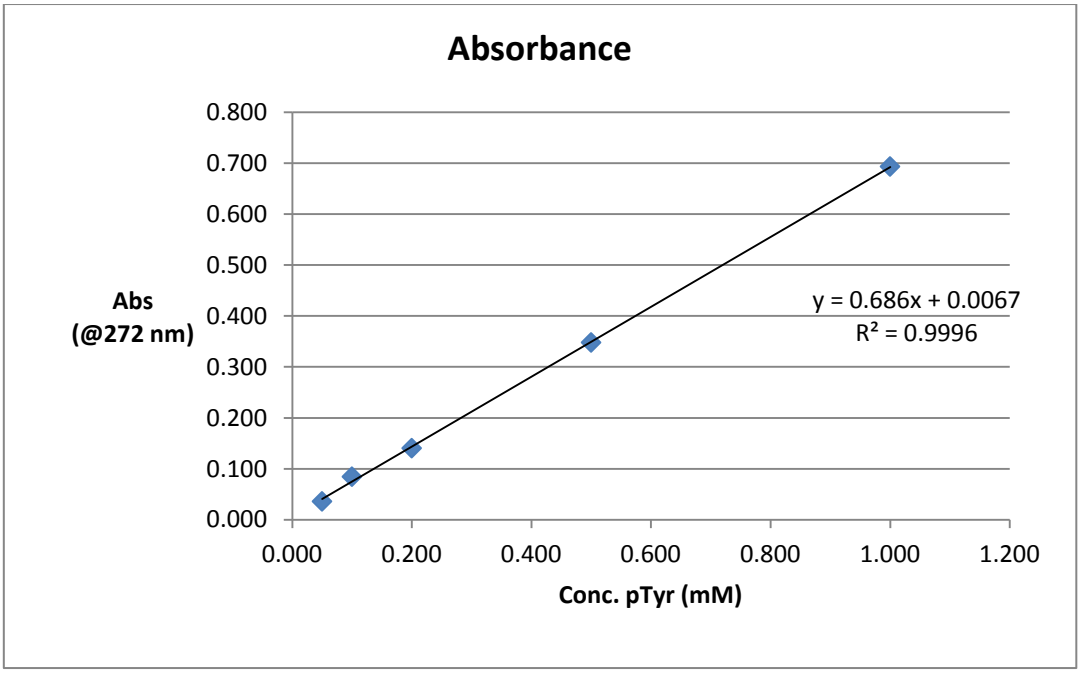

Fig. 2-45. Calibration curve for increasing concentration of pTyr.

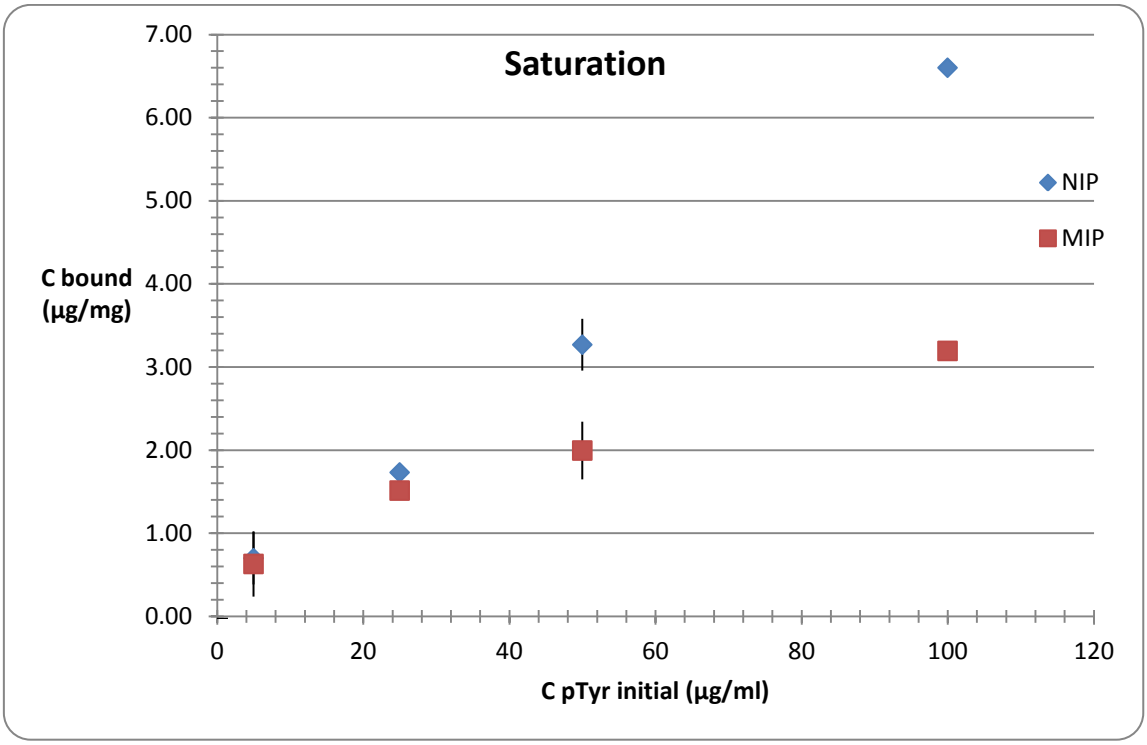

Fig. 2-46. Saturation curve for increasing concentration of pTyr.

From the graphs it emerges that the MIP polymer has a saturation behaviour, while NIP definitely increases the substrate incorporation at increasing concentrations. The capacity of the MIP resin tends to settle around 3 µg/mg resin (11 nmol/mg). The apparent better functioning of NIP polymer with respect to MIP could be explained with the presence of residual Fmoc-pTyr in the imprinted polymer, that saturates binding sites and repels substrate with the same charge. A more extensive washing of the polymer should therefore be tried to improve the MIP behaviour. Another possibility is the different structure of the NIP and MIP polymers, with the template contributing to the formation of less accessible binding sites.

2.5.6.8 Cleaning of polymers after rebinding

The graph shown here reports the cleaning passages. Absorbance data of NIP and MIP were put together given their identical behaviour in pTyr release.

Tab. 2-11. Absorbance data at 272nm for the cleaning solutions.

	HEMA/BIS and HEMA/BIS + pTyr	time (h)	total time (h)
MeOH/HCl 1:1	0.33	2	2
MeOH/HCl 1:1	0.31	1	3
MeOH/HCl 1:1	0.24	15	18
MeOH/HCl 1:1	0.16	1	19
MeOH/HCl 1:1	0.12	1	20
MeOH/HCl 1:1	0.06	1	21
MeOH/HCl 1:1	0.04	1	22
MeOH/HCl 1:1	0.18	15	37
MeOH/HCl 1:1	0.05	1	38
MeOH/HCl 1:1	0.003	2	40
Tris	0.001	2	42
Tris		final	final

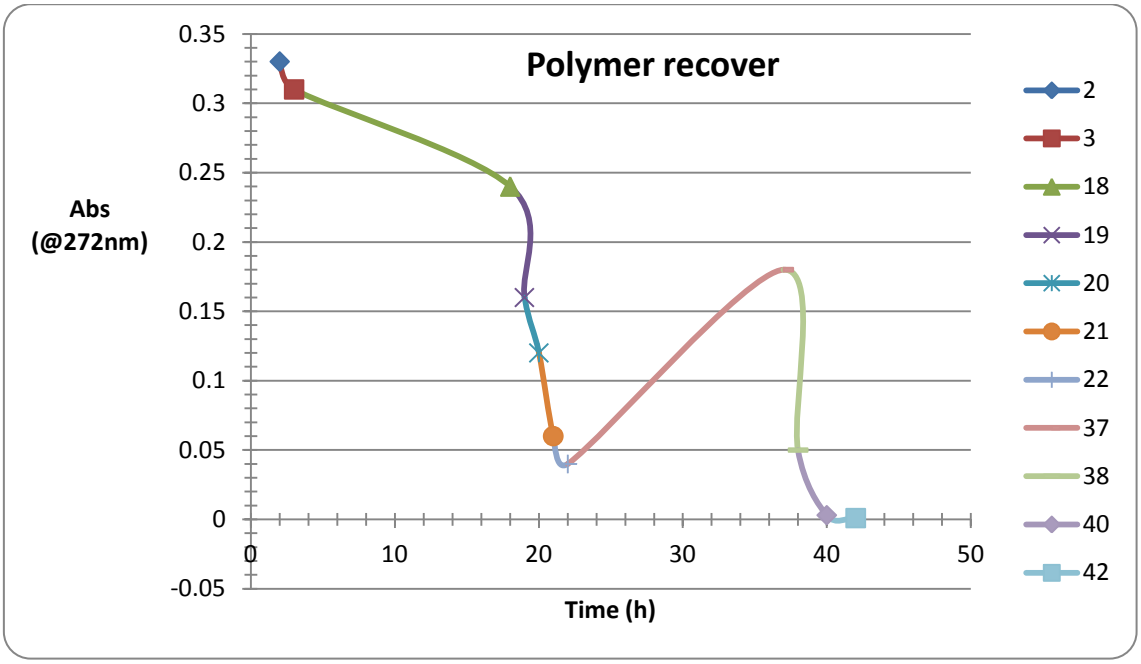

Fig. 2-47. Trend of pTyr amount extracted from the polymers.

Two days were necessary for the complete cleaning of the polymers from the substrate pTyr (Abs <0.01).

2.5.6.9 Rebinding after cleaning

The graph presented here shows the results of rebinding experiments after polymer cleaning.

Tab. 2-12. Absorbance data obtained in rebinding experiments.

H/B (NIP) µg/ml	Abs	Conc (µg/ml)	C Bound (µg/ml)	C Bound (µg/mg)
13	0.039	12	0.71	0.14
26	0.070	24	1.92	0.38
52	0.136	49	2.81	0.56
130	0.337	126	4.33	0.87
260	0.667	251	8.78	1.76

H/B pTyr (MIP) µg/ml	Abs	Conc (µg/ml)	C Bound (µg/ml)	C Bound (µg/mg)
13	0.038	12	1.09	0.22
26	0.076	26	-0.37	-0.07
52	0.138	50	2.04	0.41
130	0.344	128	1.67	0.33
260	0.676	255	5.35	1.07

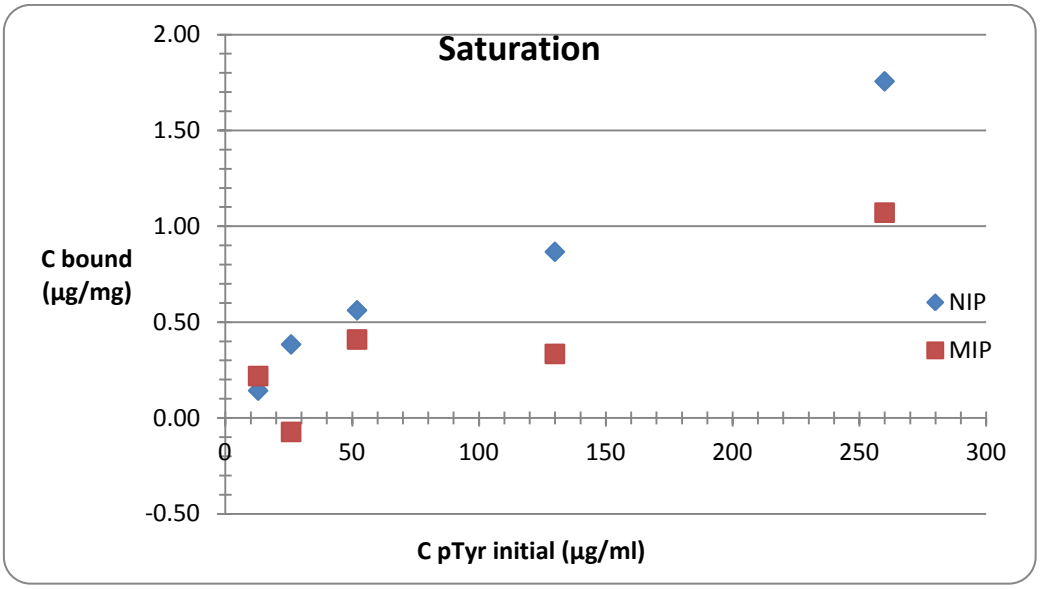

Fig. 2-48. Graph reporting the saturation of NIP and MIP polymers.

From the graph it can be noted that MIP tends to bind less substrate than NIP. The binding capacity after cleaning was shown to be much lower than before the cleaning, being 6 times less.

The complete saturation of the polymers could not be reached, anyway higher concentrations of substrate would give absorbance values out of the range of confidence of the instrument (0.001<Abs<1.0).

2.6 Conclusion

A photopolymerisation method for the production of MIP nanoparticles was evaluated here.

The method was tested under different conditions, including use of different monomers, cross-linkers and solvents.

A remarkable result, already reported by Wulff et al. (Wulff G, 2012), regards the effect of a “bad” solvent, that keeps the size of the particles small avoiding their continuous growth in solution through precipitation.

Good results both for size and polydispersity were obtained with the following recipe (“F”): HEMA/BIS 1%T, 80%C, MB 100µM, TSIA 1mM, DPI 50µM, agitation, 5 min polymerisation. Zave was 163 ± 16 nm and PdI 0.332 ± 0.101, with good reproducibility.

Good size results were obtained also with the use of BAP as cross-linker (“G” recipe: Zave 81 ± 29 nm), but for the price of a higher polydispersity (PdI 0.756 ± 0.219).

Lowering the monomers content from 1% to 0.2% brings unexpected enlargement of nanoparticles both in TRIS buffer and acetonitrile/water 9:1 v/v (recipes F-I, P-Q, Fig. 2-10).

DAU shows faster polymerisation kinetics than HEMA in TRIS buffer, having a turbidity point of 3 min at 1%T and 15 min at 0.2%T (HEMA does not give turbidity for both recipes after 60 min). Moreover DAU nanoparticles are in general bigger than those incorporating HEMA (Fig. 2-11).

The addition of Fmoc-pTyr does not produce a significant change in size or polydispersity (recipes F-P, L-S and M-T, Fig. 2-14).

The yields were between 0.5% and 5.5%, with no significant difference between the use of different monomers (Tab.2-8).

HEMA/BIS recipe was produced with a standard bulk synthesis and subjected to rebinding experiments. The results show a saturation behaviour for the MIP and the tendency to accumulate the substrate for the NIP. The binding capacity for the MIP was 3 µg/mg (11 nmol/mg) resin.

The results can be considered as still preliminary, with the perspective to evaluate binding characteristics for other recipes.

Nevertheless the DLS analysis showed that our method of synthesis is effective in the production of particles with size around 100 nm, confirmed through AFM microscopy. Moreover an interesting result was the low polydispersity of the particles that in many cases was below 0.2.

AFM showed particles with a flattened shape, probably due to the fact that a hydrogel is soft and the combined effect of gravity, surface attraction and pressure of the tip of the probe lower their height (Weisenhornt AL, 1993).

The future perspectives of this research line consist of extending the evaluation of the binding properties to other recipes. In particular, testing the properties of the nanometric format (the four recipes produced on large scale) would give us an indication of the possibility of production of a valid alternative material to phosphospecific antibodies.

A peculiar characteristic of MIPs is in fact the possibility of being shaped around a template creating a cleft complementary to it: in the case of phosphopeptides this could mean creating a material with complementarity not only for a phosphate group but also for an extended epitope, such as an aminoacidic sequence flanking a phosphoamino acid. This is an enhanced characteristic with respect to the usual resins employed in phosphoproteomics, such as TiO_2, that are specific only for the phosphate group (Helling S, 2011).

Not many examples of phosphoamino acid imprinting can be found in the literature, and these studies can be considered directed towards the creation of a first generation of materials. Helling et al. (Helling S, 2011) tested the chromatographic performance of a crushed monolith with respect to TiO_2, finding a significant advantage in the selectivity for pTyr down to the low fmol level with respect to other amino acids, plus a preference for pTyr containing peptides, recovering a 18-fold more p-angiotensin II than the non-phosphorylated peptide (Helling S, 2011). A further advantage of the nanometric format over microparticles could be the enhanced characteristics with respect to the time of diffusion, thus reducing the time for analysis, plus a better homogeneity of the binding sites.

In practice, the next experiments will be to test the material against pTyr-containing peptides to evaluate its selectivity towards the non-phosphorylated counterparts and pSer/pThr containing peptides. A stable suspension with known concentration of nano-MIPs could be directly added to a peptide mixture and ultrafiltered after incubation: the solid material will contain bound phosphopeptides that can be subsequently extracted with a proper choice of buffer.

3 Chapter

DEVELOPMENT OF AN SPR BIOSENSOR FOR HEPCIDIN HORMONE

3.1 Introduction

Iron homeostasis related disorders have a high incidence in the population. Both anemias, in which iron is deficient, affecting at least 500,000,000 people in the world, including at least 2-5% of adolescent at every latitude (Andrews NC, 1999), and iron overload disorders, as Hereditary Haemocromatosis (HH) are widespread. The C282Y allele on the HFE gene, which is mainly linked to HH, occurs in 5-10% of the European population (Andrews NC, 1999). It was demonstrated that iron homeostasis is regulated by the 25 amino acid peptide hormone Hepcidin (Hepc) and that urinary and blood levels of Hepc are associated with dis-regulation of iron metabolism (Pigeon C, 2001).

Hepcidin regulates iron export from enterocytes and macrophages by binding the only known iron export protein, ferroportin (Nemeth E, 2004). It is synthesised in the liver as an 84-amino acid pre-pro-hormone and matured by proteolysis through a furin cleavage to generate the biologically active 25-aa peptide (Hepc-25) that is secreted into circulation (Gagliardo B, 2009). Hepc-25 leaves the body via secretion through the kidneys (Park CH, 2001).

In contrast to serum, where the Hepc-25 (2789.4 Da) form is detected almost exclusively, urine also contains N-terminally truncated peptides of 22 amino acids (Hepc-22; 2436 Da) and 20 amino acids (Hepc-20; 2191.7 Da) (Park CH, 2001, Krause A, 2000).

Structurally, hepcidin shows a secondary amphipathic structure and is particularly rich in basic amino acids that confer a positive charge with an isoelectric point of 8.2 (Krause A, 2000). The eight cysteine residues contained within hepcidin form four disulfide bridges (Fig. 3-1) (Park CH, 2001).

Fig. 3-1. NMR structure of the major form of human hepcidin The amino and carboxy termini are labelled as N and C respectively Disulfide bridges are in yellow (This research was originally published in Journal of Biological Chemistry Jordan JB, Poppe L, Haniu M, Arvedson T, Syed R, Li V, Kohno H, Kim H, Schnier PD, Kim H, Schnier PD, Harvey TS, Miranda LP, Cheetham J, Sasu BJ, Journal of Biological Chemistry 2009, 284, 24155, 24167 © The American Society for Biochemistry and Molecular Biology.

Because hepcidin levels reveal important clinical information about pathological states, measurement of hepcidin in urine or plasma as a biomarker may be interesting to apply in clinical practice.

Despite significant efforts, the development of a robust assay to detect hepcidin proved to be problematic. Initially, hepatic hepcidin mRNA expression in the liver was successfully used as a marker, but liver biopsies are rarely clinically indicated (Kemna EHJM, 2008). Immunoassays are commercially available for prohepcidin (DRG Diagnostics, Marburg, Germany), however, the assay does not recognise the biologically active Hepc-25 (Frazer DM, 2009). By contrast, the only available immunoassay against Hepc-25 is not widely available yet as a commercial product (Ganz T, 2008, Koliaraki V, 2009, Schwarz P, 2011). Therefore, several groups have developed assays to detect Hepc-25 based on mass spectroscopy (Ward DG, 2008, Bozzini C, 2008, Kemna E, 2005, Kemna EH, 2007, Tomosugi N, 2006, Altamura S, 2009).

These latter techniques have the disadvantage to be quite expensive and demanding in terms of sophisticated instrumentation and dedicated staff. Moreover, MS methods revealed the presence, in biological fluids, of non-functional truncated isoforms of Hepc (e.g. Hepc-22 and Hepc-20), which further complicated the interpretation of the most advanced immunological assays. These forms, in fact, are detected by the immunoassays but do not intervene in iron balance regulation (Swinkels D, 2008).

It can be concluded that, notwithstanding the very latest progress, a method for blood and urine Hepc measurement having the characteristics of accuracy, ease of implementation, and large scale distribution at fairly low cost is still not available.

De Domenico et al. (I De Domenico, 2008) identified the hepcidin-binding domain (HBD, Fig. 3-2) on ferroportin and showed that a synthetic 20 amino acid peptide corresponding to the HBD summarises the characteristics and specificity of hepcidin binding to cell-surface ferroportin. They subsequently developed a competitive assay to measure hepcidin concentrations in small volumes of biological fluids.

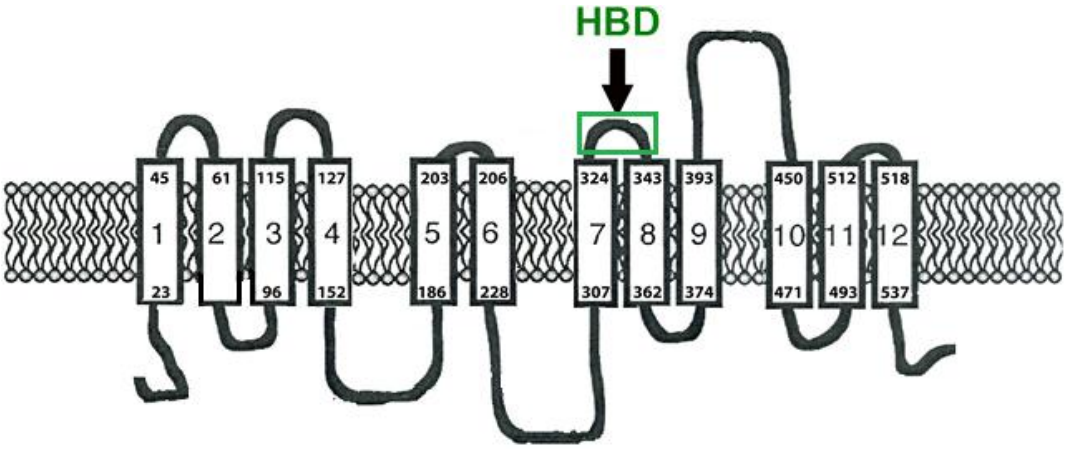

Fig. 3-2. Predicted topology of ferroportin (Fpn) The structure of Fpn is based on the study of Liu et al, 2005 [adapted from ref.108]. We can note the HBD synthetically mimicked.

Our attempt is to improve the measurement of the hepcidin levels in body fluids by developing a point-of-care and label-free assay based on the affinity

between hepcidin and this synthetic peptide. For the purpose we exploited the Surface Plasmon Resonance (SPR) technique (see next paragraph) and the immobilisation of the synthetic ligand on CM5 Biacore chips. These chips present a carboxymethyl dextran matrix on the surface, to which the N-terminal of HBD can be bound through the use of EDC/NHS chemistry.

The sequence of the wild-type HBD is FDCITTGYAYTQGLSGSILS (pI=3.8). To increase solubility, the peptide was synthesised with two arginines added at the amino and carboxyl termini (pI=10.0). The arginines did not affect the specificity, temperature dependence, or affinity of HBD for hepcidin (Liu X, 2005). The presence of these extremities could favour the binding of hepcidin, freeing amino acids able to link the hormone. We tested the effectiveness of the peptide bait linking it to the chip and evaluating the instrumental response to different concentrations of hepcidin-25.

3.2 Surface Plasmon Resonance

Surface Plasmon Resonance is a biosensing technique widely employed in testing the affinity between ligands and analytes. Biosensors can be defined as "…devices comprising a biologically sensitive material immobilised in intimate contact with a suitable transducing system to convert the biochemical signal into a quantifiable and processable electric signal" (Lowe CR, 1984). The physical phenomenon at the core of the SPR system is the variation of refractive index of a dielectric medium in contact with a metal (Cooper MA, 2009). Usually gold is chosen for its better performance and inertness.

When a linearly polarised beam of light (polarisation parallel to the plane of incidence) hits the surface of the metal, the radiation is totally internally reflected if the angle of incidence is higher than the critical angle. At a certain angle of incidence, called the SPR angle (Θ_{SPR}), the component of the wave of light parallel to the surface excites the polaritons, waves of electrons along the surface of the metal, if their wavelength corresponds to the wavelength of the incident light (i.e. there is resonance). In this case an evanescent field is generated at the interface between metal and medium. The amplitude of this field decays exponentially from the surface and is sensed usually at a maximum distance of ~100 nm from the surface. The SPR angle depends on the

wavelength, on the metal, on the temperature and on the polarisability of the medium at the interface with the metal, strictly connected to its refractive index (*n*) by the Eq. 3-1:

$$n = \sqrt{\epsilon_r \mu_r}$$

Eq. 3-1.

where ε_r is the relative permittivity of the material and μ_r is its relative permeability.

This absorption is evidenced by a minimum of reflected light that arrives to a detector (usually a photodiode array) at the SPR angle (Θ_{SPR}). The dependence of Θ_{SPR} from the refractive index of the medium in contact with the metal is the principle at the basis of the system. By immobilising a ligand on the surface, for example, the binding events of analytes to the ligand can be monitored through the variation of the refractive index, proportional to the mass of analyte in proximity to the interface metal/dielectric (Fig. 3-3).

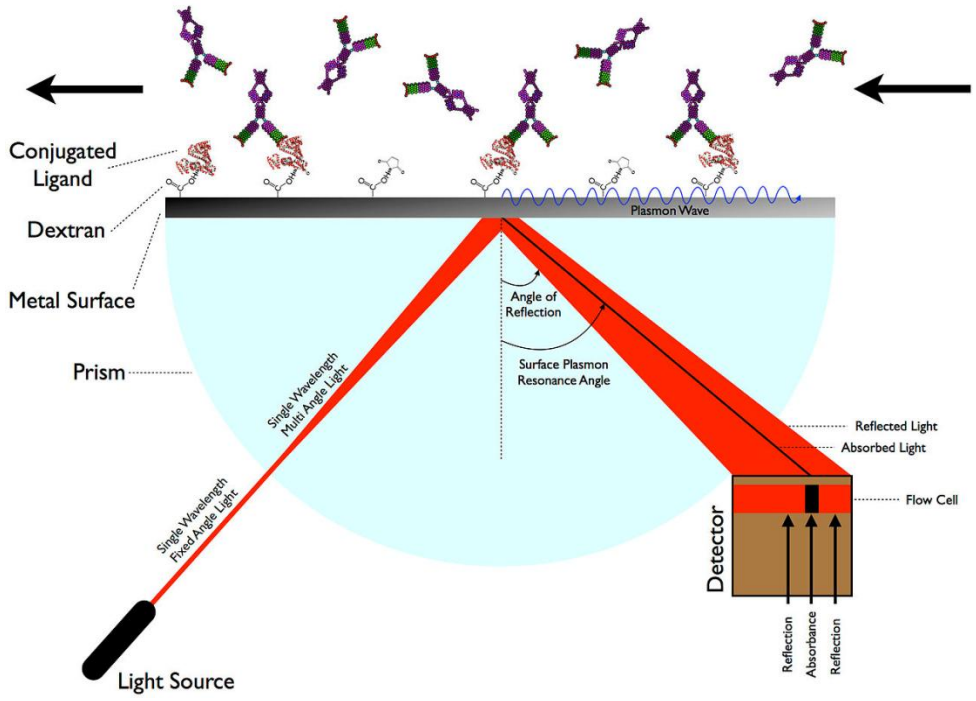

Fig. 3-3. Representation of the SPR principle. The SPR angle (angle at which the incident light is absorbed and not totally reflected) depends on the refractive index of the medium in contact with the metal layer on which the light impinges. This refractive index is directly proportional to the mass of analyte bound to the metal surface (Picture taken from: Wikipedia).

The variation of *n* is converted in Responsive Units (RU), proportional to the mass of analyte. In the case of proteins, these molecules all have a similar *n*, thus a binding event or simply the presence of any protein in proximity of the surface generates a signal proportional to the mass: 1RU corresponds to 1 pg/mm^2 of protein. The binding event is actually a dynamic process that is expressed by a profile of RU variation, called a sensorgram (Fig. 3-4).

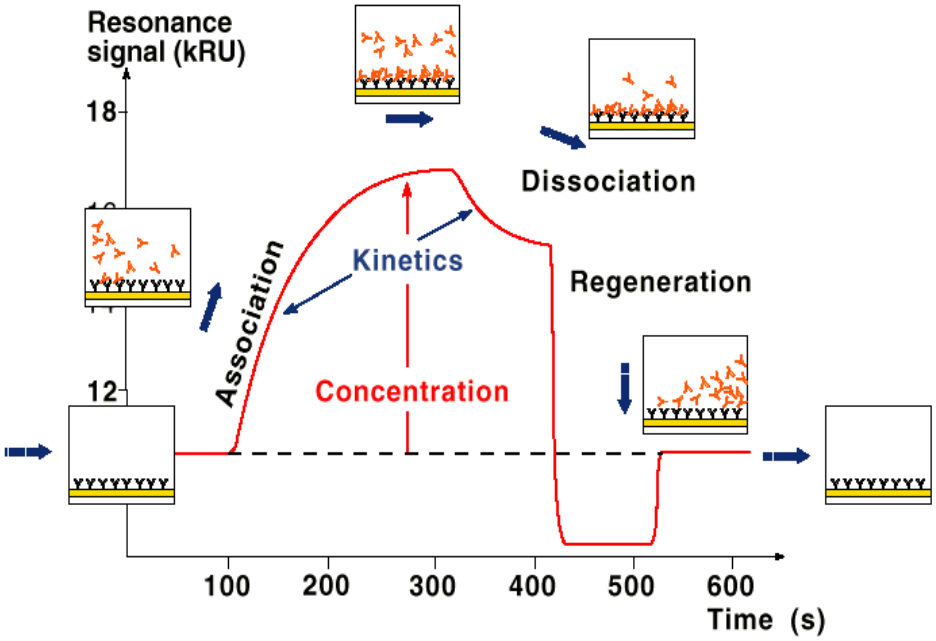

Fig. 3-4. Typical SPR sensorgram depicting a binding event (picture taken from: Biacore website).

When a solution of analyte is injected in the system and arrives to the detecting zone, firstly a variation of RU due to the different refractive index of the media is sensed: this is called a “bulk effect”.

The binding of the analyte to the surface is subsequently detected, generating an increase of the signal that finally reaches a plateau, when a dynamic equilibrium occurs. By stopping the injection of analyte a decrease of the signal is detected, and this decrease depends on the affinity between analyte and ligand. With SPR the strength of interaction between partners, one of which is immobilised on the surface, can be evaluated, as explained in Par. 3.4. Kinetic constants can also be measured by fitting the profile of binding and detachment (Fig. 3-4).

Biacore furnishes chips with different matrixes on a golden layer, to meet the need of the researchers. For example a carboxymethylated matrix gives good performance with proteins by furnishing sites of attachment through EDC/NHS chemistry and by minimizing the non-specific binding, a relevant problem when SPR technique is used with complex matrixes.

A commonly used Biacore chip is CM5, with a carboxymethylated highly branched matrix able to furnish multiple points of attachment to the ligand molecules.

3.3 Materials and methods

3.3.1 Reagents

CM5 chips were purchased from Biacore (Sweden). Ethanolamine (Eth), 1-ethyl-3-(3-dimethylaminopropyl)carbodiimide (EDC), N-hydroxysuccinimide (NHS) were from Sigma Aldrich (UK). Synthetic Hepc-20 and Hepc-25 were purchased from AbCam (UK); peptide ligands (HBD 20-mer and RR-HBD-RR 24-mer) are custom made at Peptide 2.0 (USA). All reagents and solvents were used at analytical grade.

3.3.2 Peptide immobilisation on CM5 chips

The CM5 chips were activated with the coupling mixture EDC/NHS (200 mM/50 mM) for 75 min (75 µl at 10 µl/min). The peptide RR-HBD-RR was dissolved at concentration of 50 µg/mL in 10 mM phosphate buffer at pH 7.0 and flushed for 12 sec at 10 µL/min flow rate. Quenching of reaction was performed with 1M Eth at flow rate 10 µl/min for 25 min (total volume: 25 µl) One channel was kept as reference by injecting only Eth after EDC/NHS activation.

3.3.3 Hepcidin measurements

Hepcidin-25 was injected simultaneously in three flow channels of the IFC (Integrated Microfluidic Cartridge). A fourth channel was kept as reference. The signal from this reference channel was subtracted from the RU response of the three channels to give the final value of RU. The chosen concentrations were: 1, 5, 10, 25, 50, 100 ng/mL. Running buffer was PBS, whose flow was kept at 2 µl/min.

3.4 K_D estimation

An estimation of the affinity between the ligand RR-HBD-RR and hepcidin-25 was attempted through the use of Biacore Biasimulation software.

Curve-fitting of the experimental data enables the association and dissociation rate constants and the equilibrium dissociation constant to be determined. Of the models proposed by Biacore®, the “1:1 binding” model was the one that gave the best fit (the lowest χ2). It is the simplest model and describes the interaction between an analyte A and a ligand B as:

$$A + B \rightleftharpoons AB$$

Eq. 3-2.

The association rate ka (in L/(mol s)) corresponding to the number of complexes formed per second in a molar solution of HBD and Hepc-25, is defined by the formula:

$$\frac{d[AB]}{dt} = k_a[A][B].$$

Eq. 3-3.

Where [A], [B] and [AB] are the concentrations of A, B and the AB complex The dissociation rate constant kd (in s^{-1}), corresponding to the portion of the complex that dissociates in 1 s, is given by the formula:

$$-\frac{d[AB]}{dt} = k_d[AB]$$

Eq. 3-4.

Association and dissociation actually occur at the same time. Furthermore, association is equal to dissociation at equilibrium, resulting in an equilibrium dissociation constant of:

$$K_{\mathrm{D}} = \frac{[A][B]}{[AB]} = \frac{k_{\mathrm{d}}}{k_{\mathrm{a}}}.$$

Eq. 3-5.

A high K_D therefore means that there is low affinity between the analyte and the ligand. By fitting the analytical expressions of the response R(t) to the R(t) curves in RU obtained in real time by the Biacore® system, it is possible to deduce these various constants, ka, kd and K_D, that characterise the binding of the analyte (Hepc-25 or Hepc-20) to the ligand (RR-HBD-RR).

3.4 Results and discussion

3.4.1 Immobilisation

The maximum amount of ligand to be bound to a CM5 chips was assessed to be 5500 ± 500 RU (1000 RU = 1 ng/mm^2). The choice was therefore to keep the ligand level around 3000 RU, to permit the analyte to 'sneak' between the immobilised ligands avoiding steric crowding on the chip surface.
This result was obtained with a 12 µl injection at 10 µl/min flow (Tab. 3-1).

Tab. 3-1. Immobilised peptide amount in three channels, expressed in RU (1000RU=1ng/mm^2).

	Flow channel 1	Flow channel 2	Flow channel 3
Peptide (RU)	2800	3700	2250

3.4.2 Detection

Increasing amounts of hepcidin-25 and hepcidin-20 were injected, starting from 1 ng/mL increasing to 100 ng/mL. The response for the three channels is reported in Tab.. In this case a regenerating solution was not used during the experiment between the different injections, because the level of saturation of

the surface was minimal compared to the total amount of binding sites available (<5% considering the mass of analyte compared to the mass of ligand bound).

3.4.3 Regeneration

Different regenerating solutions were tried with the purpose of removing bound hepcidin while not to spoil or remove the ligand bound on the chip surface. Salt solutions were initially considered, with the idea of a “soft” regeneration. Increasing concentrations of NaCl were injected, and finally NaCl 500mM proved to be effective for the purpose. Other regenerating solutions (NaOH 1 mM, 10 mM glycine pH 2.5) had the drawback of significantly reducing the binding capacity of the ligand after their use.

Tab. 3-2. Hepcidin concentrations and relative instrumental response.

Hepcidins concentration (ng/mL)	Hepc-25 media (RU)	Hepc-20 media (RU)
1	10 ± 4	5 ± 2
5	15 ± 3	10 ± 2
10	21 ± 6	14 ± 3
25	26 ± 8	16 ± 3
50	36 ± 9	14 ± 3
100	67 ± 21	5 ± 2

Fig. 3-5 shows a sensorgram depicting the instrumental response due to different concentrations of analyte in a single flow channel. It can be noticed the proportionality of slope due to increasing concentrations of analyte. Stabilisation of baseline was allowed to occur after every injection.

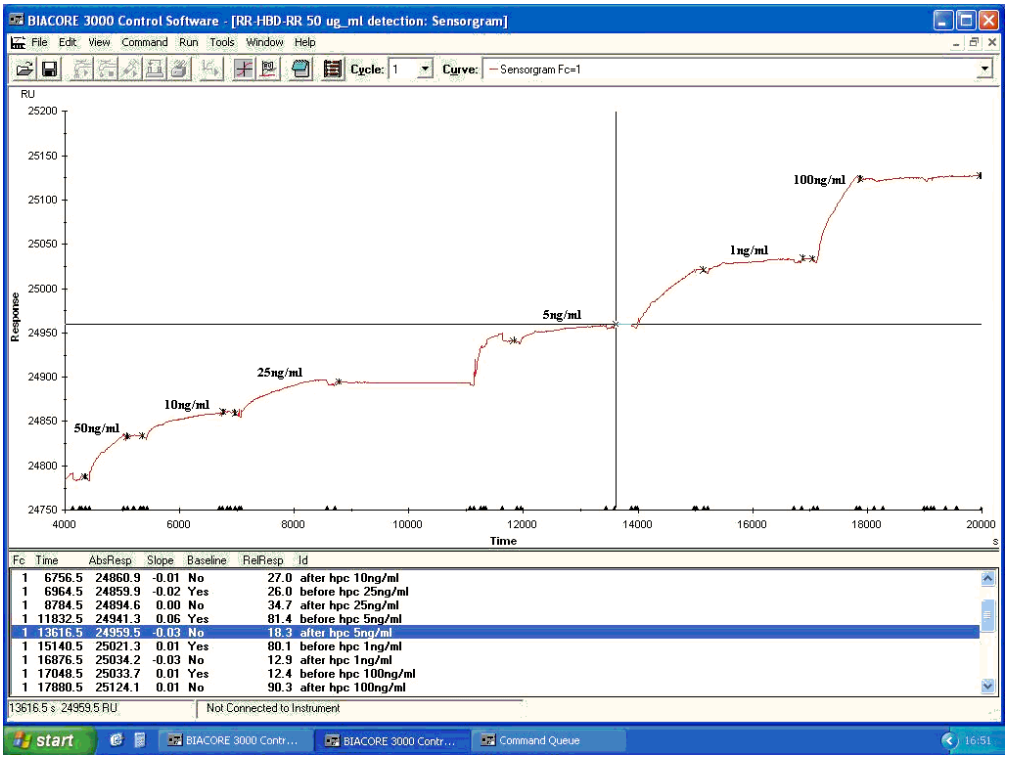

Fig. 3-5. Instrumental response following sequential injections of hepcidin in one of the available channels.

The binding curves following the sequential injections of increasing concentrations of hepcidin were then superimposed to highlight the proportionality of the signal to the presence of hepcidin (Fig. 3-6).

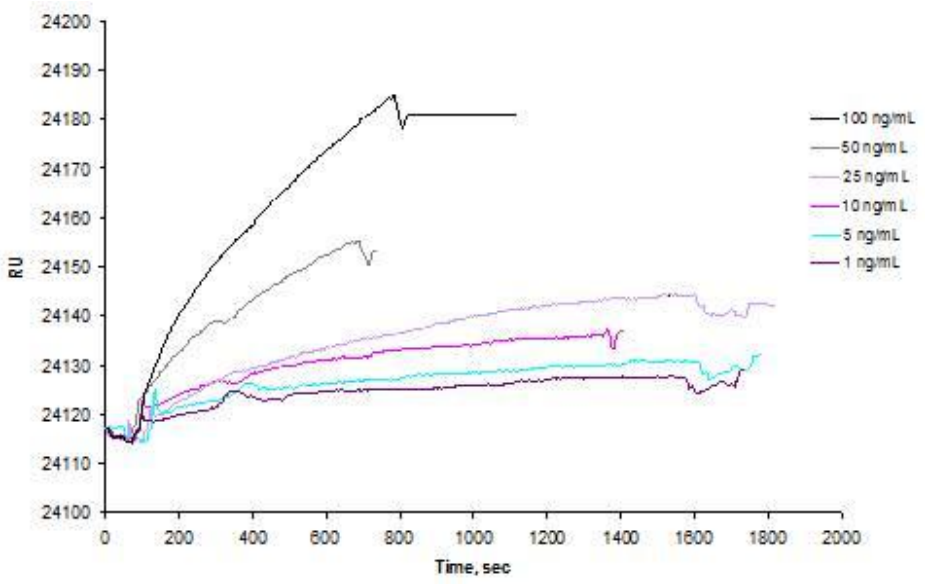

Fig. 3-6. Superimposition of instrumental responses due to increasing concentrations of hepcidin-25.

The response of the system to the increasing hepcidin concentration was used to produce a calibration curve (Fig. 3-7).

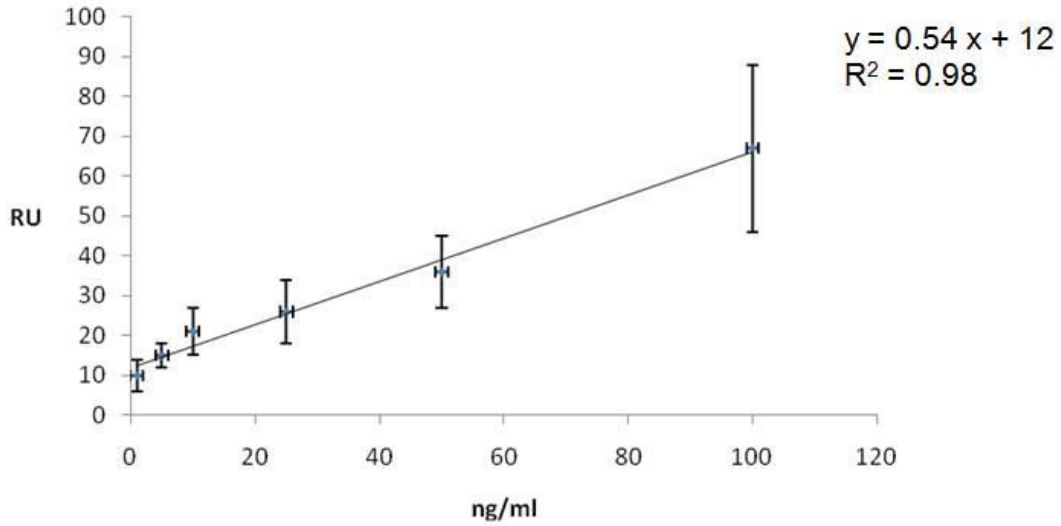

Fig. 3-7. Calibration curve related to increasing hepcidin-25 concentrations.

The response of the system was linear in the range of concentrations evaluated (R^2 = 0.98). Sensitivity was moderate (slope = 0.54), as well as the intermediate precision (average intra-assay CV% = 29). The specificity against the competitor hepcidin-20 is however good, even though not quantified for not having reached a saturation value of concentration. Anyway the response for hepcidin-20 at the highest concentration measured (100 ng/mL) was 7% than the response of hepcidin-25 (Tab.), and this result is therefore encouraging.

A couple of considerations should be made here: the first one regards the high standard deviation of the data, increasing at increasing concentrations. This fact could be explained with the big differences on the amount of the immobilised fishing ligand on the channels. More experiments with other chips could be made to shed light on this problem. Another consideration regards the high value of the intercept, meaning that there is a high response at concentration of analyte close to zero. An injection of the buffer alone does not give a response higher than 2 RU, meaning that it is hepcidin that causes the increase of the signal. Anyway the calibration curve tries to fit in a linear fashion data that do

not show an exactly linear trend. This could give an estimation of the intercept value higher than expected.

3.4.4 K_D estimation

The evaluation of K_D with our data gave us an attempted value of K_D of 50 nM, consistent with data previously reported for measuements made in solution. De Domenico et al., in fact, estimated the value of dissociation constant of RR-HBD-RR with hepcidin to be 200 nM (De Domenico I, 2008). The small difference could be explained by the difference in interaction between partners in solution and when a ligand is immobilised on a surface (Cochran S, 2009).

3.4.5 LLOD estimation

The Lower Limit Of Detection (LLOD), considered as a signal 3 times the standard deviation of the blank (injection of the buffer alone), was assessed to be 5 ng/mL.

3.5 Conclusion

The clinical relevance of hepcidin quantification is elevated. Therefore, the measurement of hepcidin in serum and urine has been identified as a valuable parameter for the differential diagnosis of physiopathological states. In iron overload syndromes the hepcidin level allows a diagnostic pre-genetic scheme to be drawn for grouping of patients (Kaneko Y, 2010). Whereas in anaemic patients, a hepcidin level threshold was proposed to be 129.5 µg/L to help diagnose iron deficiency in critically ill patients, thus directing them towards an appropriate therapy (Lasocki S, 2010). After myocardial infarction the levels of hepcidin have been observed to increase both in the ischemic and in the remote myocardium; such up-regulation seems to be specifically associated with hepcidin, as other iron-regulatory molecules did not show changes, and it was hypothesised to correlate with a defence mechanism to reduce iron toxicity and thus to reduce the expansion of the infarction (Simonis G, 2010). Hepcidin expression does correlate with inflammation and increases with increased interleukin-6 (IL6) (Nemeth E, 2004) and is negatively correlated with erythropoietin as shown in kidney impairment patients (Ashby DR, 2009).

Our results show the ability of the HBD ligand to bind hepcidin-25, indicating the possibility of the measurement of the analyte by the use of the SPR technique.
The system showed poor binding for the competitor hepcidin-20, an interferent in the measurement of hepcidin-25 by ELISA, at least for the higher concentrations of analytes (Kroot T, 2010). Regarding this aspect our system could therefore have a significant advantage.
SPR is also a rather straightforward technique: once the protocol of analysis has been optimised the measurement could be made by non-specialist personnel. The system permitted the measurement of hepcidin in the patho-physiological concentration range of 5-100 ng/L (1.5 – 35 nM), with LLOD of 5 ng/mL (1.5 nM). This limit is higher compared to c-ELISA (0.01 nM) (Kroot T, 2010) and similar to that of MS approaches (0.55 – 1.55 nM for SELDI-TOF (Swinkels D, 2008), 0.5 nM for WCX-TOF (Kroot T, 2010), 0.75 nM for MALDI-TOF (Anderson DS, 2010)) but nevertheless can reveal an hepcidin deficit, that starts to be pathological at 5 nM (Ganz T, 2008, Galesloot TE, 2011).
One of the main problems of this technique is to overcome the non-specific binding. This is actually the main problem to solve when needing to deal with complex matrices such as serum. Some proteins such as albumin have an overwhelming presence in blood that can be more than 6 orders of magnitude higher than the concentration of disease markers. Its physiological concentration is in fact assessed to be 35-50 mg/mL (Anderson NL, 2002), while hepcidin concentration was evaluated to be between 5 and 350 ng/mL considering both sexes (Ganz T, 2008). The natural proceeding in the method development could therefore be the analysis of serum samples after filtration on a high MW cut-off membrane. Kobold et al, for example, obtained a recovery of hepcidin between 95 and 100% by filtering serum samples on a 10 kDa cut-off cellulose acetate membrane (Kobold U, 2008).
In conclusion, the system under development here described has the potential to permit an easy and straightforward measurement of hepcidin in body fluids, a highly desired goal of the scientific community.

4 Chapter

GENERAL CONCLUSIONS

Proteomics showed a pivotal role in the process of the discovery of new potential biomarkers for diseases (Calligaris D, 2011). The methods are quite well established, but improvements at all levels are needed if we want to dig in the subproteome (proteins present in picomolar amount). Disease biomarkers are in fact often in this range of concentration in body fluids (Righetti PG, 2005). The detection and quantification of established biomarkers can also take advantage of biosensing techniques that are emerging as valuable diagnostic tools. Their inner potential lays in the possibility of developing the so-called point-of-care diagnostics, i.e. directly at the patient's bedside (Mascini M, 2008).
The use of proteomics techniques, in particular 2D-PAGE, has been applied here to discover up- or down-regulated proteins in umbilical cord serum and amniotic fluids of Intrauterine Growth Restricted (IUGR) foetuses. A total of 14 and 11 proteins were found to be modulated in IUGR umbilical cord serum and amniotic fluids respectively. In particular, proteins related to blood pressure, coagulation, immunity, oxidative stress and iron/copper metabolism were found to be involved in the IUGR pathological picture. Proteomics furnishes a snapshot of the whole protein complement in a particular stage of life and/or in a particular condition. This is however just the first step: the data obtained in this study necessitates a further validation on a larger scale and a deeper analysis to shed light on the pathological mechanisms. The final goal is in fact to detect diagnostic biomarkers which could help a specific and early diagnosis of IUGR.
The improvement of the analysis methods is at the basis of the process of biomarkers discovery. Phosphoproteomics is definitely a subject of importance to identify deranged mechanisms, it being involved in so many life processes such as signalling, cell duplication and apoptosis. Altered phosphorylation pathways are in fact present in pathologies such as cancer, neurodegeneration and diabetes (Thingholm TE, 2009).

A small step was made here in the production of Molecularly Imprinted Polymer nanoparticles (nanoMIPs) for the sequestration of phosphoproteins and/or phosphopeptides from complex protein mixtures. The challenge in the production of nano-MIPs is in fact to create a valid alternative to antibodies, whose cost is nowadays high and stability is low (Ye L, 2008). The experiments allowed the definition of a photoactivated synthesis protocol for the production of nanoMIPs and in the first experiments to evaluate the efficiency of the material towards the binding of phosphotyrosine. The loading capacity of the nanoMIPs was assessed. More experiments are however needed in order to extend the binding experiments to a wide range of nanoMIPs compositions (Wulff G, 2012).

The field of biosensors is definitely a sparkling one, with many papers published in recent years. Biosensors can give a boost to the process of biomarker detection, having the potential of miniaturization and thus employment directly at the patient's bedside, when not directly implanted under the skin (Lowe CR, 2011). An interesting subject for which to devise a biosensor is hepcidin, the major regulator of systemic iron homeostasis in mammals. Its quantification could be useful in the deepening the knowledge of iron imbalance-related diseases, in stratifying patients as well as in monitoring disease progression (Castagna A, 2010).

The detection and quantification of hepcidin-25 was here attempted with by employment of Surface Plasmon Resonance as the biosensing technique. A protocol for chip preparation was established and a calibration curve in the physiopathological range of concentrations was made. Moreover, the affinity between hepcidin-25 and its binding domain on ferroportin (HBD) was evaluated, assessing the negligible binding of HBD for the competitor hepcidin-20 above 50 ng/mL. This part of experiments should be considered as preliminary, and it has to be extended to the analysis of real samples, with the intention of selecting hepcidin as primary analyte to be measured, overcoming the hurdle of non-specific binding, in particular of highly abundant proteins of serum, such as albumin (Righetti PG, 2003).

In conclusion, the field of biomarkers discovery and quantification was here explored on three research topics. The results obtained are some steps on the path. More steps need to be taken in order to deepen our knowledge of these subjects in the near future.

REFERENCES

Airede, A.I. (1998). Serial copper and ceruloplasmin levels in African newborns with emphasis on the sick and stable preterm infant, and their antioxidant capacities. *Early Human Development* **52**, 199-210.

Albuquerque, C.P., Smolka, M.B., Payne, S.H., Bafna, V., Eng, J. & Zhou, H. (2008). A multidimensional chromatography technology for in-depth phosphoproteome analysis. *Molecular and Cellular Proteomics* **7**, 1389–1396.

Alpert, A.J. (1990). Hydrophilic-interaction chromatography for the separation of peptides, nucleic acids and other polar compounds. *Journal of Chromatography* **499**, 177–196.

Alpert, A.J. (2008). Electrostatic repulsion hydrophilic interaction chromatography for isocratic separation of charged solutes and selective isolation of phosphopeptides. *Analytical Chemistry* **80**, 62-76.

Altamura, S., Kiss, J., Blattmann, C., Gilles, W. & Muckenthaler, M.U. (2009). SELDI-TOF MS detection of urinary hepcidin. *Biochimie* **91**, 1335-1338.

Amarilyo, G., Oren, A., Mimouni, F.B., Ochshorn, Y., Deutsch, V. & Mandel, D. (2011). Increased cord serum inflammatory markers in small-for-gestational-age neonates. *Journal of Perinatology* **31**(1), 30-32.

Andersen, H.S., Gambling, L., Holtrop, G. & McArdle, H.J. (2007). Effect of dietary copper deficiency on iron metabolism in the pregnant rat. *British Journal of Nutrition* **97**, 239-246.

Anderson, D.S., Heeney, M.M., Roth, U., Menzel, C., Fleming, M.D. & Steen, H. (2010). High-throughput matrix-assisted laser desorption ionization-time-of-flight mass spectrometry method for quantification of hepcidin in human urine. *Analytical Chemistry* **82**(4), 1551-1555.

Anderson, N.L. & Anderson, N.G. (2002). The human plasma proteome: history, character, and diagnostic prospects. *Molecular and Cellular Proteomics* **1**, 845-867.

Andrews, N.C. (1999). Disorders of Iron Metabolism. The *New England Journal of Medicine* **341**, 1986-1995.

Ashby, D.R., Gale, D.P., Busbridge, M., Murphy, K.G., Duncan, N.D., Cairns, T.D., Taube, D.H., Bloom, S.R., Tam, F.W., Chapman, R.S., Maxwell, P.H. & Choi, P. (2009). Plasma hepcidin levels are elevated but responsive to erythropoietin therapy in renal disease. *Kidney international* **75**, 976-981.

Bairoch, A.& Apweiler, R. (2000). The SWISS-PROT protein sequence database and its supplement TrEMBL in 2000. *Nucleic Acids Research*, **28**, 45-48.

Bantscheff, M., Schirle, M., Sweetman, G., Rick, J. & Kuster B. (2007). Quantitative mass spectrometry in proteomics: a critical review. *Analytical Bioanalytical Chemistry* **389**, 1017–1031.

Baumann, M. & Meri, S. (2004). Techniques for studying protein heterogeneity and post-translational modifications. *Expert Reviews of Proteomics* **1**, 207-217.
Beausoleil, S.A., Jedrychowski, M., Schwartz, D., Elias, J.E., Villen, J., Li, J., Cohn, M.A., Cantley, L.C. & Gygi, S.P. (2004). Large-scale characterization of HeLa cell nuclear phosphoproteins. *Proceedings National Academy Science USA* **101**, 560-570.
Bellart, J., Gilabert, R., Fontcuberta, J. & Carreras, E. (1998). Coagulation and fibrinolytic parameters in normal pregnancy and in pregnancy complicated by intrauterine growth retardation. *American Journal of Perinatology* **15**, 81-85.
Belluco, C., Mammano, E., Petricoin, E., Prevedello, L., Calvert, V., Liotta, L., Nitti, D. & Lise, M. (2005). Kinase substrate protein microarray analysis of human colon cancer and hepatic metastasis. *Clinica Chimica Acta* **357**, 99-111.
Benedetto, C., Marozio, L., Tavella, A.M. & Salton, L. (2010). Coagulation disorders in pregnancy: acquired and inherited thrombophilias. *Annals of the New York Academy of Sciences* **1205**, 106-117.
Berne, B.J. & Pecora, R. (2000). Dynamic Light Scattering with Applications to Chemistry, Biology, and Physics. *Courier Dover Publications.* ISBN 0486411559.
Bernstein, I.M., Horbar, J.D., Badger, G.J., Ohlsson, A., Golan, A. (2000). Morbidity and mortality among very-low-birth-weight neonates with intrauterine growth restriction. *American Journal Obstetrics Gynaecology* **182** (1), 198-206.
Biemann, K. (1988). Contributions of mass spectrometry to peptide and protein structure. *Biomedical Environmental Mass Spectrometry* **16**, 99–111.
Blagoev, B., Ong, S.E., Kratchmarova, I. & Mann M. (2004). Temporal analysis of phosphotyrosine-dependent signaling networks by quantitative proteomics**.** *Nature Biotechnology* **22**, 1139–1145.
Blumenstein, M., Prakash, R., Cooper, G.J. & North, R.A. (2009)*.* Aberrant processing of plasma vitronectin and high-molecular-weight kininogen precedes the onset of preeclampsia.
Bodenmiller, B., Mueller, L.N., Mueller, M., Domon, B & Aebersold, R. (2007). Reproducible isolation of distinct, overlapping segments of the phosphoproteome. *Nature Methods* **4**, 231–237.
Bodenmiller, B., Mueller, L.N., Pedrioli, P.G., Pflieger, D., Jünger, M.A., Eng, J.K., Aebersold, R. & Tao, W.A. (2007). An integrated chemical, mass spectrometric and computational strategy for (quantitative) phosphoproteomics: application to Drosophila melanogaster Kc167 cells. *Molecular Biosystems* **3**, 275-286.
Bondarenko, P.V., Chelius, D. & Shaler, T.A. (2002). Identification and relative quantitation of protein mixtures by enzymatic digestion followed by capillary reversed-phase liquid chromatography-tandem mass spectrometry. *Analytical Chemistry* **74**, 4741-4749.

Bossi, A., Bonini, F., Turner, A.P.F. & Piletsky, S.A. (2007). Molecularly imprinted polymers for the recognition of proteins: The state of the art. *Biosensors and Bioelectronics* **22**, 1131-1137.

Bossi, A., Piletsky, S.A., Piletska, E.V., Righetti, P.G. & Turner, A.P.F. (2001). Surface-grafted molecularly imprinted polymers for protein recognition. *Analytical Chemistry* **73**, 5281-5286.

Bossi, A., Piletsky, S.A., Piletska, E.V., Righetti, P.G. & Turner, A.P.F. (2000). An assay for ascorbic acid based on polyaniline-coated microplates. *Analytical Chemistry* **72**, 4296-4300.

Bouba, I., Makrydimas, G., Kalaitzidis, R., Lolis, D.E., Siamopoulos, K.C. & Georgiou, I. (2003). Interaction between the polymorphisms of the renin-angiotensin system in preeclampsia. *European Journal of Obstetrics, Gynecology and Reproductive Biology* **110**, 8-11.

Bozzini, C., Campostrini, N., Trombini, P., Nemeth, E., Castagna, A., Tenuti, I., Corrocher, R., Camaschella, C., Ganz, T., Olivieri, O., Piperno, A. & Girelli, D. (2008). Measurement of urinary hepcidin levels by SELDI-TOF-MS in HFE-hemochromatosis. *Blood Cells, Molecules and Diseases* **40**, 347–352.

Brahim, S., Narinesingh, D. & Guiseppi-Elie, A. (2002). Kinetics of glucose oxidase immobilised in p(HEMA)-hydrogel microspheres in a packed-bed bioreactor.

Breeze, A.C.G. & Lees, C.C. (2007). Prediction and perinatal outcomes of fetal restriction. *Seminars in Fetal and Neonatal Medicine* **12**, 383-397.

Brenner, B. (2004). Haemostatic changes in pregnancy. *Thrombosis Research* **114**, 409–414.

Butt, H., Cappella, B. & Kappl, M. (2005). Force measurements with the atomic force microscope: technique, interpretation and applications. *Surface Science Reports* **59**, 1–152.

Calligaris, D., Villard, C. & Lafitte, D. (2011). Advances in top-down proteomics for disease biomarker discovery. *Journal of proteomics* **74** (7), 920-934.

Camilleri, R.S., Peebles, D., Portmann, C., Everington, T., Cohen, H. (2004). -455G/A beta-fibrinogen gene polymorphism, factor V Leiden, prothrombin G20210A mutation and MTHFR C677T, and placental vascular complications. *Blood coagulation and fibrinolysis* **15**, 139-147.

Castagna, A., Campostrini, N., Zaninotto, F. & Girelli, D. (2010). Hepcidin assay in serum by SELDI-TOF-MS and other approaches. *Journal of Proteomics* **73**, 527-536.

Cecconi, D., Zamò, A., Parisi, A. & Bianchi, E. (2008). Induction of apoptosis in Jeko-1 mantle cell lymphoma cell line by resveratrol: a proteomic analysis. *Journal of Proteome Research* **7**, 2670-2680.

Cecìlia, A., Roque, A., Christopher, R. & Lowe, G. (2005). Lessons from nature: on the molecular recognition elements of the phosphoprotein binding-domains. *Biotechnology & Bioengineering* **91**, 546-555.

Chang, C.K, Wu, C.C., Wang, Y.S. & Chang, H.C. (2008). Selective extraction and enrichment of multiphosphorylated peptides using polyarginine-coated diamond nanoparticles**.** *Analytical Chemistry* **80**, 3791–3797.

Chao, G.T., Qian, Z.Y., Huang, M.J., Kan, B., Gu, Y.C., Gong, C.Y., Yang, J.L., Wang, K., Dai, M., Li, X.Y., Gou, M.L., Tu, M.J. & Wei, Y.Q. (2008). Synthesis, characterization, and hydrolytic degradation behavior of a novel biodegradable pH-sensitive hydrogel based on polycaprolactone, methacrylic acid, and poly(ethylene glycol). *Journal of biomedical materials research Part A* **85**, 36-46.

Chen, C.H. (2008) Review of a current role of mass spectrometry for proteome research**.** *Analytica Chimica Acta* **624**, 16–36.

Chen, C.T. & Chen, Y.C. (2005). Fe3O4/TiO2 core/shell nanoparticles as affinity probes for the analysis of phosphopeptides using TiO2 surface-assisted laser desorption/ionization mass spectrometry. *Analysis* **77**, 5912-5919.

Chen, X., Wu, D., Zhao, Y., Wong, B.H.C. & Guo, L. (2011). Increasing phosphoproteome coverage and identification of phosphorylation motifs through combination of different HPLC fractionation methods. *Journal of Chromatography B* **879**, 25-34.

Chu, B. (1992). Laser Light scattering: Basic Principles and Practice*. Academic Press.* ISBN 0121745511.

Clevenger, C.V. (2004). Roles and regulation of stat family transcription factors in human breast cancer. *American Journal of Pathology* **165**, 1449–1460.

Cliver, S.P., Goldenberg, R.L., Neel, N.R. & Tamura, T. (1993). Neonatal cord serum alpha 2-macroglobulin and fetal size at birth. *Early Human Development* **33**: 201-206.

Cochran, S., Li, C.P. & Ferro, V. (2009). A surface plasmon resonance-based solution affinity assay for heparan sulfate-binding proteins. *Glycoconjugate Journal* **26**(5), 577-587.

Collins, M.O., Lu, Yu & Choudhary, J.S. (2007). Analysis of protein phosphorylation on a proteome-scale. *Proteomics* **7**, 2751–2768.

Collins, M.O., Yu, L., Coba, M.P., Husi, H., Campuzano, I., Blackstock, W.P., Choudhary, J.S. & Grant, S.G. (2005). Proteomic analysis of in vivo phosphorylated synaptic proteins. *Journal of Biological Chemistry* **280**, 5972–5982.

Cooper, M.A. (2009). Label-Free Biosensors: techniques and applications. *Cambridge University Press, New York.* Sono troppo ubriaca per capire se ho inserito o meno il titolo

Cormack, P.A.G., Haupt, K. & Mosbach, K. (2007). Affinity separation: Imprint polymers. *Encyclopedia of Separation Science,* 288-296.

Cunliffe, D., Kirby, A. & Alexander, C. (2005). Molecularly imprinted drug delivery systems. *Advanced Drug Delivery Reviews* **57**, 1836-1853.

Cvirn, G., Gallistl, S., Koestenberger, M. & Kutschera, J. (2002). Alpha 2-macroglobulin enhances prothrombin activation and thrombin potential by inhibiting the anticoagulant protein C/protein S system in cord and adult plasma. *Thrombosis Research* **105**, 433-439.

De Domenico, I., Nemeth, E., Nelson, J.M., Phillips, J.D., Ajioka, R.S., Kay, M.S., Kushner, J.P., Ganz, T., Ward, D.M. & Kaplan, J. (2008). The hepcidin-binding site on ferroportin is evolutionarily conserved. *Cell Metabolism* **8**, 146–156.

Dengjel, J., Akimov, V., Olsen, J.V., Bunkenborg, J., Mann, M., Blagoev, B. & Andersen, J.S. (2007). Quantitative proteomic assessment of very early cellular signaling events. *Nature Biotechnology* **25**, 566–568.

Domon, R.B. & Aebersold, R. (2006). Mass spectrometry and protein analysis. *Science* **312**, 212–217.

Ducloy-Bouthors, A.S. (2010). Clotting disorders and preeclampsia. *Annales Françaises d'Anesthésie et de Réanimation* **29**, 121-134.

Ducret, A., Van Oostveen, I., Eng, J.K., Yates. J.R. III & Aebersold, R. (1998). High throughput protein characterization by automated reverse-phase chromatography/electrospray tandem mass spectrometry. *Protein Science* **7**, 706–719.

Egerton, R. (2005). Physical principles of electron microscopy. *Springer.* ISBN 0387258000.

Emgenbroich, M., Borrell, C., Shinde, S., Lazraq, I., Vilela, F., Hall, A.J., Oxelbark, J., De Lorenzi, E., Courtois, J., Simanova, A. & Sellergren, B. (2008). A phosphotyrosine-imprinted polymer receptor for the recognition of tyrosine phosphorylated peptides. *Chemistry, a European Journal* **14**, 9516-9529.

Eymann, C., Becher, D., Bernhardt, J., Gronau, K., Klutzny, A. & Hecker, M. (2007). Dynamics of protein phosphorylation on Ser/Thr/Tyr in Bacillus subtilis. *Proteomics*, **7**, 3509–3526.

Feng, S., Ye, M., Zhou, H., Jiang, X., Jiang, X., Zou, H. & Gong, B. (2007). Immobilized zirconium ion affinity chromatography for specific enrichment of phosphopeptides in phosphoproteome analysis. *Molecular and Cellular Proteomics* **6**, 1656–1665.

Ficarro, S., Chertihin, O., Westbrook, V.A., White, F., Shabanowitz, J., Herr, J.C., Hunt, D.F. & Visconti, P.E. (2003). Phosphoproteome analysis of capacitated human sperm. Evidence of tyrosine phosphorylation of a kinase-anchoring protein 3 and valosin-containing protein/p97 during capacitation. *Journal of Biological Chemistry* **278**, 11579-11589.

Ficarro, S., Parikh, J.R., Blank, N.C. & Marto, J.A. (2008). Niobium(V) oxide (Nb2O5): application to phosphoproteomics. *Analytical Chemistry* **80**, 4606–4613 .

Ficarro, S.B., Mc Cleland, M.L., Stukenberg, P.T., Burke, D.J., Ross, M.M., Shabanowitz, J., Hunt, D.F. & White, F.M. (2002). Phosphoproteome analysis by mass spectrometry and its application to Saccharomyces cerevisiae. *Nature Biotechnology* **20**, 301–400.

Frazer, D.M. & Anderson, G.J. (2009). Hepcidin compared with prohepcidin: an absorbing story. *American Journal of Clinical Nutrition* **89**, 475–476.

Gagliardo, B. Kubat, N., Faye, A., Jaouen, M., Durel, B., Deschemin, J.C., Canonne-Hergaux, F., Sari, M.A. & Vaulont, S. (2009). Pro-hepcidin is unable to degrade the iron exporter ferroportin unless maturated by a furin-dependent process. *Journal of Hepatology* **50**, 394–401.

Galesloot, T.E., Vermuelen, S.H., Geurst-Moespot, A.J., Klaver, S.M., Kroot, J.J., van Tienoven, D., Wetzels, J.F.M., Kiemeney, L.A., Sweep, F.C., den Heijer, M. & Swinkels, D.W. (2011). Serum hepcidin: reference ranges and biochemical correlates in the general population. *Blood* **117**(25), e218-e225.

Gambling, L,, Danzeisen, R., Fosset, C., Andersen, H.S., Dunford, S., Srai, S.K. & McArdle, H.J. (2003). Iron and copper interactions in development and the effect on pregnancy outcome. *Journal of Nutrition* **133**, 1554S-1556S.

Ganz, T., Olbina, D., Girelli, D., Nemeth, E. & Westerman, M. (2008). Immunoassay for human serum hepcidin. *Blood* **112**, 4292–4297.

Gardosi, J. (2006). New Definition of Small for Gestational Age Based on Fetal Growth Potential. *Hormone Research* **65,** 15-18.

Gazzolo, D., Marinoni, E., Di Iorio, R., Bruschettini, M., Kornacka, M., Lituania, M., Majewska, U., Serra, G. & Michetti, F. (2004). Urinary S100B protein measurements: A tool for the early identification of hypoxic-ischemic encephalopathy in asphyxiated full-term infants. *Critical Care Medicine* **32**, 131-136.

Gembitsky, D.S., Lawlor, K., Jacovina, A., Yaneva, M. & Tempst P. (2004). A prototype antibody microarray platform to monitor changes in protein tyrosine phosphorylation. *Molecular and Cellular Proteomics* **3**, 1102-1118.

Gerber, S.A., Rush, J., Stemman, O., Kirschner, M.W. & Gygi, S.P. Absolute quantification of proteins and phosphoproteins from cell lysates by tandem MS. *Proceedings National Academy of Science USA* **100**, 6940–6945.

Giessibl, F.J. (2003). Advances in atomic force microscopy. *Reviews of modern physics* **75**, 949-983.

Girardi, G. (2008). Complement inhibition keeps mothers calm and avoids fetal rejection. *Immunological Investigation* **37**, 645-659.

Glad, M., Norrlöw, O., Sellergren, B., Siegbahn, N. & Mosbach, K. (1985). Use of silane monomers for molecular imprinting and enzyme entrapment in polysiloxane-coated porous silica. *Journal of Chromatography A* **347**, 11-23.

Gnad, F., Ren, S., Cox, J., Olsen, J.V., Macek, B., Oroshi, M. & Mann, M. (2007). PHOSIDA (phosphorylation site database): management, structural and evolutionary investigation, and prediction of phosphosites. *Genome Biology* **8**, R250.

Goldenberg, R.L., Tamura, T., Cliver, S.P. & Cutter, G.R. (1991). Maternal serum alpha 2-macroglobulin and fetal growth retardation. *Obstetrics and Gynecology* **78**, 594-599.

Goodlett, D.R., Keller, A., Watts, J.D., Newitt, R., Yi, E.C., von Haller, P., Aebersold, R. & Kolker, E. (2001). Differential stable isotope labeling of peptides for quantitation and de novo sequence derivation. *Rapid Communication Mass Spectrometry* **15**, 1214–1221.

Goss, V.L., Lee, K.A., Moritz, A., Nardone, J., Spek, E.J., MacNeill, J., Rush, J., Comb, M.J. & Polakiewicz, R.D. (2006). A common phosphotyrosine signature for the Bcr-Abl kinase. *Blood* **107**, 4888–4897.

Goto, H. & Inagaki, M. (2007). Production of a site- and phosphorylation state-specific antibody. *Nature Protocols* **2**, 2574– 2581.

Graham, M.E., Anggono, V., Bache, N., Larsen, M.R., Craft, G.E. & Robinson, P.J. (2007). The in vivo phosphorylation sites of rat brain dynamin I. *Journal of Biological Chemistry* **282**, 14695–14707.

Graves, J. & Krebs, D. (1999). Protein Phosphorylation and Signal Transduction. *Pharmacology & Therapeutics* **82**, 111–121.

Grigore, D., Ojeda, N.B., Robertson, E.B. & Dawson, A.S. (2007). Placental insufficiency results in temporal alterations in the renin angiotensin system in male hypertensive growth restricted offspring. *American Journal of Physiology. Regulatory, Integrative and Comparative Physiology* **293**, R804-811.

Grønborg, M., Kristiansen, T.Z., Stensballe, A., Andersen, J.S., Ohara, O., Mann, M., Jensen, O.N. & Pandey, A. (**2002).** A mass spectrometry-based proteomic approach for identification of serine/threonine-phosphorylated proteins by enrichment with phospho-specific antibodies: identification of a novel protein, Frigg, as a protein kinase A substrate. *Molecular and Cellular Proteomics* **1**, 517-527.

Guy, G.R., Philip, R. & Tan, Y.H. (**1994).** Analysis of cellular phosphoproteins by two-dimensional gel electrophoresis: applications for cell signaling in normal and cancer cells. *Electrophoresis* **15**, 417–440.

Han, G., Ye, M., Zhou, H., Jiang, X., Tian, R., Wan, D., Zou, H. & Gu, A. (2008). Large-scale phosphoproteome analysis of human liver tissue by enrichment and fractionation of phosphopeptides with strong anion exchange chromatography. *Proteomics* **8**, 1346-1361.

Harry, J.L., Wilkins, M.R., Herbert, B.R., Packer, N.H., Gooley, A. & Williams, K. (2000). Proteomics: capacity versus utility. *Electrophoresis* **21**, 1071-1081.

Hart, B.R. & Shea, K.J. (2001). Synthetic peptide receptors: molecularly imprinted polymers for the recognition of peptides using peptide-metal interactions. *Journal of the American Chemical Society* **123**, 2072-2073.

Heibeck, T.H., Shi-Jian, D., Opresko, L.K.,Tolmachev, A.V., Monroe, M.E., Camp II, D.G., Smith, R.D., Wiley, H.S. & Wei-Jun Qian. (2009). An extensive survey of tyrosine phosphorylation revealing new sites in human mammary epithelial cells. *Journal of Proteome Research* **8**, 3852-3861.

Helling, S., Shinde, S., Brosseron, F., Schnabel, A., Müller, T., Meyer, H.E., Marcus, K. & Sellergren, B. (2011). Ultratrace Enrichment of Tyrosine Phosphorylated Peptides on an Imprinted Polymer. *Analytical Chemistry* **83**, 1862–1865.

Hellstrom-Westas, L., Rosen, I. & Svenningsen, N.W. (1995). Predictive value of early continuous amplitude integrated EEG recordings on outcome after severe birth asphyxia in full term infants. *Archives of Disease in Childhood* **72,** 34–38.

Hinterdorfer, P. & Dufrêne, Y.F. (2006). Detection and localization of single molecular recognition events using atomic force microscopy. *Nature methods* **3** (5), 347–355.

Hjertén, S., Liao, J.L. & Zhang, R. (1989). High-performance liquid chromatography on continuous polymer beds. *Journal of Chromatography A* **473**, 273-275.

Hochstrasser, D.F., Patchornik, A. & Merril, C.R. (1988). Development of polyacrylamide gels that improve the separation of proteins and their detection by silver staining. *Analytical Biochemistry* **173**, 412-423.

Hornbeck, P.V., Chabra, I., Kornhauser, J.M., Skrzypek, E. & Zhang, B. (2004). PhosphoSite: A bioinformatics resource dedicated to physiological protein phosphorylation. *Proteomics* **4**, 1551–1561.

Hoshino, Y., Koide, H., Urakami, T., Kanazawa, H., Kodama, T., Oku, N. & Shea, K.J. (2010). Recognition, neutralization, and clearance of target peptides in the bloodstream of living mice by molecularly imprinted polymer nanoparticles: a plastic antibody. *Journal of the American Chemical Society* **132**, 6644–6645.

Hu, V.W., Heikka, D.S., Dieffenbach, P.B. & Ha L. (2001). Metabolic radiolabeling: experimental tool or Trojan horse? (35)S-Methionine induces DNA fragmentation and p53-dependent ROS production. *FASEB Journal* **15**, 1562–1568.

Huang, C.C., Wang, S.T. & Chang, Y.C. (1999). Measurement of the Urinary Lactate:Creatinine Ratio for the Early Identification of Newborn Infants at Risk

for Hypoxic–Ischemic Encephalopathy. *New England Journal of Medicine* **341**, 328–335.

Hui, L.& Challis, D. (2008) Diagnosis and management of fetal growth restriction: the role of fetal therapy. *Best Practice & Research Clinical Obstetrics and Gynaecology* **22**, 139-158.

Hunt, S.M.N., Thomas, M.R., Sebastian, L.T., Pedersen, S.K., Harcourt, R.L., Sloane, A.J. & Wilkins, M.R. (2005). Optimal replication and the importance of experimental design for gel-based quantitative proteomics. *Journal of Proteome Research* **4**, 809-819.

Hunter, T. (2000). Signaling--2000 and beyond. *Cell* **100**, 113–127.

Huttlin, E.L., Jedrychowski, M.P., Elias, J.E., Goswami, T., Rad, R., Beausoleil, S.A., Villen, J., Haas, W., Sowa, M.E. & Gygi, L. (2010). A tissue-specific atlas of mouse protein phosphorylation and expression. *Cell* **143**, 1174–1189.

Ibarrola, N., Kalume, D.E., Gronborg, M., Iwahori, A. & Pandey, A. (2003). A proteomic approach for quantitation of phosphorylation using stable isotope labeling in cell culture. *Analytical Chemistry* **75**, 6043–6049.

Ikeguchi, Y. & Nakamura, H. (2000). Selective enrichment of phospholipids by titania. *Analytical Sciences* **16**, 541-543.

Jaffe, H. (1998). Characterization of serine and threonine phosphorylation sites in beta-elimination/ethanethiol addition-modified proteins by electrospray tandem mass spectrometry and database searching. *Biochemistry* **37**, 16211–16224.

Jauniaux, E., Jurkovic, D., Gulbis, B., Collins, W.P., Zaidi, J. & Campbell, S. (1994). Investigation of the acid-base balance of coelomic and amniotic fluids in early human pregnancy. *American Journal of Obstetrics and Gynecology* **170**, 1365–1369.

Jensen, S.S. & Larsen, M.R. (2007). Evaluation of the impact of some experimental procedures on different phosphopeptide enrichment techniques**.** *Rapid Communication in Mass Spectrometry* **21**, 3635–3645.

Jones, R.B., Gordus, A., Krall, J.A. & Mac Beath, G. (2006). A quantitative protein interaction network for the ErbB receptors using protein microarrays. *Nature* **439**, 168-174.

Kaneko, Y., Miyajima, H., Piperno, A., Tomosugi, N., Hayashi, H., Morotomi, N., Tsuchida, K., Ikeda, T., Ishikawa, A., Ota, Y., Wakusawa, S., Yoshioka, K., Kono, S., Pelucchi, S., Hattori, A., Tatsumi, Y., Okada, T. & Yamagishi, M. (2010). Measurement of serum hepcidin-25 levels as a potential test for diagnosing hemochromatosis and related disorders. *Journal of Gastroenterology* **45**,1163-1171.

Karlgard, C.C.S., Wong, N.S., Jones, L.W. & Moresoli, C. (2003). In vitro uptake and release studies of ocular pharmaceutical agents by silicon-

containing and p-HEMA hydrogel contact lens materials. *International Journal of Pharmaceutics* **257**, 141-151.

Kaufmann, H., Bailey, J.E. & Fussenegger, M. (2001). Use of antibodies for detection of phosphorylated proteins separated by two-dimensional gel electrophoresis. *Proteomics* **1**, 194–199.

Kemna, E,H,, Tjalsma, H., Podust, V.N. & Swinkels, D.W. (2007). Mass spectrometry-based hepcidin measurements in serum and urine: analytical aspects and clinical implications. *Clinical Chemistry* 53, 620–628.

Kemna, E.H., Tjalsma, H., Laarakkers, C., Nemeth, E., Willems, H. & Swinkels, D. (2005). Novel urine hepcidin assay by mass spectrometry. *Blood* **106**, 3268–3270.

Kemna, E.H., Tjalsma, H., Willems, H.L. & Swinkels, D.W. (2008). Hepcidin: from discovery to differential diagnosis. *Haematologica* **93**(1), 90-97.

Kempe, M. & Mosbach, K. (1994). Direct resolution of naproxen on a non-covalently molecularly imprinted chiral stationary phase. *Journal of Chromatography A* **664**, 276-279 .

Kempe, M. & Mosbach, K. (1995). Separation of amino acids, peptides and proteins on molecularly imprinted stationary phases. *Journal of Chromatography A* **694**, 3-13.

Kempe, M. (2000). Oxytocin receptor mimetics prepared by molecular imprinting. *Letters in peptide science* **7**, 27-33.

Kersten, B., Agrawal, G.K., Iwahashi, H. & Rakwal, R. (2006). Plant phosphoproteomics: A long road ahead. *Proteomics* **6**, 5517–5528.

Khan, I.H., Mendoza, S., Rhyne, P., Ziman, M., Tuscano, J., Eisinger, D., Kung, H.J. & Luciw, P.A. (2006). Multiplex analysis of intracellular signaling pathways in lymphoid cells by microbead suspension arrays. *Molecular and Cellular Proteomics* **5**, 758-768.

Kim, D. & Scranton, A. (2004). Analysis of association constant for ground state dye-electron acceptor complex of photoinitiator systems and the association constant effect on the kinetics of visible-light-induced polymerizations. *Journal of Polymer Science: Part A: Polymer Chemistry* **42**, 5863–5871.

Kim, S., Mischerikow, N., Bandeira, N., Navarro, N.J.D., Wich, L., Mohammed, S., Heck, A.J.R. & Pevzner, P.A. (2010). The generating function of CID, ETD, and CID/ETD pairs of tandem mass spectra: applications to database search. *Molecular and Cellular Proteomics* **9**, 2840-2852.

Kirat, K.E., Bartkowski, M. & Haupt, K. (2009). Probing the recognition specificity of a protein molecularly imprinted polymer using force spectroscopy. *Biosensors and Bioelectronics* **24**, 2618-2624.

Kirkpatrick, D.S., Gerber, S.A. & Gygi, S.P. (2005). High throughput proteome screening for biomarker detection. *Methods* **35**, 265–273.

Kjeldsen, F., Giessing, A.M., Ingrell, C.R. & Jensen, O.N. (2007). Peptide sequencing and characterization of post-translational modifications by enhanced ion-charging and liquid chromatography electron-transfer dissociation tandem mass spectrometry. *Analytical Chemistry* **79**, 9243-9252.

Klein, J.U., Whitcombe, M.J., Mulholland, F. & Vulfson, E.N. (1999). Template-mediated synthesis of a polymeric receptor specific to amino acid sequences. *Angewandte Chemie International Edition* **38**, 2057-2060.

Kleinnijenhuis, A.J., Kjeldsen, F., Kallipolitis, B. & Haselmann K.F. & Jensen, O.N. (**2007).** Analysis of histidine phosphorylation using tandem MS and ion-electron reactions. *Analytical Chemistry* **79**, 7450–7456.

Knight, Z.A., Schilling, B., Row, R.H., Kenski, D.M., Gibson, B.W. & Shokat, K.M. (2003). Phosphospecific proteolysis for mapping sites of protein phosphorylation. *Nature Biotechnology* **21**, 1047–1054.

Kobold U, Dülffer, T., Dangl, M., Escherich, A., Kubbies, M., Röddiger, R. & Wright, J.A. (2008). Quantification of hepcidin-25 in human serum by isotope dilution micro-HPLC-tandem mass spectrometry**.** *Clinical Chemistry* **54**, 1584-1586.

Kolialexi, A., Mavrou, A. & Tsangaris, G.T. (2007). Proteomic analysis of human reproductive fluids. *Proteomics Clinical Applications* **1**, 853–860.

Koliaraki, V., Marinou, M., Vassilakopoulos, T.P., Vavourakis, E., Tsochatzis, E., Pangalis, G.A., Papatheodoridis, G., Stamoulakatou, A., Swinkels, D.W., Papanikolaou, G. & Mamalaki, A. (2009). A novel immunological assay for hepcidin quantification in human serum. *PLoS ONE* **4**, e4581.

Krause, A., Neitz, S., Mägert, H.J., Schulz, A., Forssmann, W.G., Schulz-Knappe, P. & Adermann, K. (2000). LEAP-1, a novel highly disulfide-bonded human peptide, exhibits antimicrobial activity. *FEBS Letters* **480**, 147-150.

Kroot, T., Laarakkers, C.M., Geurts-Moespot, A.J., Grebenchtchikov, N., Pickkers, P., van Ede, A.E., Peters, H.P., van Dongen-Lases, E., Wetzels, J.F., Sweep, F.C., Tjalsma, H. & Swinkels, D.W. (2010). Immunochemical and mass-spectrometry-based serum hepcidin assays for iron metabolism disorders. *Clinical Chemistry* **56**, 1570-1579.

Kryscio, D.R. & Peppas, N.A. **(2012).** Critical review and perspective of macromolecularly imprinted polymers. *Acta Biomaterialia* **8**(2), 461-473.

Kugimiya, A. & Takei, H. (2008). Selectivity and recovery performance of phosphate-selective molecularly imprinted polymer. *Analytica Chimica Acta* **606, 252-256.**

Kumar, Y., Khachane, A., Belwal, M., Das, S., Somsundaram, K. & Tatu, U. (2004). ProteoMod: A new tool to quantitate protein post-translational modifications. *Proteomics* **4**, 1672-1683.

Kweon, H.K. & Hakansson, K. (2006). Selective zirconium dioxide-based enrichment of phosphorylated peptides for mass spectrometric analysis. *Analytical Chemistry* **78**, 1743–1749.

Labarrere, C.A. & Althabe, O.H. (1986). Intrauterine growth retardation of unknown etiology: II. Serum complement and circulating immune complexes in maternal sera and their relationship with parity and chronic villitis. *American Journal of Reproductive Immunology and Microbiology* **12**, 4-6.

Labarrere, C.A., Manni, J., Salas, P. & Althabe, O. (1985). Intrauterine growth retardation of unknown etiology. I. Serum complement and circulating immune complexes in mothers and infants. *American Journal of Reproductive Immunology and Microbiology* **8**, 87-93.

Larsen, M.R., Thingholm, T.E., Jensen, O.N., Roepstorff, P. & Jorgensen, T.J. **(2005).** Highly selective enrichment of phosphorylated peptides from peptide mixtures using titanium dioxide microcolumns. *Molecular and Cellular Proteomics* **4**, 873–886.

Lasocki, S., Baron, G., Driss, F., Westerman, M., Puy, H., Boutron, I., Beaumont, C. & Montravers, P. (2010). Diagnostic accuracy of serum hepcidin for iron deficiency in critically ill patients with anemia. *Intensive care medicine* **36**,1044-1048.

Leitner, A. (2010). Phosphopeptide enrichment using metal oxide affinity chromatography. *Trends in Analytical Chemistry* **29**, 177-185 .

Leonhardt, A. & Mosbach, K. (1987). Enzyme-mimicking polymers exhibiting specific substrate binding and catalytic functions. *Reactive Polymers, Ion Exchangers, Sorbents* **6**, 285-290.

Lipinski, S., Bremer, L., Lammers, T., Thieme, F., Schreiber, S. & Rosentiel, P. (2010). Coagulation and inflammation. Molecular insights and diagnostic implications. *Hamostaseologie* **31**(2), 94-102.

Liu, X.B., Yang, F. & Haile, D.J. (2005). Functional consequences of ferroportin 1 mutations. *Blood Cells, Molecules, and Diseases* **35**, 133-146.

Loue, S. (2010). Forensic epidemiology. *Jones and Bartlett publishers Washington USA.* ISBN 978-0-7637-3849-5.

Lowe, C.R. **(1984).** Biosensors. *Trends in Biotechnology* **2**(3), 59-65.

Lowe, C.R. (2011). The future: biomarkers, biosensors, neuroinformatics, and e-neuropsychiatry. *International Review of Neurobiology* **101**, 375–400.

Lu, P., Vogel, C., Wang, R., Yao, X. & Marcotte, E.M. (2007). Absolute protein expression profiling estimates the relative contributions of transcriptional and translational regulation. *Nature Biotechnology* **25**, 117–124.

Lulka, M.F., Iqbal, S.S., Chambers, J.P., Valdes, E.R., Thompson, R.G., Goode, M.T. & Valdes, J.J. (2000). Molecular imprinting of Ricin and its A and B chains to organic silanes: fluorescence detection. *Materials Science and Engineering: C* **11**, 101-105.

Lynch, A.M., Gibbs, R.S., Murphy, J.R. & Giclas, P.C. (2010). Early elevations of the complement activation fragment C3a and adverse pregnancy outcomes. *Obstetrics and Gynecology* **117**, 75-83.

Lyubimova, T., Caglio, S., Gelfi, C., Righetti, P.G. & Rabilloud, T. (1993). Photopolymerization of polyacrylamide gels with methylene blue. *Electrophoresis* **14**, 40-50.

Magi, B., Bini, L., Marzocchi, B., Liberatori, S., Raggiaschi, R. & Pallini, V. (**1999).** Immunoaffinity identification of 2-DE separated proteins. *Methods in Molecular Biology* **112**, 431–443.

Mamone, G., Picariello, G., Ferranti, P. & Addeo, F. (2010). Hydroxyapatite affinity chromatography for the highly selective enrichment of mono- and multi-phosphorylated peptides in phosphoproteome analysis. *Proteomics* **10**, 380–393.

Mando, C., Tabano, S., Colapietro, P., Pileri, P., Colleoni, F., Avagliano, L., Doi, P., Bulfamante, G., Miozzo, M. & Cetin, I. (2010). Transferrin receptor gene and protein expression and localization in human IUGR and normal term placentas. *Placenta* 32, 44-50.

Mandruzzato, G., Antsaklis, A., Botet, F., Chervenak, F.A., Figueras, F., Grunebaum, A., Puerto, B., Skupski, D. & Stanojevic, M. (2008). Intrauterine restriction (IUGR). *Journal of Perinatal Medicine* **36,** 277-281.

Mann, M. & Jensen, O.N. (2003). Proteomic analysis of post-translational modifications. *Nature Biotechnology* **21**, 255-261.

Manning, G., Whyte, D.B., Martinez, R., Hunter, T. & Sudarsanam, S. (2002). The protein kinase complement of the human genome. *Human Genome Science* **298**, 1912–1934.

Mascini, M. & Tombelli, S. (2008). Biosensors for biomarkers in medical diagnostics. *Biomarkers* **13**(7), 637-657.

Matsui, J., Miyoshi, Y., Doblhoff-Dier, O. & Takeuchi, T. (1995). A molecularly imprinted synthetic polymer receptor selective for atrazine *Analytical Chemistry* **67**, 4404-4408.

McNulty, D.E. & Annan, R.S. (2008). Hydrophilic interaction chromatography reduces the complexity of the phosphoproteome and improves global phosphopeptide isolation and detection. *Molecular and Cellular Proteomics* **7**, 971-980.

Mohammed, S. & Heck, A.J.R. (2011). Strong cation exchange (SCX) based analytical methods for the targeted analysis of protein post-translational modifications**.** *Current Opinion in Biotechnology* **22**, 9–16.

Molina, H., Horn, D.M., Tang, N., Mathivanan, S. & Pandey, A. (2007). Global proteomic profiling of phosphopeptides using electron transfer dissociation tandem mass spectrometry. *Proceedings National Academy Science USA.* **104**, 2199–2204.

Mosbach, K. (1994). Molecular imprinting. *Trends in Biochemical Sciences* **19**, 9.

Mosbach, K., Zimmermann, H., Laurell, J.N., Csöregi, E. & Schuhmann, W. (2001). Picodroplet-deposition of enzymes on functionalized self-assembled monolayers as a basis for miniaturized multi-sensor structures. *Biosensors and Bioelectronics* **16**, 827-837.

Müller, R.H. (1993). Fat emulsions for parenteral nutrition II: Characterisation and physical long-term stability of Lipofundin MCT LCT. *Clinical Nutrition* **12**, 298-309.

Nelson, L. & Cox, M. (2004). *Lehninger principles of biochemistry, WHFreeman.*, 4th edition.

Nemeth, E., Rivera, S., Gabayan, V., Keller, C., Taudorf, S., Pedersen, B.K. & Ganz, T. (2004). IL-6 mediates hypoferremia of inflammation by inducing the synthesis of the iron regulatory hormone hepcidin. *The Journal of Clinical Investigation* **113**, 1271-1276.

Nemeth, E., Tuttle, M.S., Powelson, J., Vaughn, M.B., Donovan, A., Ward, D.M., Ganz, T. & Kaplan, J. (2004). Hepcidin regulates cellular iron efflux by binding to ferroportin and inducing its internalization. *Science* **306**, 2090–2093.

Neta, G.I., von Ehrenstein, O.S., Goldman, L.R., Lum, K., Sundaram, R., Andrews, W. & Zhang, J. (2010). Umbilical cord serum cytokine levels and risks of small-for-gestational-age and preterm birth. *American Journal of Epidemiology* **171**, 859-867.

Neuhoff, V., Arold, N., Taube, D.& Ehrhardt, W. (1988). Improved staining of proteins in polyacrylamide gels including isoelectric focusing gels with clear background at nanogram sensitivity using Coomassie Brilliant Blue G-250 and R-250. *Electrophoresis* **9**, 255-262.

Nishino, H., Huang, C.S. & Shea, K.J. (2006). Selective protein capture by epitope imprinting. *Angewandte Chemie International Edition* **45**, 2392-2396.

Nühse, T.S., Stensballe, A., Jensen, O.N. & Peck, S.C. (2003). Large-scale analysis of in vivo phosphorylated membrane proteins by immobilized metal ion affinity chromatography and mass spectrometry. *Molecular and Cellular Proteomics* **2**, 1234– 1243.

Nühse, T.S., Stensballe, A., Jensen, O.N. & Peck, S.C. (2004). Phosphoproteomics of the Arabidopsis plasma membrane and a new phosphorylation site database. *The Plant Cell* **16**, 2394-2405.

Oda, Y., Huang, K., Cross, F.R., Cowburn, D. & Chait, B.T. (1999). Accurate quantitation of protein expression and site-specific phosphorylation. *Proceedings National Academy Science USA.* **96**, 6591–6596.

Oda, Y., Nagasu, T. & Chait, B.T. (2001). Enrichment analysis of phosphorylated proteins as a tool for probing the phosphoproteome. *Nature Biotechnology* **19**, 379–382.

Olsen, J.V., Blagoev, B., Gnad, F., Macek, B., Kumar, C., Mortensen, P. & Mann, M. (2006). Global, in vivo, and site-specific phosphorylation dynamics in signaling networks. *Cell* **127**, 635–648.

Olsen, J.V., Macek, B., Lange, O., Makarov, A., Horning, S. & Mann, M. (2007). Higher-energy C-trap dissociation for peptide modification analysis. *Nature Methods* **4,** 709–712.

Olsen, J.V., Vermeulen, M., Santamaria, A., Kumar, C., Miller, M.L., Jensen, L.J., Gnad, F., Cox, J., Jensen, T.S., Nigg, E.A., Brunak, S. & Mann, M. (2010). Quantitative phosphoproteomics reveals widespread full phosphorylation site occupancy during mitosis**.** *Science Signaling* **3**: p ra3.

Ong, S.E., Blagoev, B., Kratchmarova, I., Kristensen, D.B., Steen, H., Pandey, A. & Mann, M. (**2002).** Stable isotope labeling by amino acids in cell culture, SILAC, as a simple and accurate approach to expression proteomics. *Molecular and Cellular Proteomics* **1**, 376–386.

Ou, S.H., Wu, M.C., Chou, T.C. & Liu, C.C. (2004). Polyacrylamide gels with electrostatic functional groups for the molecular imprinting of lysozyme. *Analytica Chimica Acta* **504**, 163-166.

Pan, S., Zhang, H., Rush, J., Eng, J., Zhang, N., Patterson, D., Comb, M.J. & Aebersold, R. (2005). High throughput proteome screening for biomarker detection. *Molecular and Cellular Proteomics* **4**, 182–190.

Park, C.H., Valore, E.V., Waring, A.J. & Ganz, T. (2001). Hepcidin, a urinary antimicrobial peptide synthesized in the liver. *Journal of Biological Chemistry* **276**, 7806–7810.

Perkins, D.N., Pappin, D.J., Creasy, D.M. & Cottrell, J.S. (1999). Probability-based protein identification by searching sequence databases using mass spectrometry data**.** *Electrophoresis* **20**, 3551–3567.

Perrault, S.D. (2009). Mediating tumor targeting efficiency of nanoparticles through design. *Nano Letters* **9**, 1909-1915.

Persson, B.L., Holmberg, L., Astedt, B. & Nilsson, I.M. (1982). Coagulation and fibrinolysis in pregnancy complicated by intrauterine growth retardation. *Acta Obstetricia et Gynecologica Scandinavica* **61**, 455-459.

Pigeon, C., Ilyin, G., Courselaud, B., Leroyer, P., Turlin, B., Brissot, P. & Loréal, O. (2001). A new mouse liver-specific gene, encoding a protein homologous to human antimicrobial peptide hepcidin, is overexpressed during iron overload. *Journal of Biological Chemistry* **276**, 7811-7819.

Piletska, E.V., Guerreiro, A.R., Romero-Guerra, M., Chianella, I., Turner, A.P.F. & Piletsky, S.A. (2008). Design of molecular imprinted polymers compatible with aqueous environment. *Analytica Chimica ACTA* **607**, 54–60.

Piletsky, S.A., Piletska, E.V., Bossi, A.M., Karim, K., Anthony, P.L. & Turner, P.F. (2001). Substitution of antibodies and receptors with molecularly imprinted polymers in enzyme-linked and fluorescent assays. *Biosensors and Bioelectronics* **16**, 701-707.

Pinkse, M.W., Uitto, P.M., Hilhorst, M.J., Ooms, B. & Heck, A.J. (2004). Selective isolation at the femtomole level of phosphopeptides from proteolytic digests using 2D-NanoLC-ESI-MS/MS and titanium oxide precolumns. *Analytical Chemistry* **76**, 3935–3943.

Porath, J., Carlsson, J., Olsson, I. & Belfrage G. **(1975).** Metal chelate affinity chromatography, a new approach to protein fractionation. *Nature* **258**, 598–599.

Posewitz, M.C. & Tempst, P. (1999). Immobilized gallium(III) affinity chromatography of phosphopeptides. *Chemistry* **71**, 2883–2892.

Ptacek, J., Devgan, G., Michaud, G., Zhu, H., Zhu, X., Fasolo, J., Guo, H., Jona, G., Breitkreutz, A., Sopko, R., Stern, D.F., De Virgilio, C., Tyers, M., Andrews, B., Gerstein, M., Schweitzer, B., Predki, P.F. & Snyder, M. (2005). Global analysis of protein phosphorylation in yeast. *Nature* **438**, 679–684.

Qi, D., Lu, J., Deng, C. & Zhang, X. (2009). Magnetically Responsive Fe(3)O(4)@C@SnO(2) core-shell microspheres: synthesis, characterization and application in phosphoproteomics. *Journal of Physical Chemistry* **113**, 15854–15861. Non lo go catà

Rabilloud, T. (2010). Variations on a theme: changes to electrophoretic separations that can make a difference. *Journal of Proteomics* **73**, 1562–1572.

Rachkov, A. & Minoura, N. (2001). Towards molecularly imprinted polymers selective to peptides and proteins. The epitope approach. *Biochimica et Biophysica Acta* **1544**, 255-266.

Raggiaschi, R., Gotta, S. & Terstappen, G.C. (2005). Phosphoproteome analysis. *Bioscience Reports* **25**, 33-44.

Rappsilber, J., Ryder, U., Lamond, A.I. & Mann, M. (2002). Large-scale proteomic analysis of the human spliceosome. *Genome Research* **12**, 1231–1245.

Reinders, J. & Sickmann, A. (2005). State-of-the-art in phosphoproteomics. *Proteomics* **5**, 4052–4061.

Reproductive Sciences, **16**, 1144-1152.

Reynolds, E.C., Riley, P.F. & Adamson, N.J. (1994). A selective precipitation purification procedure for multiple phosphoseryl-containing peptides and methods for their identification. *Analytical Biochemistry* **217**, 277–284.

Richani, K., Soto, E., Romero, R., Espinoza, J., Chaiworapongsa, T., Nien, J.K., Edwin, S., Kim, Y.M., Hong, J.S. & Mazor, M. (2005). Normal pregnancy is characterized by systemic activation of the complement system**.** *Journal of Maternal and Fetal Neonatal Medicine* **17**, 239-245.

Rick, J. & Chou, T-C. (2006). Amperometric protein sensor fabricated as a polypyrrole, poly-aminophenylboronic acid bilayer. *Biosensors and Bioelectronics* **22**, 329-335.

Rigbolt, K.T., Prokhorova, T.A., Akimov, V., Henningsen, J., Johansen, P.T., Kratchmarova, I., Kassem, M., Mann, M., Olsen, J.V. & Blagoev, B. (2011). System-wide temporal characterization of the proteome and

phosphoproteome of human embryonic stem cell differentiation. *Science Signaling* **4**, rs3.

Righetti, P.G. (2005) Polyacrylamide Gels. *Encyclopedia of Analytical Science* (2nd edition) Elsevier, Amsterdam. 396-407.

Righetti, P.G., Castagna, A., Antonucci, F., Piubelli, C., Cecconi, D., Campostrini, N., Rustichelli, C., Antonioli, P., Zanusso, G., Monaco, S., Lomas, L. & Boschetti, E. (2005). Proteome analysis in the clinical chemistry laboratory: myth or reality? *Clinica Chimica Acta* **357**, 123-139.

Righetti, P.G., Castagna, A., Antonucci, F., Piubelli, C., Cecconi, D., Campostrini, N., Zanusso, G. & Monaco, S. (2003). The proteome: anno Domini 2002. *Clinical Chemistry and Laboratory Medicine* **41**, 425-438.

Roepstorff, P. & Fohlman, J. **(1984).** Proposal for a common nomenclature for sequence ions in mass spectra of peptides. *Biomedical Mass Spectrometry* **11**, 601.

Ross, P.L., Huang, Y.N., Marchese, J.N., Williamson, B., Parker, K., Hattan, S., Khainovski, N., Pillai, S., Dey, S., Daniels, S., Purkayastha, S., Juhasz, P., Martin, S., Bartlet-Jones, M., He, F., Jacobson, A. & Pappin, D.J. (2005). Multiplexed protein quantitation in Saccharomyces cerevisiae using amine-reactive isobaric tagging reagents**.** *Molecular and Cellular Proteomics* **3**, 1154–1169.

Rudenberg, H.G. (2010). Origin and background of the invention of the electron microscope: commentary and expanded notes on memoir of Reinhold Rüdenberg. *Advances in Imaging and Electron Physics (Elsevier).* Vol. **160**, Chapter 6.

Rush, J., Moritz, A., Lee, K.A., Guo, A., Goss, V.L., Spek, E.J., Zhang, H., Xiang-Ming, Z., Polakiewicz, R.D. & Comb, M.J. (2004). Immunoaffinity profiling of tyrosine phosphorylation in cancer cells. *Nature Biotechnology* **23**, 94-101.

Sachs, K., Perez, O., Pe'er, D., Lauffenburger, D.A. & Nolan, G.P. (2005). Causal protein-signaling networks derived from multiparameter single-cell data. *Science* **308**, 523-529.

Salas, S.P., Giacaman, A., Romero, W., Downey, P., Aranda, E., Mezzano, D. & Vío, C.P. (2007). Pregnant rats treated with a serotonin precursor have reduced fetal weight and lower plasma volume and kallikrein levels. *Hypertension* **50**, 773-779.

Salas, S.P., Rosso, P., Espinoza, R. & Robert, J.A. (1993). Maternal plasma volume expansion and hormonal changes in women with idiopathic fetal growth retardation. *Obstetrics and Gynecology* **81**, 1029-1033.

Salimonu, L.S. (1992). Acute phase proteins in "small for dates" babies. II. Haptoglobin, transferrin, alpha-1-feto protein, alpha-1-acid glycoprotein and caeruloplasmin levels. *African Journal of Medicine and Medical Sciences* **21**, 55-59.

Schmelzle, K. & White, F.M. (2006). Phosphoproteomic approaches to elucidate cellular signaling networks. *Current Opinion in Biotechnology* **17**, 406-414.

Schmidt, A., Kellermann, J. & Lottspeich, F. (2005). A novel strategy for quantitative proteomics using isotope-coded protein labels. *Proteomics* **5**, 4–15.

Schmidt, S.R., Schweikart, F. & Andersson, M.E. (2007). Current methods for phosphoprotein isolation and enrichment. *Journal of Chromatography B* **849**, 154-162.

Schroeder, M.J., Webb, D.J., Shabanowitz, J., Horwitz, A.F. & Hunt, D.F. (2005). Methods for the detection of paxillin post-translational modifications and interacting proteins by mass spectrometry. *Journal of Proteome Research* **4**, 1832–1840.

Schürenberg, M., Dreisewerd, K. & Hillenkamp, F. (1999). Laser desorption/ionization mass spectrometry of peptides and proteins with particle suspension matrixes. *Analytical Chemistry* **71**, 221-229.

Schwarz, P., Strnad, P., von Figura, G., Janetzko, A., Krayenbu, P., Adler, G., Kulaksiz, H. (2011). A novel monoclonal antibody immunoassay for the detection of human serum hepcidin. *Journal of Gastroenterology* **46**, 648–656.

Sellergren, B. & Allender, C.J. (2005). Molecularly imprinted polymers: a bridge to advanced drug delivery. *Advanced Drug Delivery Reviews* **57**, 1733-1741.

Sellergren, B., Lepistö, M. & Mosbach, K. (1989). Highly enantio- and substrate-selective polymers obtained by molecular imprinting based on non-covalent interactions. *Reactive Polymers* **10**, 306-307.

Shevchenko, A., Wilm, M., Vorm, O., Mann, M. (1996). Mass spectrometric sequencing of proteins silver-stained polyacrylamide gels *Analytical Chemistry* **68**, 850-858.

Shi, H.Q., Tsai, W.B., Garrison, M.D., Ferrari, S. & Ratner, B.D. (1999). Template-imprinted nanostructured surfaces for protein recognition. *Nature* **398**, 593-597.

Shiomi, T., Matsui, M., Mizukami, F. & Sakaguchi, K. (2005). A method for the molecular imprinting of hemoglobin on silica surfaces using silanes. *Biomaterials* **26**, 5564-5571.

Sickmann, A. & Meyer, H.E. (2001). Phosphoamino acid analysis. *Proteomics* **1**, 200-206.

Simonis, G., Mueller, K., Schwarz, P., Wiedemann, S., Adler, G., Strasser, R.H. & Kulaksiz, H. (2010). The iron-regulatory peptide hepcidin is upregulated in the ischemic and in the remote myocardium after myocardial infarction. *Peptides* **31**,1786-1790.

Soubasi, V., Petridou, S., Sarafidis, K., Tsantali, C.H., Diamanti, E., Buonocore, G. & Drossou-Agakidou, V. (2010). Association of increased

maternal ferritin levels with gestational diabetes and intra-uterine growth retardation. *Diabetes and Metabolism* **36**, 58-63.

Stannard, C., Soskic, V. & Godovac-Zimmermann, J. (**2003).** Rapid changes in the phosphoproteome show diverse cellular responses following stimulation of human lung fibroblasts with endothelin-1. *Biochemistry* **42**, 13919–13928.

Steen, H., Jebanathirajah, J.A., Springer, M., Kirschner, M.W. (2005). Stable isotope-free relative and absolute quantitation of protein phosphorylation stoichiometry by MS. *Proceedings National Academy of Science USA* **102**, 3948–3953.

Steen, H., Kuster, B. & Mann, M. (2001). Quadrupole time-of-flight versus triple-quadrupole mass spectrometry for the determination of phosphopeptides by precursor ion scanning. *Journal Mass Spectrometry* **367**, 782–790.

Steen, H., Kuster, B., Fernandez, M., Pandey, A. & Mann, M. (2001). Tyrosine phosphorylation mapping of the epidermal growth factor receptor signaling pathway. *Journal of Biological Chemistry* **277**, 1031–1039.

Steinberg, T.H., Agnew, B.J., Gee, K.R., Leung, W.Y., Goodman, T., Schulenberg, B., Hendrickson, J., Beechem, J.M., Haugland, R.P. & Patton, W.F. (2003). Global quantitative phosphoprotein analysis using Multiplexed Proteomics technology. *Proteomics* **3**, 1128–1144.

Steinberg, T.H., Agnew, B.J., Gee, K.R., Leung, W.Y., Goodman, T., Schulenberg, B., Hendrickson, J., Beechem, J.M., Haugland, R.P. & Patton, W.F. (2003). Global quantitative phosphoprotein analysis using Multiplexed Proteomics technology. *Proteomics* **3**, 1128–1144.

Sugiyama, N., Nakagami, H., Mochida, K., Daudi, A., Tomita, M., Shirasu, K. & Ishihama, Y. (2008). Large-scale phosphorylation mapping reveals the extent of tyrosine phosphorylation in Arabidopsis. *Molecular Systems Biology* 4, 193.

Swinkels, D., Girelli, D., Laarakkers, C., Kroot, J., Campostrini, N., Kemna, E.H.& Tjalsma, H. (2008). Advances in quantitative hepcidin measurements by time-of-flight mass spectrometry. *PLoS ONE* **3**, e2706.

Syka, J.E., Coon, J.J., Schroeder, M.J., Shabanowitz, J. & Hunt, D.F. (2004). Peptide and protein sequence analysis by electron transfer dissociation mass spectrometry. *Proceedings National Academy Science USA.* **101**, 9528–9533.

Tamayo, F.G., Turiel, E. & Martìn-Esteban, A. (2007). Molecularly imprinted polymers for solid-phase extraction and solid-phase microextraction: recent developments and future trends. *Journal of Chromatography A* **1152**, 32-40.

Tao, W.A., Wollscheid, B., O'Brien, R., Eng, J.K., Li, X.J., Bodenmiller, B., Watts, J.D., Hood, L. & Aebersold, R. (2005). Quantitative phosphoproteome analysis using a dendrimer conjugation chemistry and tandem mass spectrometry. *Nature Methods* **2**, 591-598.

Thingholm ,T.E., Jensen, O.N. & Larsen, M.R. (2009). *Phospho-Proteomics – Methods and Protocols. Humana Press, Totowa, NJ.*, Chapter **4**, 47–56.

Thingholm, T.E., Jensen, O.N., Robinson, P.J. & Larsen, M.R. (2008). SIMAC (sequential elution from IMAC), a phosphoproteomics strategy for the rapid separation of monophosphorylated from multiply phosphorylated peptides. *Molecular and Cellular Proteomics* **7**, 661-671.

Thingholm, T.E., Larsen, M.R., Ingrell, C.R., Kassem, M. & Jensen, O.N. (**2008).** TiO(2)-based phosphoproteomic analysis of the plasma membrane and the effects of phosphatase inhibitor treatment. *Journal of Proteome Research* **7**, 3304–3313.

Thompson, A., Schafer, J., Kuhn, K., Kienle, S., Schwarz, J., Schmidt, G., Neumann, T., Johnstone, R., Mohammed, A.K. & Hamon, C. (2003). Tandem mass tags: a novel quantification strategy for comparative analysis of complex protein mixtures by MS/MS. *Analytical Chemistry* **75**, 1895–1904.

Tincani, A., Cavazzana, I., Ziglioli, T., Lojacono, A., De Angelis, V. & Meroni, P. (2010). Complement activation and pregnancy failure. *Clinical Reviews in Allergy and Immunology* **39**, 153-159.

Tiselius, A., Hjerten, S. & Levin, O. (1956). Protein chromatography on calcium phosphate columns. *Archives of biochemistry and biophysics* **65**, 32–155.

Tomosugi, N., Kawabata, H., Wakatabe, R, Higuchi, M., Yamaya, H., Umehara, H. & Ishikawa I. (2006). Detection of serum hepcidin in renal failure and inflammation by using ProteinChip System. *Blood* **108**, 1381–1387.

Trinidad, J.C., Specht, C.G., Thalhammer, A., Schoepfer, R. & Burlingame, A.L. (2006). Comprehensive identification of phosphorylation sites in postsynaptic density preparations. *Molecular and Cellular Proteomics* **5**, 914–922 .

Twyman, R.M. (**2004).** *Principles of proteomics, BIOS Scientific Publishers, Taylor and Francis Group.* 273-275.

Valdes, T.I., Ciridon, W., Ratner, B.D. & Bryers, J.D. (2008). Surface modification of a perfluorinated ionomer using a glow discharge deposition method to control protein adsorption. *Biomaterials* **29**, 1356-1366.

Venter, J.C. et al. (2001). The sequence of the human genome**.** *Science* **291**, 1304–1351.

Villen, J., Beausoleil, S.A., Gerber, S.A. & Gygi, S.P. (2007). Large-scale phosphorylation analysis of mouse liver. *Proceedings National Academy of Science USA.* **104**, 1488–1493.

Vlatakis, G., Andersson, L.I., Miller, R. & Mosbach, K. (1993). Drug assay using antibody mimics made by molecular imprinting. *Nature* **361**- 645-647.

von Tempelhoff, G.F., Velten, E., Yilmaz, A., Hommel, G., Heilmann, L. & Koscielny, J. **(2009).** Blood rheology at term in normal pregnancy and in

patients with adverse outcome events. *Clinical Hemorheology and Microcirculation* **42**, 127-139.

Vuadens, F., Benay, C., Crettaz, D., Gallot, D., Sapin, V., Schneider, P., Bienvenut, W.V., Lemery, D., Quadroni, M., Dastugue, B. & Tissot, J.D. (2003). Identification of biologic markers of the premature rupture of fetal membranes: proteomic approach. *Proteomics* **3,** 1521–1525.

Wang, G., Wu, W.W., Zeng, W., Chou, C.L. & Shen, R.F. (2006). Label-free protein quantification using LC-coupled ion trap or FT mass spectrometry: reproducibility, linearity, and application with complex proteomes. *Journal of Proteome Research* **5**, 1214–1223.

Ward, D.G., Roberts, K., Stonelake, P., Goon, P., Zampronio, C.G., Martin, A., Johnson, P.J., Iqbal, T. & Tselepis, C. (2008). SELDI-TOF-MS determination of hepcidin in clinical samples using stable isotope labelled hepcidin as an internal standard. *Proteome Science* **6**, 28.

Weisenhornt, A.L., Khorsandit, M., Kasast, S., Gotzost, V. & Butt, H.J. (1993). Deformation and height anomaly of soft surfaces studied with an AFM. *Nanotechnology* **4**, 106-113.

Wolf-Yadlin, A., Hautaniemi, S., Lauffenburger, D.A. & White, F.M. (2007). Multiple reaction monitoring for robust quantitative proteomic analysis of cellular signaling networks. *Proceedings National Academy of Science USA* **104**, 5860–5865.

Wu, Y., Sakamoto, H., Kanenishi, K., Li, J., Khatun, R. & Hata, T. (2003). Transferrin microheterogeneity in pregnancies with preeclampsia. *Clinica Chimica Acta* **332**, 103-110.

Wulff, G. & Liu, J. (2012). Design of biomimetic catalysts by molecular imprinting in synthetic polymers: the role of transition state stabilization. *Accounts of Chemical research* **45** (2), 239-247.

Wulff, G. (1991). Molecular recognition in polymers prepared by imprinting with templates. *Reactive Polymers* **15**, 233.

Wulff, G. (2002). Molecular imprinting-a way to prepare effective mimics of natural antibodies and enzymes. *Studies in Surface Science and Catalysis* **141**, 35-44.

Xia, Q.W., Cheng, D., Duong, D.M., Gearing, M., Lah, J.J., Levey, A.I. & Peng, J. (2008). Phosphoproteomic analysis of human brain by calcium phosphate precipitation and mass spectrometry. *Journal of Proteome Research* **7**, 2845–2851.

Xia, Y., Wen, H.Y., Kellems, R.E. (2002). Angiotensin II inhibits human trophoblast invasion through AT1 receptor activation. *Journal of Biological Chemistry* **277**, 24601-24608.

Yamagata, A., Kristensen, D.B., Takeda, Y., Miyamoto, Y., Okada, K., Inamatsu, M. & Yoshizato, K. (**2002).** Mapping of phosphorylated proteins on

two-dimensional polyacrylamide gels using protein phosphatase. *Proteomics* **2**, 1267–1276.

Yamazaki, T., Yilmaz, E., Mosbach, K. & Sode, K. (2001). Towards the use of molecularly imprinted polymers containing imidazoles and bivalent metal complexes for the detection and degradation of organophosphotriester pesticides. *Analytica Chimica Acta* **435**, 209-214.

Yan, J.X., Harry, R.A., Spibey, C. & Dunn, M.J. (2000). Postelectrophoretic staining of proteins separated by two-dimensional gel electrophoresis using SYPRO dyes. *Electrophoresis* **21**, 3657-3665.

Yaoi, T., Chamnongpol, S., Jiang, X. & Li, X. (2006). Src homology 2 domain-based high throughput assays for profiling downstream molecules in receptor tyrosine kinase pathways. *Molecular Cellular Proteomics* **5**, 959-968.

Ye, L. & Mosbach, K. (2001). Molecularly imprinted microspheres as antibody binding mimics. *Reactive & Functional Polymers* **48**, 149–157.

Ye, L. & Mosbach, K. (2008). Molecular Imprinting: synthetic materials as substitutes for biological antibodies and receptors. *Chemistry of Materials* **20**(3), 859-868.

Yoshimatsu, K., Yamazaki, T., Ioannis, S., Chronakis, I.S. & Ye, L. (2012). Influence of template/functional monomer/cross-linking monomer ratio on particle size and binding properties of molecularly imprinted nanoparticles. *Journal of Applied Polymer Science* **124,** 1249–1255.

Yu, Y.H., Shen, L.Y., Zhong, M., Zhang, Y., Su, G.D., Gao, Y.F., Quan, S.& Zeng, L. (2004). Effect of heparin on fetal growth restriction. *Zhonghua Fu Chan Ke Za Zhi* (Article in chinese) **39**, 793-796.

Yu, Y.H., Shen, L.Y., Zou, H., Wang, Z.J. & Gong, S.P. (2010). Heparin for patients with growth restricted fetus: a prospective randomized controlled trial. *Journal of Maternal and Fetal Neonatal Medicine* **23**, 980-987.

Zadrozna, M., Gawlik, M., Nowak, B., Marcinek, A., Mrowiec, H., Walas, S., Wietecha-Posłuszny, R. & Zagrodzki, P. (2009). Antioxidants activities and concentration of selenium, zinc and copper in preterm and IUGR human placentas. *Journal of Trace Elements in Medicine and Biology* **23**, 144-148.

Zarei, M., Sprenger, A., Metzger, F., Gretzmeier, C. & Dengjel, J. (2011). Comparison of ERLIC-TiO2, HILIC-TiO2, and SCX-TiO2 for global phosphoproteomics approaches. *Journal of Proteome Research* **10**, 3474-3483.

Zhai, B., Villen, J., Beausoleil, S.A., Mintseris, J., Gygi, S.P. (2008). Phosphoproteome analysis of Drosophila melanogaster embryos. *Journal of Proteome Research* **7**, 1675-1682.

Zhang, H., Zha, X., Tan, Y., Hornbeck, P.V., Mastrangelo, A.J., Alessi, D.R., Polakiewicz, R.D. & Comb, M.J. (**2002).** Phosphoprotein analysis using antibodies broadly reactive against phosphorylated motifs. *Journal of Biological Chemistry* 277, 39379-39387.

Zhang, K. (2006). From purification of large amounts of phospho-compounds (nucleotides) to enrichment of phospho-peptides using anion-exchanging resin. *Analytical Biochemistry* **357**, 225–231.

Zhang, X., Jin, Q.K., Carr, S.A. & Annan. R.S. (2002). N-Terminal peptide labeling strategy for incorporation of isotopic tags: a method for the determination of site-specific absolute phosphorylation stoichiometry. *Rapid Communication Mass Spectrometry* **16**, 2325-2332.

Zhang, X., Ye, J., Jensen, O.N.& Roepstorff, P. (2007). Highly Efficient Phosphopeptide Enrichment by Calcium Phosphate Precipitation Combined with Subsequent IMAC Enrichment. *Molecular and Cellular Proteomics* **6**, 2032–2042.

Zhang, X.Q., Varner, M., Dizon-Townson, D., Song, F. & Ward, K. (2003). A molecular variant of angiotensinogen is associated with idiopathic intrauterine growth restriction. *Obstetrics and Gynecology* **101**, 237-242.

Zhou, H., Watts, J.D. & Aebersold, R. (2001). A systematic approach to the analysis of protein phosphorylation. *Nature Biotechnology* **19**, 375–378.

Zhu, W.P., Gou, P.F., Zhu, K. & Shen, Z. (2008). Synthesis, extraction, and adsorption properties of calix[4]arene-poly(ethylene-glycol) crosslinked polymer.

Zhu, X., Lee, H., Raina, A.K., Perry, G. & Smith, R.D. (2002). The role of mitogen-activated protein kinase pathways in Alzheimer's disease. *Neurosignals* **11**, 270–281.

Zohdi, V., Moritz, K.M., Bubb, K.J. & Cock, M.L. *(*2007). Nephrogenesis and the renal renin-angiotensin system in fetal sheep: effects of intrauterine growth restriction during late gestation.*American Journal of Physiology. Regulatory, Integrative and Comparative Physiology* **293**, R1267-1273.

Zubarev, R.A., Kelleher, N.L., McLafferty, F.W. (1998). Electron capture dissociation of multiply charged protein cations. A nonergodic process. *Journal of American Chemical Society* **120**, 3265–3266.

PAPERS PUBLISHED DURING THE PHD STUDIES

Cecconi, D., Lonardoni, F., Favretto, D., Cosmi, E., Tucci, M., Visentin, S., Cecchetto, G., Fais, P., Viel, G. & Ferrara, S.D. (2011). Changes in amniotic fluid and umbilical cord serum proteomic profiles of foetuses with intrauterine growth retardation. *Electrophoresis* **32** (24):3630-7.

Lonardoni, F. & Bossi, A.M. (2012). Phosphoproteomics. Source: *Protein Purification*, ISBN 978-953-307-831-1. Edited by: Rizwan Ahmad. Publisher: InTech.